論文 / 著書情報
Article / Book Information

題目(和文)	合成高分子のコイル・グロビュール転移に基づくsiRNA 周囲の空間支配と薬理機構制御への展開
Title(English)	Development of a Methodology for an Artificial Control of siRNA Bioactivity Based on the Coil-Globule Transition Behavior of the Conjugated Polymeric Molecule
著者(和文)	NOORFaizah
Author(English)	Noor Faizah
出典(和文)	学位:博士(工学), 学位授与機関:東京工業大学, 報告番号:甲第10530号, 授与年月日:2017年3月26日, 学位の種別:課程博士, 審査員:西山 伸宏,小畠 英理,金原 数,宍戸 厚,田巻 孝敬
Citation(English)	Degree:Doctor (Engineering), Conferring organization: Tokyo Institute of Technology, Report number:甲第10530号, Conferred date:2017/3/26, Degree Type:Course doctor, Examiner:,,,,
学位種別(和文)	博士論文
Type(English)	Doctoral Thesis

Development of a Methodology for an Artificial Control of siRNA Bioactivity Based on the Coil-Globule Transition Behavior of the Conjugated Polymeric Molecule

(合成高分子のコイル・グロビュール転移に基づく
siRNA 周囲の空間支配と薬理機構制御への展開)

Noor Faizah Binti Che Harun

A thesis submitted in partial fulfillment of the requirements for the degree of
DOCTOR OF ENGINEERING
in the Interdisciplinary Graduate School of Science and Engineering
Tokyo Institute of Technology

March 2017

Dedication

This humble effort is dedicated to my beloved family members, especially to my sweet and loving mother, Nor Aswana Yusuff, and father, Che Harun Ismail, for all of unconditional love and support throughout my life.

Preface

This thesis is ultimately based on the experimental research for the development of a new scientific methodology for an artificial control of siRNA bioactivity in Prof. Nishiyama laboratory at Tokyo Institute of Technology, Tokyo, Japan. In October 2013, I started my research as a Ph.D. student in the laboratory, and I dedicated to a research for design a new methodology for artificial induction of siRNA bioactivity, based on conjugation with stimuli-responsive polymer. I believe that this work provides a new trend for molecular design of siRNA-based medicine and associated therapeutics.

I would like to appreciate many people who gave me a lot of supports and advices not only for my research but also for my daily life. I would like to express my first and foremost gratitude to Professor Nobuhiro Nishiyama, for his excellent guidance and aid from the beginning to the completion of my research. I also would like to express my gratitude to all of the members in the Nishiyama Laboratory. The last but not least, I also appreciate my family and friends for all of the supports to me.

Noor Faizah Binti Che Harun

Department of Environmental Chemistry and Engineering

Interdisciplinary Graduate School of Science and Engineering

Tokyo Institute of Technology

March 2017

Table of Contents

List of Abbreviations

AA: acrylic acid

AGO2 (Ago2): Argonaute-2

ATRP: atom transfer radical polymerization

asRNA: antisense-RNA

$CDCl_3$: deuterated chloroform

CHS: chalcone synthase

CTA: chain transfer agent

CuBr: Copper (I) bromide

CuCl: Copper (I) chloride

DMAA: *N, N*-dimethyl acrylamide

EtBriB: ethyl-2-bromoisobutyrate

FCS: fluorescence correlation spectroscopy

GSH: glutathione

LCST: lower critical solution temperature

MAA: methacrylic acid

MALDI-TOF MS: matrix-assisted laser desorption/ionization

MCP: Methyl 2-chloropropionate

MeOD: deuterated methanol

Me_6TREN: tris[2-(dimethylamino)ethyl]amine

Mw: molecular weight

Mw/Mn: molecular weight distribution

NMP: nitroxide-mediated polymerization

PAA: poly(acrylic acid)

PAsp: poly(aspartic acid)

PBAVE: poly(butyl amino vinyl ether)

PEG: poly(ethylene glycol)

PEI: polyethylenimine

PEO-PPO-PEO: poly(ethylene oxide)-poly(propylene oxide)-poly(ethylene oxide)

PIC: polyion complex

PKR: protein kinase R

PMAA: poly(methacrylic acid)

PNIPAAm: poly(*N*-isopropylacrylamide)

PNIPAAm-Br: bromide terminated-poly (*n*-isopropyl acrylamide)

PNIPAAm-Cl: bromide terminated- poly (*n*-isopropyl acrylamide)

PNIPAAm-CTA: trithiocarbonate terminated- poly (*n*-isopropyl acrylamide)

PNIPAAm-DBCO: DBCO terminated- poly (*n*-isopropyl acrylamide)

PNIPAAm-NH_2: amine terminated-poly (*n*-isopropyl acrylamide)

PNIPAAm-phthalimide: phthalimide terminated-poly (*n*-isopropyl acrylamide)

PNIPAAm-SH: thiol terminated-poly (*n*-isopropylacrylamide)

PNIPAAm-TE: thioether terminated-poly (*n*-isopropyl acrylamide)

PNVC: poly(*N*-vinylcaprolactam)

RAFT: reversible addition-fragmentation radical polymerization

RISC: RNA-induced silencing complex

RNAi: RNA interference

siRNA: small interfering RNA

ssRNA: sense-strand

TAMRA: Carboxytetramethylrhodamine

TLRs: toll-like receptors

UCST: upper critical solution temperature

Chapter 1. General Introduction

1.1. Introduction

Enormous efforts have been devoted to the design of small interfering RNA (siRNA)-based therapeutics because of its strong gene silencing ability in a sequence specific manner [1-9]. siRNA-based therapy has been employed as a promising therapy for cure several intractable diseases such as genetic disorder and cancer [10, 11]. The strategy of employing siRNA-based therapy with sequences complementary to specific target genes to cure gene defect-derived diseases can improve the drug discovery as well as target validation.

It is known that siRNA-based treatment can efficiently inhibit the tumor growth in *in vitro* and in *in vivo*. However, siRNA-based treatment faces several barriers along the pathway from administration to the body to the intracellular target site. After systemically administered, siRNA is rapidly degraded by RNases in the bloodstream and/or eliminated by the kidney because they are smaller than 6 nm [6]. Moreover, at the cellular level, when siRNA successfully be uptaken into the cell through endocytosis, siRNA needs to escape from endosomal compartment to function the RNAi process. Thus, the release from endosome is an important barrier. In addition, to initiate the gene silencing pathway, the recognition by gene silencing-related protein in RNA-induced silencing complex (RISC) in the cytoplasm cell is also another important barrier. Therefore, enormous efforts have been developed in order to realize the clinical potential of siRNA. Chemically modified siRNA structures as well as sophisticatedly designed delivery materials for siRNA are among the approaches. For example, researchers modified siRNA structure for physiological resistance leading to prolonged bioactivity of siRNA, and created sophisticated carriers with targeting ligand for siRNA delivery to the targeted site [12-16].

siRNA conjugation is also one of the approaches. siRNA conjugation not only improves inherent gene silencing ability, but also endows new functions. For example, siRNA has been chemically modified with fluorescence for the detection, antibody modification for the active

targeting as well as modification with polymer such as poly(ethylene glycol) (PEG) for enzymatic tolerability [9, 17, 18]. However, chemically modified siRNA with polymeric molecule often undergoes weak recognition with the gene silencing related protein due to the steric hindrance effect of the conjugated polymer [19-21]. Thus, in the present study, a new methodology for an artificial control of siRNA activity is developed based on steric hindrance effect of the conjugated polymer. The artificial control of siRNA bioactivity was developed utilizing stimuli-responsive polymer having coil-globule transition behavior. The artificial control of therapeutic activity of siRNA has a high potential to provide another solution to realize targeted-site specific gene silencing toward the siRNA-based therapeutics.

1.2. siRNA-based RNA interference (RNAi)

In 1978, the first study of gene expression has been discovered using antisense oligonucleotide. In that discovery, using a 13-mer of DNA oligonucleotide to inhibit Rous sarcoma virus translation in a sequence-specific manner [22, 23]. Then, in early 1990 Napoli et al. discovered siRNA after they attempted to determine the rate-limiting enzyme in anthocyanin biosynthesis. At first, they attempted to generate violet petunia, however, they overexpressed chalcone synthase (CHS) and unexpectedly it resulted in white petunia in wild-type petunia. They named this phenomenon as “co-suppression” [24].

Several years later, Fire and Mello reported the first explanation of gene silencing for RNA interference (RNAi) using double-stranded RNA (dsRNA) and the high significance of their discovery and being recognized by award of the Nobel Prize in Physiology or Medicine in 2006. In the first report, they introduced synthetic dsRNA into nematode, *Caenorhabditis elegans*. They observed that, the expression of the complementary gene of introduced synthetic dsRNA was blocked [1].

Then, in 2000, Zamore, Hammond et al discovered small interfering RNA (siRNA) with 21 -23 nucleotide in length during the examination of molecular mechanism of RNAi in *Drosopilla* cells. Those siRNA were able to bind the complementary sequence target in mRNA, and lead to the mRNA degradation [25, 26]. Moreover, Elbashir et al. reported that synthetic siRNA could silence the genes and also discovered the RNAi process possible in mammalian cells [3]. Since that discovery, siRNA has provided a new tool for studying gene function in mammalian cells. siRNA also has a potential as a drug for intractable disease such as genetic disorder and cancer. siRNA also provided powerful new tools for biological research and drug discovery.

Several components that are related to the mechanism of siRNA-based RNAi have been reported as shown in Figure 1-1. In nature, when long dsRNA introduced into the cytoplasm is cleaved by the enzyme complex dicer to produce 21-23 nucleotide fragments with 2 nucleotide overhangs on the 3' ends siRNA. Dicer is one of the RNase III type enzymes [27-32]. Then, Argonaute-2 (AGO2) in ribonucleoprotein complex RISC (RNA induced silencing complex) will employ antisense strand (asRNA) in either endogenous siRNA or synthetic siRNA and package asRNA to form activated RISC, while sense-strand in siRNA (ssRNA) will degrade. The asRNA in activated RISC binds to its complementary sequence in mRNA and cleave the mRNA [33,34]. AGO2 is a main catalytic compound in RISC and act as a slicer that cleaves the target mRNA [35].

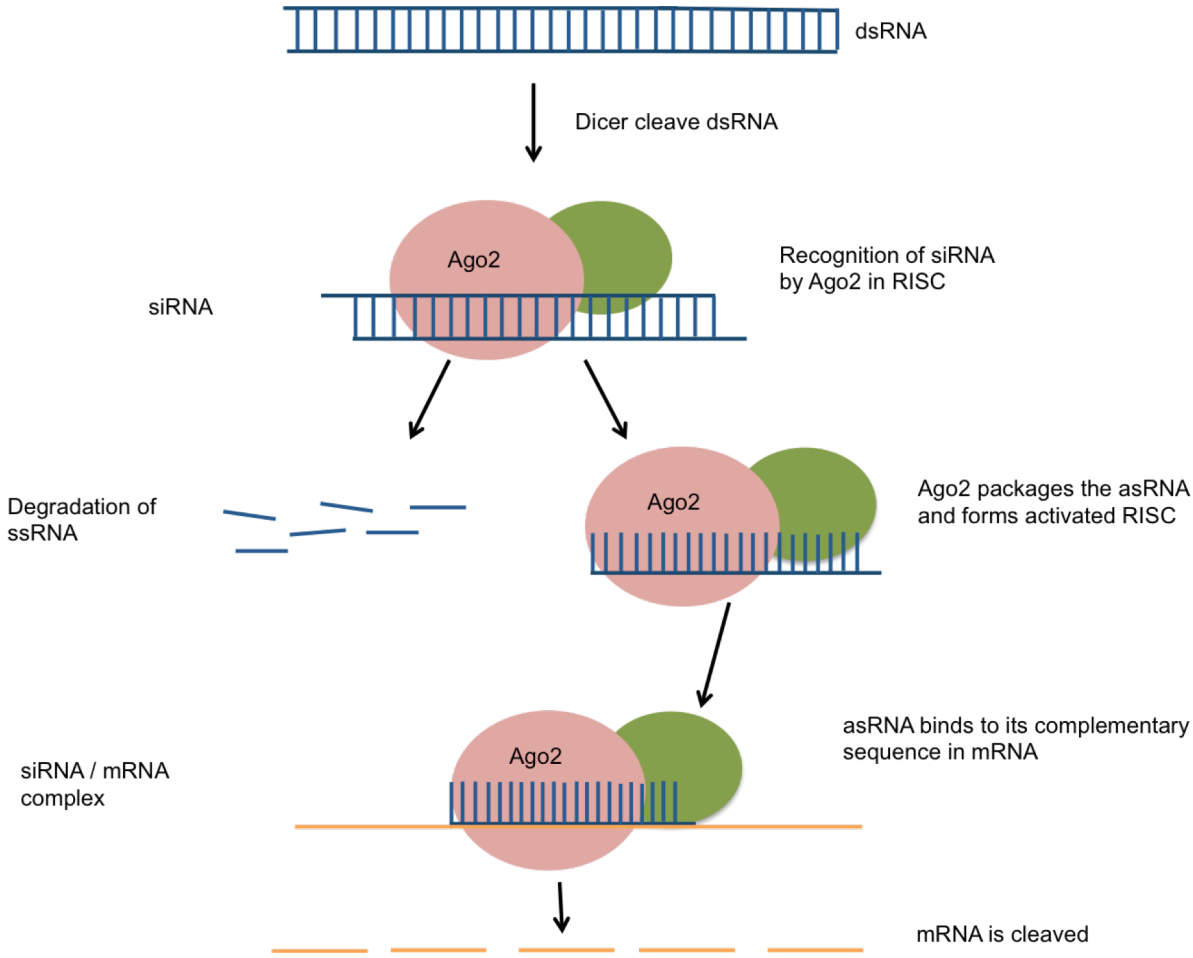

Figure 1-1. Mechanism of RNA interference by siRNA in the cytoplasm cell.

1.3. siRNA and its barriers for therapeutics agent

siRNA has generated a great number of attention as a research tool and a therapeutic agent. siRNA is a large water soluble polyanionic macromolecules possessing molecular weight around 13 kDa and the average size of an siRNA molecule is below than 6 nm length and 2.3 nm width [6]. In general, siRNA structure comprises of two RNA strands, i.e., an antisense strand (guide strand) and a sense strand (passenger strand). Both strands of siRNA have their 5'- and 3' ends. Usually, siRNA is 19-23 base-pair (bp) in length (Figure 1-2). siRNA forms a right-handed and tightly packed A-form helix with deep and narrow major grooves, which is a main character for RNA to trigger the gene silencing. The A-form helix structure could be

important in RNAi mechanism at two steps, i.e., at RISC formation and the loading of the guide strand [6].

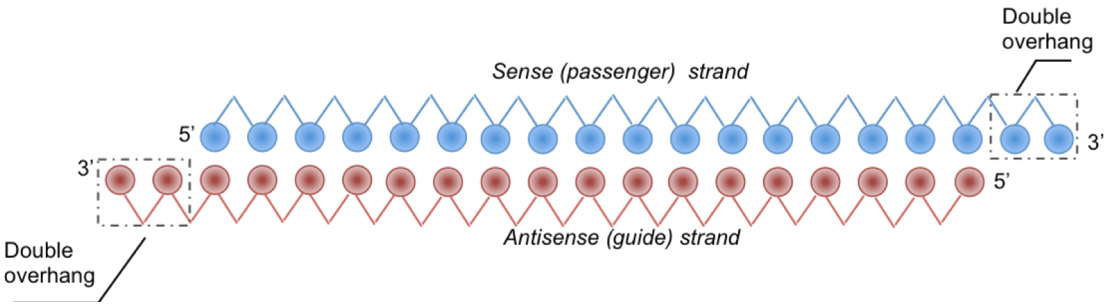

Figure 1-2. Structure of siRNA. siRNA consists of sense (passenger) strand and antisense (guide) strand with 3' double nucleotide overhangs on each strand. [6]

siRNA faces several barriers along the pathway from administration to the body to the intracellular target site. In order to be used as a therapeutic agent, siRNA has to be stable in the environment to which it is exposed. However, after administrated, siRNA is susceptible to digestion by RNases and also can easily be degraded in human plasma. Therefore, siRNA has a short half-life of less than ~ 15 min in physiological condition [37-39].

In addition, siRNA has the potential to induce the innate immune system [12, 40, 41]. The interaction between siRNA and the immune system are complex. In brief, the process of immunological recognition and response to siRNA is governed by the innate immune system. Innate immune responses are characterized by an induction of small signaling molecules called cytokines, including interleukins, type I interferons, and tumor necrosis factor- α. The induction of innate immune response by siRNA is dependent on several factors such as the siRNA sequence and structure, the material used to construct delivery carrier of siRNA, and cell type. The interaction between siRNA and innate immune response system are complex. In general, innate immune response is triggered by two common siRNA–recognition receptors, i.e., toll-like receptors (TLRs) and cytoplasmic receptors such as RIG-1 and PKR.

TLR family is responsible for the detection of various pathogen-associated molecules, and among them, TLR3, TLR7 and/or TLR8 are common to siRNA. TLR3 responds to double-stranded RNA (dsRNA), which, in human, it expresses in endosomes and on the cell surface of selected cell population. Meanwhile, TLR7 and TLR8 are located in the intracellular vesicles, including endosomes, lysosomes and endoplasmic reticulum, important in responding to single-strand RNA (ssRNA) in a sequence-specific manner. In addition, PKR, a protein kinase, which is one of the cytoplasmic receptors, responds to dsRNA, and siRNA would inhibit the protein translation and an interferon response when activated. On the other hand, RIG-1 would trigger interferon response in the presence of various forms of siRNA. For example, RIG-1 has been shown to bind to ssRNA and dsRNA containing uncapped 5'-triphosphate group resulting in an interferon-mediated immune response. Nevertheless, it is also known that nucleotide structure would affect activation of the innate immune response system as some studies had established to modify the 2' group on the ribose ring of the RNA backbone could reduce the innate immune response [42-47].

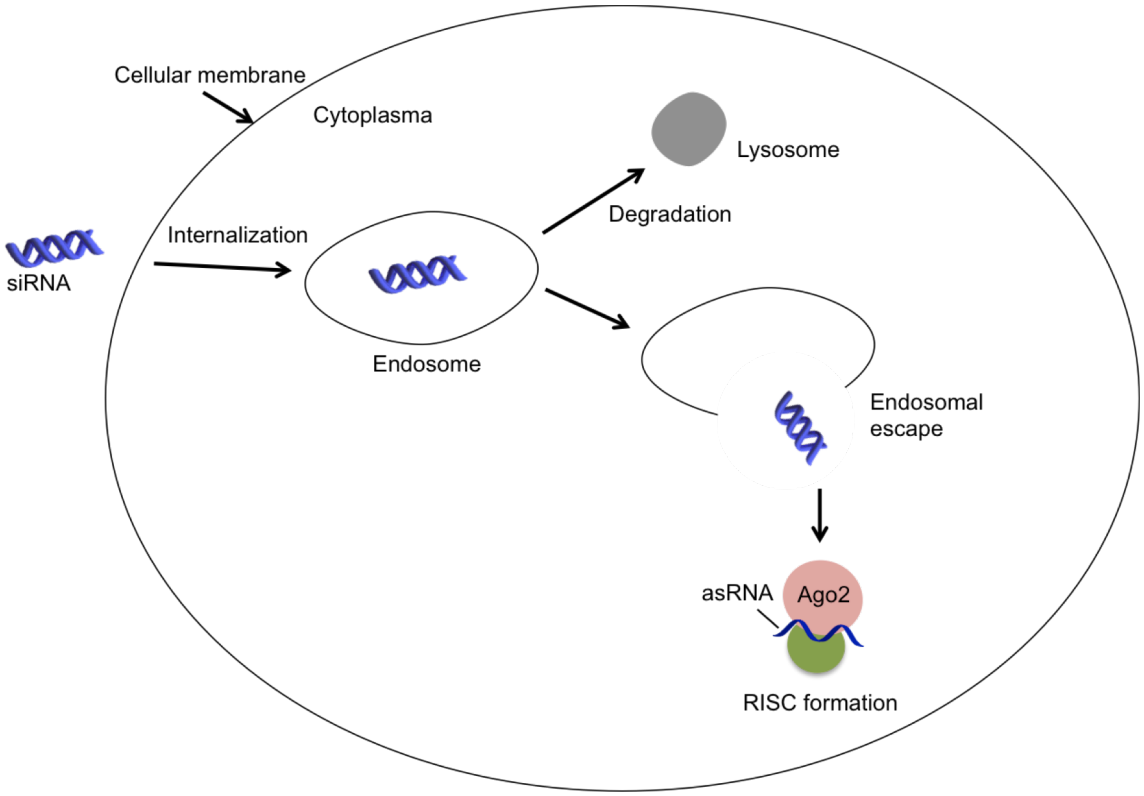

Figure 1-3. Illustration for internalization, endosome escape and RISC formation of siRNA at the cellular level

The last, but the most challenging barrier is the delivery of siRNA to the targeted site. In particular, at the cellular level, siRNA needs to cross the cytoplasmic membrane, escape from endosome, and be recognized by Ago2 in RISC in the cytosol (Figure 1-3). However, siRNA is a large hydrophilic and polyanionic molecule, and therefore, siRNA has a difficulty to penetrate cytoplasmic membrane due to the electrostatic repulsion between cellular membrane and siRNA. Cellular membrane has glycocalix [48]. Glycocalix contains anionic polysaccharide, for example, heparin, heparan sulfate, hyaluronic acid, and etc. Because of the anionic characteristic of siRNA molecule, siRNA has a difficulty to cross the cell membrane through passive diffusion, and thus, it will be taken up into the cell through endocytosis by the assistance with delivery carriers. It is reported that, almost 95% of siRNA internalizations are through endocytosis [49].

Moreover, once siRNA cross the cellular membrane through endocytosis, siRNA has to escape from the endosome, and have to be recognized by Ago2 protein in RISC to initiate RNAi process. It is known that, the endosome and/or lysosome compartment in the cell is in acidic environment and in order to avoid lysosomal degradation, siRNA must escape from endosome into the cytosol. In this regard, the endosomal escape is a major barrier for an efficient gene silencing. In addition, the recognition to the gene silencing protein in the cytosol, where siRNA associate with the RNAi machinery, is also another challenging matters for an efficient gene silencing.

1.4. Chemical modification of siRNA and siRNA delivery

In order to improve the safety of potential RNAi-based therapeutics as well as to realize it as an outstanding candidate for future clinical use, many researchers have attempted to overcome the barriers, such as poor stability, activation of immune response and inefficient cellular uptake. The chemical modifications of siRNA structure and the suitable design of delivery materials for siRNA are common approaches, i.e., chemically modified siRNA structure and the delivery materials of siRNA could provide an ideal opportunity to modify current treatment in a substantial way.

It is known that siRNA has poor RNase resistance both in ex vivo or in vivo. The catalytic mechanism of RNases involves the interaction between the ribose 2'-OH and phosphate groups of the RNA molecule, and thus, the modification of these groups are the key points for the increasing the stability of siRNA as well as enhancing the nuclease resistance. For example, the modification of 2'-*O*-methyl (2' OMe) and 2'-deoxy-2'-fluoro (2'F) had been demonstrated to show the increase of siRNA stability [6, 9, 49, 50]. Also, 2'-*O*-methyl modifications of siRNA can also reduced the off-target effect without loss the silencing ability of intended target gene [51].

Moreover, siRNA is a hybridized product of sense strand and antisense strand, and thus, there are four ends in siRNA structure, which could potentially be conjugation sites for designing siRNA-conjugates. Indeed, many researchers designed siRNA-conjugates for utilizing in drug delivery system. Those siRNA-conjugates not only could improve the inherent ability, but also could provide entirely new functions for siRNA. For example, lipid modification for improved cellular uptake (Figure 1-4a), ligand molecule modification for target specificity (Figure 1-4b), and PEGylation for tolerance against enzyme (Figure 1-4c), [52-56].

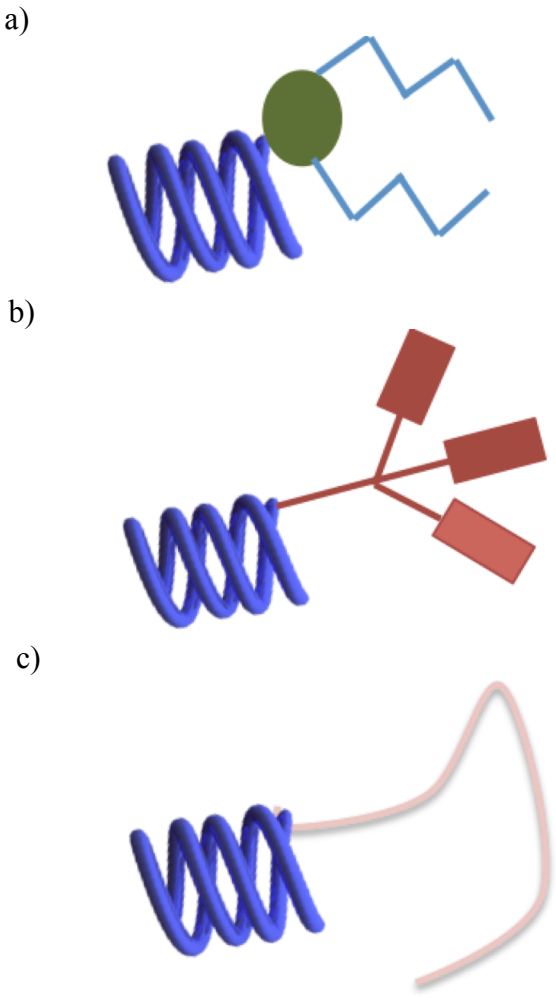

Figure 1-4. Examples of siRNA-conjugates. a) lipid-conjugated siRNA, b) ligand-conjugated siRNA and c) PEG-conjugated siRNA.

Furthermore, in order to activate the RNAi pathway, siRNA must be delivered to the target cells and be incorporated into RNAi machinery. Various types of carrier materials, including lipids, polymers, and inorganic nanoparticles, have been designed for use as the delivery carriers of siRNA [12, 49, 57-59]. Those carrier materials were sophisticatedly designed and decorated with several functionalities. For example, in order to initiate gene silencing at the target site, those carriers were often prepared with ligand molecules, such as tumor-targeted cyclic RGD peptide and folate, and liver targeted galactose and cholesterol [16, 54, 60, 61].

In particular, polyion complexes (PIC) are one of the promising nucleic acids carriers, i.e., it is formed from negative charge of nucleic acids and oppositely charged polycations. PIC has been widely studied as a carrier because the polycations could be chemically designed in a variety of modifications [62-66]. The utilization of PIC as a nucleic acid carriers not only protected nucleic acid from enzymatic degradation but also showed enhanced cellular uptake [66]. Moreover, in order to obtain a stable PIC, much efforts have been devoted to design of the polycations as well as employed chemically modified siRNA structure as a part of PIC, such as, PEG-siRNA, sticky-siRNA and poly-siRNA [67-71]. In addition, Kataoka and co-workers demonstrated siRNA-grafted at backbone of poly(aspartic acid) [PAsp] derivative through a disulfide linkage formed not only more stable PIC with inherent gene silencing ability than those formed from mono-siRNA, but also showed negligible immunogenicity [72].

In addition, another approach to achieve an efficient delivery of siRNA to the appropriate target cell, a carrier called siRNA Dynamic PolyConjugate (DPC) was successfully developed by Rozema et al. for the delivery of siRNA to hepatocytes both in vitro and in vivo. siRNA was conjugated to the endosomolytic amphiphilic poly (vinyl ether) to enhance endosomal escape after endocytosis. The poly(butyl amino vinyl ether) (PBAVE) was decorated with a bifunctional maleimide linkage to reversibly attach the shielding PEG and the *n*-

acetylgalactosamine ligand to enhance hepatocyte specific targeting. siRNA was attached to PBAVE through a reversible disulfide linkage, resulting an effective to knockdown two endogenous gene in liver, i.e., apoB-1 and apoB-2 with negligible immunogenicity [73].

1.5. Stimuli-responsive polymer in drug delivery system study.

Stimuli-responsive polymer is called 'smart' polymer because of its unique property, i.e., it can change the structure depending on the environment they are in. The development of 'smart' polymeric system has attracted a great deal of attention due to its versatile ability of reversibly altering of their properties on receiving external stimuli, and thus, enormous research has highlighted potential applications of stimuli-responsive polymers in the biomedical field, especially in the drug delivery, cell culture surface, and diagnostics [74, 75]. The triggers in biomedical study for stimuli-responsive polymers can be divided into exogenous and endogenous triggers. Temperature, magnetic field, ultrasound and light are among the exogenous triggers. On the other hand, pH gradient, redox-potential and enzyme concentrations are endogenous triggers [76, 77].

pH-responsive polymers are polymers containing ionizable groups of a weak acid such as carboxylic acid or a weak base such as amino group. It is known that pH-responsive polymer having phase transition, i.e., for acidic polymers at high pH, polymer will swell due to negatively charged polymer, and however, at low pH polymers collapse their structure to become unswollen. The opposite phase transition behavior for basic polymers, due to the ionization of the basic groups will increase when decreasing the pH. Numerous pH-responsive polymeric systems have been investigated for applications in biomedical areas, such as, site-specific targeting, tumor-specific delivery and sensors [76-78]. The examples of pH-responsive acidic polymer are poly(acrylic acid) (PAA), and poly(methacrylic acid) (PMAA) [79]. Polysulfonamide derivatives of *p*-aminobenzenesulfonamide is another weak

acidic pH-responsive polymer having pKa varies from 3 to 11, which are influenced by the nature of the substituent R on the nitrogen (Figure 1-5) [80]. On the other hand, the examples of basic pH-responsive polymer are poly (dimethylaminoethyl methacrylate) (PDMAEMA), poly (ethylenimine) (PEI) and chitosan [81].

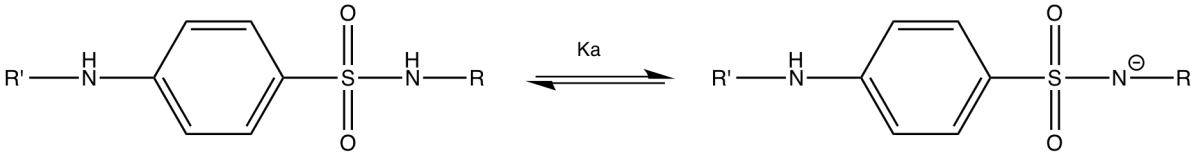

R = electron withdrawing or donating group
R' = polymerizable group or polymer (R' =H: sulfonamide)

Figure 1-5. Chemical structure of *p*-aminobenzenesulfonamide.

It is also known that at the cellular level, glutathione (GSH) is a tripeptide found at approximately 2-10 mM in the cytosol than at the extracellular milieu (2 – 20 μM) [82]. Thus, redox potential is also one of the most studied stimuli and has widely been investigated for developing redox-responsive materials. For example, disulfide group is one of the redox-responsive moieties. Disulfides will be cleaved into thiol groups in environment that contains reducing reagents, including GSH. Moreover, the resulting thiol group can reversibly form disulfide bonds upon oxidation [82,83] Based on the reversible characteristic of thiol-disulfide chemistry, thiol groups and disulfide can be introduced into polymers either at the polymer backbone or the crosslinkers in order to design redox-responsive polymers.

1.6. Thermoresponsive polymer

Thermoresponsive polymers that undergo phase transition behavior in response to the exogenous stimuli have attracted a great number of attentions for various biotechnology application fields including drug delivery, tissue engineering [74-78]. In general, thermoresponsive polymer solutions have an upper critical solution temperature (UCST) or a lower critical solution temperature (LCST). The polymer solutions possessing UCST behavior show one polymer phase above UCST, and phase separation appears below UCST [84]. Meanwhile, for polymer having LCST behavior, polymer solution shows only one phase solution below LCST, however, above LCST, polymer solution shows a phase separation. During phase separation for both UCST and LCST, polymer chains undergo a transition from open coil form to globule form. The globule form of polymers will aggregate and thereby causes the turbidity. I mention a brief introduction about the basic mechanism of thermosensitivity. The phenomenon of thermosensitivity is based on thermodynamic rules using Gibbs equation is $\Delta G = \Delta H - T\Delta S$ (G = Gibbs free energy, H = enthalpy and S:

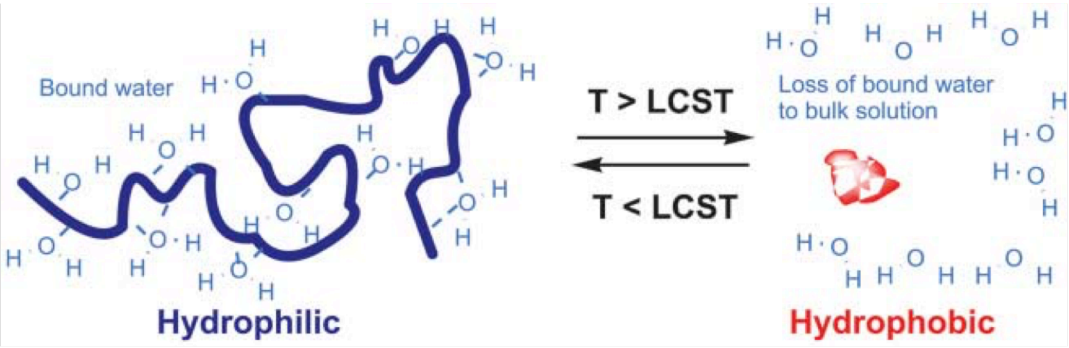

Figure 1-6. Schematic of LCST polymer in response to the temperature [85].

entropy), in which a system is more stable at its lower Gibbs free energy level. In particular, in LCST type polymer, below LCST, Gibbs free energy is negative, leading to dissolution of

polymer in water. At this time, water molecule form a thin layer surrounding the hydrophilic part of the polymer, and it is called “hydrophilic hydration”. At the same time, rigid hydrogen bond network of water also can be found around hydrophobic part of the polymer, and this is called “hydrophobic hydration”. When temperature of the polymer solution increases, entropy of the system increases. As the results, hydrogen bond between water and polymer breaks, leading to release of bounded water from polymer. When the dense and highly ordered water bound around the polymer releases into bulk water solution, polymer forms a hydrophobic globule. At this time, the entropy of water around polymer increases, due to the release from polymer, which increases the overall entropy in the system, resulting in the aggregate formation of the polymer (Figure 1-6) [86, 87].

To date, various LCST type thermoresponsive polymers have been reported such as poly(*N*-vinylcaprolactam) (PNVC), and poly (ethylene oxide)-poly(propylene oxide)-poly (ethylene oxide) (PEO-PPO-PEO) [76, 77]. Among thermoresponsive polymers, the most representative group of polymers showing LCST is the poly (*N*-substituted acrylamide) group, i.e., poly(*N,N’*-diethyl acrylamide) (PDEAAm) that shows LCST 26-35 °C [88], poly(dimethylaminoethyl methacrylate) (PDMAEMA) shows LCST close to 50 °C [89], and poly (*N*-isopropylacrylamide) (PNIPAAm) is the most investigated thermoresponsive polymer showing LSCT close to body temperature.

The controlled structure of PNIPAAm as illustrated in Figure 1-7 can be synthesized using

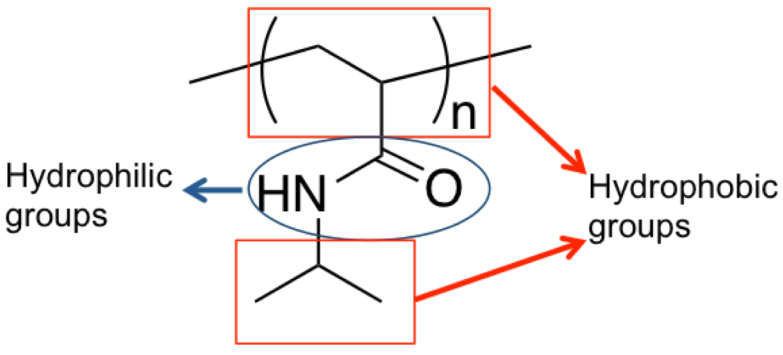

Figure 1-7. Chemical structure of poly (N-isopropyl acrylamide) (PNIPAAm)

commercial *N*-isopropylacrylamide monomer through living radical polymerization [90]. PNIPAAm having both hydrophobic and hydrophilic group in its repeating unit and it will be as a water soluble state below LCST, and change into insoluble state above LCST. The LCST of PNIPAAm exists between ca. 32 °C and 35 °C in water [91, 92]. Fujishige and co-workers investigated the structural changes of PNIPAAm while changing the solution temperature [92]. They reported that PNIPAAm undergoes a coil to globule transition upon heating the aqueous solution. Below LCST, PNIPAAm would be as a coil form due to strong hydrogen bonding of amide groups with water. However, above LCST, PNIPAAm collapsed their structure into globule form due to strong hydrophobic interaction between hydrophobic backbone and isopropyl groups [93, 94]. PNIPAAm has been utilized in multiple purposes and in very diverse forms including single chains, macroscopic gels, latexes, thin films, membranes, coatings, and fibers.

In addition, the LCST of PNIPAAm also can be tuned by incorporating hydrophilic or hydrophobic comonomers by copolymerization with NIPAAM through radical polymerization. In this regard, the introduction of hydrophilic comonomers to the PNIPAAm raises the LCST, and decreases the LCST of PNIPAAm by copolymerized with hydrophobic comonomers [95, 96]. Interestingly, the copolymerization of PNIPAAm with hydrophilic comonomers, such as *N,N*- dimethyl acrylamide (DMAA) produced polymer having the phase transition temperature near to the body temperature [97]. Moreover, it is reported that PNIPAAm is noncytotoxic at certain concentration and thus it could be applied in biological use [98]. Therefore, PNIPAAm-based thermoresponsive polymers have widely been used in biomedical field.

Furthermore, other stimuli-responsive behaviors also can be combined with PNIPAAm to prepare a variety of smart materials. pH-responsive monomers can also be combined through the copolymerization with NIPAAm. For example, carboxylic acid monomers, such as acrylic

acid (AA) or methacrylic acid (MAA), have been copolymerized with NIPAAm to form random copolymers having both temperature and pH-responsive characters [99, 100]. Kanazawa et al. copolymerized pH-responsive acrylic monomer, sulfamethazineacrylamide monomer with PNIPAAm through living radical polymerization, and eventually, the product has a potential to be applied for the selective imaging in the acidic tumor microenvironments [101].

Nevertheless, PNIPAAm-based polymer also can be conjugated with biomolecule. Hoffman, Stayton and co-workers have extensively investigated the conjugation of PNIPAAm-based polymer with biomolecule [85, 102, 103]. Their development of conjugating PNIPAAm with biomolecules has been applied for various application fields such as affinity separations, biosensors, diagnostics, and enzyme process. In particular, their PNIPAAm-conjugated biomolecules have been prepared by site-specific conjugation of the polymer to genetically engineered specific amino acid sites. For example, maleimide-terminated PNIPAAm was reacted with a streptavidin mutant engineered to contain thiol functionality through introduction of a cysteine residue close to the biotin recognition site. Biotin bound strongly to the polymer-streptavidin conjugate below 32 °C, but, no binding was observed above LCST due to the collapse of the polymer structure, thereby, inhibit the recognition site. The switching behavior showed that the regulation of binding was due to the reversible coil-globule transition of the attached PNIPAAm [102]. This approach has proved to be very versatile and provide a new platform for utilizing PNIPAAm in controlling the bioactivity of conjugated biomolecule.

1.7. Objective and strategy of the present study

Since the discovery of RNAi in mammalian cells, tremendous researches have been devoted to the design of siRNA-based therapeutics due to its strong gene silencing ability. For example, researchers chemically modified siRNA structure such as siRNA conjugation with polymeric molecule [12-16]. The siRNA conjugation with polymeric molecule enhanced inherent gene silencing ability as well as endowed new functions i.e., tolerance against enzymatic degradation, improved cellular uptake and target specificity. However, the

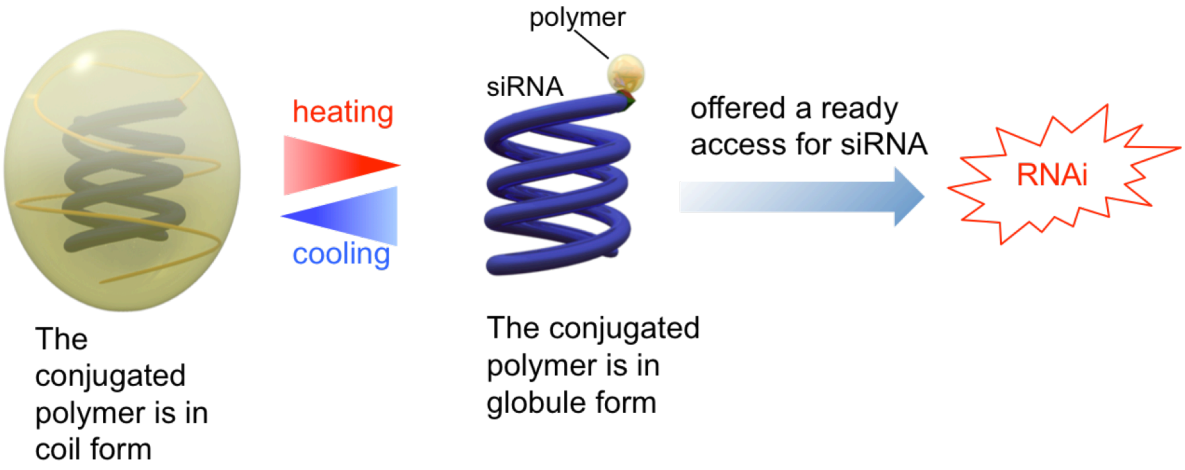

Figure 1-7. Illustration for the present study. A coil form of PNIPAAm would inhibit siRNA activity due to steric hindrance effect, however, a globule form of PNIPAAm allows for a ready access of siRNA to the gene silencing related proteins, and thus, leads to artificial gene silencing effect.

conjugation with polymeric molecule often underwent weak recognition with gene silencing related protein, and thus, compromised gene silencing ability was induced due to the steric hindrance effect of the conjugated polymer. It should be noted that the recognition of siRNA by the gene silencing protein is a main trigger to initiate the gene silencing pathway. Therefore, the steric hindrance effect of the conjugated polymeric molecule motivated me to

develop a new scientific methodology for an artificial control of siRNA bioactivity. In order to realize the artificial control of siRNA bioactivity, I selected a stimuli-responsive polymer to be conjugated with an siRNA molecule. It is known that stimuli-responsive polymer would undergo size changes in response to the external environment [75-78]. In this regard, I conjugated a stimuli-responsive polymer that undergoes coil-globule transition behavior to an siRNA molecule. The coil form of the conjugated polymer would inhibit the bioactivity of siRNA, and in contrast, the globule form of the conjugated polymer associated with the size changes would allow siRNA for a ready access to the gene silencing pathway, and leads to the efficient gene silencing ability (Figure 1-7). In order to demonstrate an artificial controlled gene silencing activity, I prepared PNIPAAm that linearly conjugated with siRNA molecule. PNIPAAm was selected in this study due to its coil-globule transition behavior and its LCST close to the body temperature. It is also known that the responsiveness of PNIPAAm is simple, i.e., it only responses to the temperature changes. Moreover, the coil-globule transition behavior of PNIPAAm has a potency to be applied as a switching device to the conjugated biomolecule [102]

For the future perspective, based on coil-globule transition behavior of conjugated polymer, I envisage to develop polymers having responsiveness to biological stimuli such as pH, redox potential and enzyme and to employ those polymers for an artificial control of therapeutic application. Moreover, in order to realize the therapeutics to the specific targeted site, the combination with the developed delivery carriers, such as liposome and micelle, is one of the future plans.

1.8. The outline of the thesis

My research is focusing on the development of a new scientific methodology for an artificial control of gene silencing activity in the cells without adverse effect. In chapter 2, I discussed the molecular design of siRNA-conjugated polymer with coil-globule transition behavior (PNIPAAm-siRNA) as shown in Figure 1-8a. In order to design polymer with controlled structure, i.e., polymer having a narrow molecular weight distribution and desired

a)

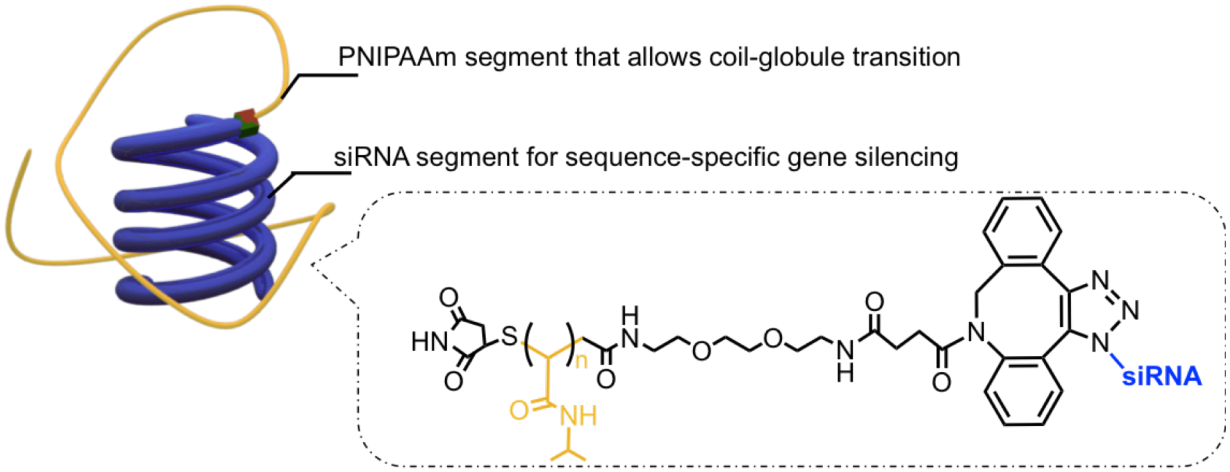

b)

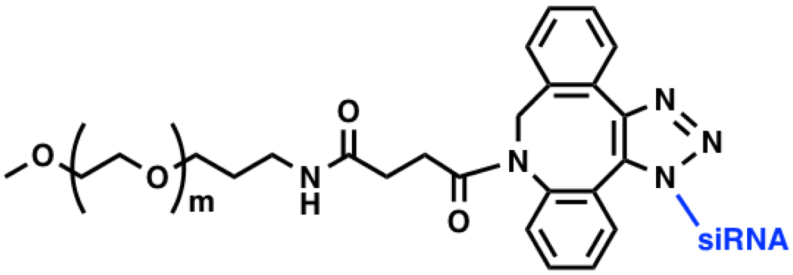

Figure 1-8. The molecular design of thermoresponsive polymer, PNIPAAm-conjugated with siRNA (PNIPAAm-siRNA) (a) and non-thermoresponsive polymer, poly(ethylene glycol)-conjugated with siRNA (PEG-siRNA) (b).

molecular weight, I prepared PNIPAAm through living radical polymerization technique. I developed PNIPAAm through both atom transfer radical polymerization (ATRP) and reversible addition-fragmentation chain-transfer polymerization (RAFT) technique. However, the development of PNIPAAm through ATRP technique faced an inter-cyclization between a

halide group at the terminus with an amide group at the side chain of PNIPAAm, leading to production of PNIPAAm with a weak livingness at the terminus. Therefore, I designed PNIPAAm through RAFT polymerization technique, and eventually, a monodisperse molecular weight distribution of PNIPAAm with targeted molecular weight was successfully synthesized. Subsequently, I modified the end groups of PNIPAAm in order to circumvent unexpected reaction in the cells and to prepare PNIPAAm for the conjugation with siRNA through click chemistry reaction. As a control system, I utilized non-thermoresponsive poly (ethylene glycol) (PEG). Both PNIPAAm-siRNA and PEG-siRNA were successfully developed through click chemistry reaction (Figure 1-8b).

In the chapter 3, I discussed about the physicochemical properties of obtained PNIPAAm-siRNA. Herein, I investigate the optical transmittance of PNIPAAm before the conjugation with siRNA through UV-vis measurement. Obtained PNIPAAm exhibited LCST around 33 °C to 35 °C, which were close to the LCST of reported PNIPAAm. Moreover, through the light scattering analysis while changing the temperature, the critical aggregation temperature of PNIPAAm was observed at 35 °C upon heating the PNIPAAm-siRNA solution, indicating PNIPAAm-segment undergoes LCST-related behavior even after the conjugation with an siRNA molecule. I also evaluated the hydrodynamic diameter of PNIPAAm-siRNA at diluted concentration, which is similar to the concentration of siRNA after entering the cells, using fluorescence correlation spectroscopy (FCS), and as a result, the decreasing of size in diameter for PNIPAAm-siRNA after changing the temperature from room temperature to 37 °C was demonstrated. These results indicate that PNIPAAm-segment undergoes a coil-globule transition behavior even in the presence at the vicinal of siRNA molecule, and strongly suggesting that the conjugated PNIPAAm segment has a high potential that allows thermoresponsive siRNA exposure and associate siRNA recruitment into gene silencing pathway.

In chapter 4, I investigated the biological properties of developed PNIPAAm-siRNA for gene silencing analysis human cervical cancer cells stably expressing luciferase (HeLa-Luc), and as a result, PNIPAAm-siRNA was close to that of unconjugated siRNA above LCST (~80%), while it was dramatically decreased to ~20 % below LCST. Meanwhile, the treatment with PEG-siRNA showed inefficient gene silencing at both temperatures (~10%), suggesting the steric hindrance effect of PEG segment inhibits siRNA activity. In addition, I investigated the recognition efficacy between Ago2 in RISC complexes with PNIPAAm-siRNA through immunoprecipitation method. The results indicate that the coil-globule transition behavior of PNIPAAm controlled the recognition siRNA with gene silencing related proteins in the cells. Through all of the results, I strongly confirmed that using coil-globule transition behavior of the conjugated polymer could artificially control the bioactivity of siRNA. The achievements described in this thesis will contribute to the realization in artificially controlled the therapeutic application with minimal side effect.

1.9. References

[1] Fire, A., Xu, S., Montgomery, M. K., Kostas, S. A., Driver, S. E., Mello, C. C. Potent and specific genetic interference by double-stranded RNA in Caenorhabditis elegans *Nature* **1998**, 391, 806-811.

[2] Zamore, P. D., Tuschl, T., Sharp, P. A., Bartel, D. P. RNAi: double-stranded RNA directs the ATP-dependent cleavage of mRNA at 21 to 23 nucleotide intervals. *Cell* **2000**, 101, 25-33.

[3] Elbashir, S. M., Harborth, J., Lendeckel, W., Yalcin, A., Weber, K., Tuschl, T. Duplexes of 21- nucleotide RNAs mediate RNA interference in cultured mammalian cells mediated. *Nature*. **2001**, 494-498.

[4] Parker, J. S., Roe, S. M., Barford, D. Structural insights into mRNA recognition from a PIWI domain-siRNA guide complex *Nature* **2005**, 434, 663-666.

[5] de Fougerolles, A., Vornlocher, H., Maraganore, J., and Lieberman, J. Interfering with disease: a progress report on siRNA-based therapeutics. *Nat. Rev. Drug Discov.* **2007**, *6*, 443–453.

[6] Rana, T. M. (2007) Illuminating the silence: understanding the structure and function of small RNAs. *Nat. Rev. Mol. Cell Biol.* **2007**,*8*, 23–36

[7] He, S., Zhang, D., Cheng, F., Gong, F., Guo, Y. Applications of RNA Interference in Cancer Therapeutics as a Powerful Tool for Suppressing Gene Expression. *Mol. Biol. Rep*. **2009**, *36*, 2153-2163.

[8] Dykxhoorn, D. M. RNA Interferences as an Anticancer Therapy: a Patent Perspective Expert Opin. Ther. Pat. **2009**, *19*, 475-491.

[9] Wittrup, A., and Lieberman, J. Knocking down disease: a progress report on siRNA therapeutics. *Nat. Rev. Genet.* **2015**, *16*, 543–552

[10] Buckingham, S. D., Esmaeili, B., Wood, M., and Sattelle, D. B. RNA interference: From model organisms towards therapy for neural and neuromuscular disorders. *Hum. Mol. Genet.* **2004**, *13*, 275–288.

[11] Kole, R., Krainer, A. R., and Altman, S. RNA therapeutics: Beyond RNA interference and antisense oligonucleotides. *Nat. Rev. Drug Discov.* **2012**, *11*, 125–140.

[12] Kanasty, R., Dorkin, J. R., Vegas, A., and Anderson, D. Delivery materials for siRNA therapeutics. *Nat. Mater.* **2013**, *12*, 967–977.

[13] Mura, S., Nicolas, J., and Couvreur, P. Stimuli-responsive nanocarriers for drug delivery. *Nat. Mater.* **2013**, *12*, 991–1003.

[14] Lee, S. J., Son, S., Yhee, J. Y., Choi, K., Kwon, I. C., Kim, S. H., and Kim, K. (2013) Structural modification of siRNA for efficient gene silencing. *Biotechnol. Adv.* **2013***, 31, 491-*

503.

[15] Liu, H., Li, Y., Mozhi, A., Zhang, L., Liu, Y., Xu, X., Xing, J., Liang, X., Ma, G., Yang, J., and Zhang, X. SiRNA-phospholipid conjugates for gene and drug delivery in cancer treatment. *Biomaterials* **2014**, *35*, 6519–6533.

[16] Nair, J. K., Willoughby, J. L. S., Chan, A., Charisse, K., Alam, M. R., Wang, Q., Hoekstra, M., Kandasamy, P., Kelin, A. V., Milstein, S., Taneja, N., Oshea, J., Shaikh, S., Zhang, L., Van Der Sluis, R. J., Jung, M. E., Akinc, A., Hutabarat, R., Kuchimanchi, S., Fitzgerald, K., Zimmermann, T., Van Berkel, T. J. C., Maier, M. A., Rajeev, K. G., and Manoharan, M. Multivalent N -acetylgalactosamine-conjugated siRNA localizes in hepatocytes and elicits robust RNAi-mediated gene silencing. *J. Am. Chem. Soc.* **2014**, *136*, 16958–16961.

[17] Akerman, M. E., Chan, W. C. W., Laakkonen, P., Bhatia, S. N., and Ruoslahti, E. Nanocrystal targeting in vivo. *Proc. Natl. Acad. Sci. U. S. A.* **2002**, *99*, 12617–12621.

[18] Gangar, A., Fegan, A., Kumarapperuma, S. C., and Wagner, C. R. Programmable self-assembly of antibody-oligonucleotide conjugates as small molecule and protein carriers. *J. Am. Chem. Soc.* **2012**, *134*, 2895–2897.

[19] Jung, S., Lee, S. H., Mok, H., Chung, H. J., and Park, T. G. Gene silencing ef fi ciency of siRNA-PEG conjugates : Effect of PEGylation site and PEG molecular weight. *J. Control. Release* **2010**, *144*, 306–313.

[20] Takemoto, H., Miyata, K., Hattori, S., Ishii, T., Suma, T., Uchida, S., Nishiyama, N., and Kataoka, K. Acidic pH-responsive siRNA conjugate for reversible carrier stability and accelerated endosomal escape with reduced IFN??-associated immune response. *Angew. Chemie - Int. Ed.* 2013, *52*, 6218–6221.

[21] Iversen, F., Yang, C., Dagnæs-Hansen, F., Schaffert, D. H., Kjems, J., and Gao, S. Optimized siRNA-PEG conjugates for extended blood circulation and reduced urine excretion in mice. *Theranostics* **2013**, *3*, 201–209

[22] Zamecnik, P. C., and Stephenson, M. L. Inhibition of Rous sarcoma viral RNA translation by a specific oligodeoxynucleotide. *Proc. Natl Acad. Sci. USA* **1978**, 75, 285-288.

[23] Zamecnik, P. C., Stephenson, M. L. Inhibition of Rous sarcoma virus replication and cell transformation by a specific oligodeoxynucleotide. *Proc. Natl Acad. Sci. USA* **1978** 75, 280-284.

[24] Napoli, C., Lemieux, C., Jorgensen, R. Introduction of a chimeric chalcone synthase gene into petunia results in reversible co-suppresion of homologous genes in trans. *The Plant Cell*, **1990**, 2, 279-289.

[25] Hammond, S. M., Bernstein, E., Beach, D., Hannon, G. J. An RNA-directed nuclease mediates post-transcritional gene silencing in Drosophilla cells. Nature **2000**, 404, 293-296.

[26] Zamore, P. D., Tuschl, T., Sharp, P. A., Bartel, D. P. RNAi: double-stranded RNA directs the ATP-dependent cleavage of mRNA at 21 to 23 nucleotide intervals. *Cell* **2000**, 101, 25-33.

[27] Bernstein, E., Caudy, A. A., Hammond, S. M., Hannon, G. J. Role for a bidentate ribonuclease in the initiation step of RNA interference. *Nature* **2001**, 404, 363-366.

[28] Lee, Y. S., Nakahara, K., Pham, J. W., Kim, K., He, Z., Sontheimer, E. J., and Carthew, R. W. Distinct roles for Drosophila Dicer-1 and Dicer-2 in the siRNA/miRNA silencing pathways. *Cell* **2004**, *117*, 69–81.

[29] Tijsterman, M., and Plasterk, R. H. A. Dicers at RISC: The mechanism of RNAi. *Cell* **2004**, *117*, 1–3.

[30] Filippov, V., Solovyev, V., Filippova, M., Gill, S. S., A novel type of RNase III family proteins in eukaryotes, *Gene* **2000**, 245, 1, 213-221.

[31] Kolb, F. A., Zhang, H., Jaronczyk, K., Tahbaz, N., Hobman, T. C., and Filipowicz, W. Human Dicer: Purification, Properties, and Interaction with PAZ PIWI Domain Proteins, in *Methods in Enzymology*, 2005, 316–336.

[32] Cook, A, Conti, E., Dicer measures up, *Nat. Struct. Mol. Biol*. **2006**, 13, 3, 190-192.

[33] Nicholson, A. W., Function, mechanism and regulation of bacterial ribonucleases, *FEMS Microbiol. Rev.* **1999** 23, 3, 371–390.

[34] Rivas, F. B., Tolia, N. H., Song, J. J., Aragon, J. P., Liu, J., Hannon, G. J., Joshua-Tor, L. Purified argonaute2 and an siRNA form recombinant human RISC. *Nature Structural and Molecular Biology* **2005**, 12(4), 340-349

[35] Hammond, S. M., Boettcher, S., Caudy, A. A., Kobayashi, R., Hannon, G. J. Argonaute2, a link between genetic and biochemical analyses of RNAi *Science* **2001**, 293, 1146-1150.

[36] Gallas, A., Alexander, C., Davies, M. C., Puri, S., and Allen, S. Chemistry and formulations for siRNA therapeutics. *Chem. Soc. Rev.* **2013**, *42*, 7983–97.

[37] Bartlett, D. W., and Davis, M. E. Physicochemical and Biological Characterization of Targeted, Nucleic Acid-Containing Nanoparticles. *Bioconjug. Chem.* **2007**, *18*, 456–468.

[38] Aliabadi, H. M., Landry, B., Sun, C., Tang, T., and Uludag, H. Supramolecular assemblies in functional siRNA delivery: Where do we stand? *Biomaterials* **2012**, *33*, 2546–2569.

[39] Xu, X., Ho, W., Zhang, X., Bertrand, N., Farokhzad, O. Cancer nanomedicine: From targeted delivery to combination therapy Trends Mol. Med. **2015**, 21, 223-232.

[40] Robbins, M., Judge, A., and MacLachlan, I. siRNA and Innate Immunity. *Oligonucleotides* **2009**, *19*, 89–102.

[41] Lennox, K. A., and Behlke, M. A. Chemical modification and design of anti-miRNA oligonucleotides. *Gene Ther.* **2011**, *18*, 1111–1120.

[42] Grivennikov, S. I., Greten, F. R., and Karin, M. Immunity, Inflammation, and Cancer. *Cell* 2010, *140*, 883–899.

[43] Takeuchi, O., and Akira, S. Pattern Recognition Receptors and Inflammation. *Cell* **2010**, *140*, 805–820.

[44] Wang, J., Lu, Z., Wientjes, M. G., and Au, J. L.-S. Delivery of siRNA Therapeutics: Barriers and Carriers. *AAPS J.* **2010**, *12*, 492–503

[45] Sioud, M. Recent advances in small interfering RNA sensing by the immune system. *New Biotech*. **2010**, 27, 3, 236-242.

[46] Judge, A., Maclachlan, I. Overcoming the innate immune response to small interfering RNA Human Gene Therapy **2008**, 19, 111-124.

[47] Rehman, K., and Akash, M. S. H. Mechanisms of inflammatory responses and development of insulin resistance: how are they interlinked? *J. Biomed. Sci.* **2016**, *23*, 87, 1-18.

[48] Palte, M. J., and Raines, R. T. Interaction of nucleic acids with the glycocalyx. *J. Am. Chem. Soc.* **2012**, *134*, 6218–6223.

[49] Bitsikas, V., Corrêa, I. R., and Nichols, B. J. Clathrin-independent pathways do not contribute significantly to endocytic flux. *Elife* **2014**, *3*, 1-26.

[50] Dominska, M., and Dykxhoorn, D. M. Breaking down the barriers: siRNA delivery and endosome escape. *J. Cell Sci.* **2010**, *123*, 1183–9.

[51] Gallas, A., Alexander, C., Davies, M. C., Puri, S., and Allen, S. Chemistry and formulations for siRNA therapeutics. *Chem. Soc. Rev.* **2013**, *42*, 7983–97.

[52] Ui-Tei, K., Naito, Y., Zenno, S., Nishi, K., Yamato, K., Takahashi, F., Juni, A., and Saigo, K. Functional dissection of siRNA sequence by systematic DNA substitution:

Modified siRNA with a DNA seed arm is a powerful tool for mammalian gene silencing with significantly reduced off-target effect. *Nucleic Acids Res.* **2008**, *36*, 2136–2151.

[53] Choung, S., Kim, Y. J., Kim, S., Park, H. O., and Choi, Y. C. Chemical modification of siRNAs to improve serum stability without loss of efficacy. *Biochem. Biophys. Res. Commun.* **2006**, *342*, 919–927

[54] Nishina, K., Unno, T., Uno, Y., Kubodera, T., Kanouchi, T., Mizusawa, H., and Yokota, T. Efficient in vivo delivery of siRNA to the liver by conjugation of alpha-tocopherol. *Mol. Ther.* **2008**, *16*, 734–740

[55] Alam, M. R., Ming, X., Fisher, M., Lackey, J. G., Rajeev, K. G., Manoharan, M., and Juliano, R. L. Multivalent cyclic RGD conjugates for targeted delivery of small interfering RNA. *Bioconjug. Chem.* **2011**, *22*, 1673–1681

[56] Lee, S. H., Mok, H., and Park, T. G. Di- and Triblock siRNA-PEG Copolymers: PEG Density Effect of Polyelectrolyte Complexes on Cellular Uptake and Gene Silencing Efficiency. *Macromol. Biosci.* **2011**, *11*, 410–418

[57] Liu, X., Wang, W., Samarsky, D., Liu, L., Xu, Q., Zhang, W., Zhu, G., Wu, P., Zuo, X., Deng, H., Zhang, J., Wu, Z., Chen, X., Zhao, L., Qiu, Z., Zhang, Z., Zeng, Q., Yang, W., Zhang, B., and Ji, A. Tumor-targeted in vivo gene silencing via systemic delivery of cRGD-conjugated siRNA. *Nucleic Acids Res.* **2014**, *42*, 11805–11817.

[58] Lee, S. H., Bae, K. H., Kim, S. H., Lee, K. R., and Park, T. G. Amine-functionalized gold nanoparticles as non-cytotoxic and efficient intracellular siRNA delivery carriers. *Int. J. Pharm.* **2008**, *364*, 94–101.

[59] Meng, H., Liong, M., Xia, T., Li, Z., Ji, Z., Zink, J. I., and Nel, A. E. Engineered design of mesoporous silica nanoparticles to deliver doxorubicin and p-glycoprotein siRNA to overcome drug resistance in a cancer cell line. *ACS Nano* **2010**, *4*, 4539–4550.

[60] Park, D. H., Cho, J., Kwon, O. J., Yun, C. O., and Choy, J. H. Biodegradable Inorganic

Nanovector: Passive versus Active Tumor Targeting in siRNA Transportation. *Angew. Chemie - Int. Ed.* **2016**,*791*, 4582–4586.

[61] Wolfrum, C., Shi, S., Jayaprakash, K. N., Jayaraman, M., Wang, G., Pandey, R. K., Rajeev, K. G., Nakayama, T., Charrise, K., Ndungo, E. M., Zimmermann, T., Koteliansky, V., Manoharan, M., and Stoffel, M. Mechanisms and optimization of in vivo delivery of lipophilic siRNAs. *Nat. Biotechnol.* **2007**, *25*, 1149–1157.

[62] Yu, B., Zhao, X., Lee, L. J., and Lee, R. J. Targeted delivery systems for oligonucleotide therapeutics. *AAPS J.* **2009**, *11*, 195–203.

[63] Kakizawa, Y., and Kataoka, K. Block copolymer micelles for delivery of gene and related compounds. *Adv. Drug Deliv. Rev.* **2002**, *54*, 203–222.

[64] Cabral, H., Nishiyama, N., and Kataoka, K. Supramolecular nanodevices: From design validation to theranostic nanomedicine. *Acc. Chem. Res.* **2001**, *44*, 999–1008

[65] Nishiyama, N., Morimoto, Y., Jang, W. D., and Kataoka, K. Design and development of dendrimer photosensitizer-incorporated polymeric micelles for enhanced photodynamic therapy. *Adv. Drug Deliv. Rev.* **2009**, *61*, 327–338.

[66] Nakai, K., Nishiuchi, M., Inoue, M., Ishihara, K., Sanada, Y., Sakurai, K., and Yusa, S. I. Preparation and characterization of polyion complex micelles with phosphobetaine shells. *Langmuir* **2013**, *29*, 9651–9661.

[67] Nishiyama, N., and Kataoka, K. Current state, achievements, and future prospects of polymeric micelles as nanocarriers for drug and gene delivery. *Pharmacol. Ther.* **2006**, *112*, 630–48.

[68] Oishi, M., Nagasaki, Y., Itaka, K., Nishiyama, N., and Kataoka, K. Lactosylated Poly(ethylene glycol)-siRNA Conjugate through Acid-Labile β-Thiopropionate Linkage to Construct pH-Sensitive Polyion Complex Micelles Achieving Enhanced Gene Silencing in Hepatoma Cells. *J. Am. Chem. Soc.* **2005**, *127*, 1624–1625.

[69] Stuart, M. A. C., Huck, W. T. S., Genzer, J., Müller, M., Ober, C., Stamm, M., Sukhorukov, G. B., Szleifer, I., Tsukruk, V. V., Urban, M., Winnik, F., Zauscher, S., Luzinov, I., and Minko, S. Emerging applications of stimuli-responsive polymer materials. *Nat. Mater.* **2010**, *9*, 101–113.

[70] Kong, W. H., Bae, K. H., Hong, C. A., Lee, Y., Hahn, S. K., and Park, T. G. Multimerized siRNA Cross-linked by Gold Nanoparticles. *Bioconjug. Chem.* **2011**, *22*, 1962–1969.

[71] Oh, Y. K., and Park, T. G. siRNA delivery systems for cancer treatment. *Adv. Drug Deliv. Rev.* **2009**, *61*, 850–862

[72] Lee, S. J., Son, S., Yhee, J. Y., Choi, K., Kwon, I. C., Kim, S. H., and Kim, K. Structural modification of siRNA for efficient gene silencing. *Biotechnol. Adv.* **2013**, *31*, 491–503.

[73] Takemoto, H., Ishii, A., Miyata, K., Nakanishi, M., Oba, M., Ishii, T., Yamasaki, Y., Nishiyama, N., and Kataoka, K. Polyion complex stability and gene silencing efficiency with a siRNA-grafted polymer delivery system. *Biomaterials* **2010**, *31*, 8097–8105.

[74] Rozema, D. B., Lewis, D. L., Wakefield, D. H., Wong, S. C., Klein, J. J., Roesch, P. L., Bertin, S. L., Reppen, T. W., Chu, Q., Blokhin, A. V, Hagstrom, J. E., and Wolff, J. A. Dynamic PolyConjugates for targeted in vivo delivery of siRNA to hepatocytes. *Proc. Natl. Acad. Sci. U. S. A.* **2007**, *104*, 12982–12987.

[75] Gil, E. S., and Hudson, S. M. Stimuli-reponsive polymers and their bioconjugates. *Prog. Polym. Sci.* **2004**, *29*, 1173–1222.

[76] Roy, D., Cambre, J. N., and Sumerlin, B. S. Future perspectives and recent advances in stimuli-responsive materials. *Prog. Polym. Sci.* **2010**, *35*, 278–301

[77] Cabane, E., Zhang, X., Langowska, K., Palivan, C. G., and Meier, W. (2012) Stimuli-responsive polymers and their applications in nanomedicine. *Biointerphases*. 2012, 7, 9, 1-4.

[78] Lu, Y., Sun, W., and Gu, Z. Stimuli-responsive nanomaterials for therapeutic protein

delivery. *J. Control. Release* **2014**, *194*, 1–19.

[79] Yin, X., Hoffman, A. S., and Stayton, P. S. (2006) Poly(N -isopropylacrylamide- c o -propylacrylic acid) Copolymers That Respond Sharply to Temperature and pH. *Biomacromolecules 7*, 1381–1385.

[80] Park, S. Y., and Bae, Y. H. Novel pH-sensitive polymers containing sulfonamide groups. *Macromol. Rapid Commun.* **1999**, *20*, 269–273.

[81] Yoshida, T., Lai, T. C., Kwon, G. S., and Sako, K. pH- and ion-sensitive polymers for drug delivery. *Expert Opin. Drug Deliv.* **2013**, *10*, 1497–1513.

[82] Takemoto, H., Miyata, K., Nishiyama, N., and Kataoka, K. Bioresponsive Polymer-Based Nucleic Acid Carriers. *Adv. Genet.* **2014***, 88, 289-323.*

[83] Lushchak, V. I., and Lushchak, V. I. Glutathione Homeostasis and Functions: Potential Targets for Medical Interventions. *J. Amino Acids* **2012**, *2012*, 1–26

[84] Zhang, Q., Tosi, F., Ü‡düler, S., Maji, S., and Hoogenboom, R. Tuning the LCST and UCST thermoresponsive behavior of poly(N,N-dimethylaminoethyl methacrylate) by electrostatic interactions with trivalent metal hexacyano anions and copolymerization. *Macromol. Rapid Commun.* **2015**, *36*, 633–639.

[85] C.de Las Heras Alarcon, C., Pennadam, S., and Alexander, C. Stimuli responsive polymers for biomedical applications. *Chem. Soc. Rev.* 2005, *34*, 276–285.

[86] Bischofberger, I., Calzolari, D. C. E., De Los Rios, P., Jelezarov, I., and Trappe, V. Hydrophobic hydration of poly-N-isopropyl acrylamide: a matter of the mean energetic state of water. *Sci. Rep.* **2014**, *4*, 4377.

[87] Shiraga, K., Naito, H., Suzuki, T., Kondo, N., and Ogawa, Y. Hydration and hydrogen bond network of water during the Coil-to-Globule transition in poly(N -isopropylacrylamide) aqueous solution at cloud point temperature. *J. Phys. Chem. B* **2015**, *119*, 5576–5587.

[88] Idziak, I., Avoce, D., Lessard, D., Gravel, D., and Zhu, X. X. Thermosensitivity of

Aqueous Solutions of Poly(N,N -diethylacrylamide). *Macromolecules* **1999**, *32*, 1260–1263

[89] Takeda, N., Nakamura, E., Yokoyama, M., and Okano, T. Temperature-responsive polymeric carriers incorporating hydrophobic monomers for effective transfection in small doses. *J. Control. Release* **2004**, *95*, 343–355.

[90] Masci, G., Giacomelli, L., and Crescenzi, V. Atom Transfer Radical Polymerization of N-Isopropylacrylamide. *Macromol. Rapid Commun.* **2005**, *25*, 559–564.

[91] Schild, H. G. POLY (N-ISOPROPYLACRYLAMIDE): EXPERIMENT , THEORY AND APPLICATION *Prog. Polym. Sci.* **1992**, *17*, 163–249.

[92] Fujishige, S., Kubota, K., Ando, I. Phase transition of aqueous solutions of poly (*N*-isopropylacrylamide) and poly (*N*-isopropylmethacrylamide) *J. Phys. Chem*. **1989**, 93, 3311-3313.

[93] Graziano, G. On the temperature-induced coil to globule transition of poly- N -isopropylacrylamide in dilute aqueous solutions **2000**, *27*, 89–97.

[94] Jeong, B., and Gutowska, A. Lessons from nature: stimuli-responsive polymers and their biomedical applications. *Trends Biotechnol.* **2002**, *20*, 305–311

[95] Xia, Y., Burke, N. A. D., and Stöver, H. D. H. End group effect on the thermal response of narrow-disperse poly(N-isopropylacrylamide) prepared by atom transfer radical polymerization. *Macromolecules* 2006, *39*, 2275–2283.

[96] Duan, Q., Narumi, A., Miura, Y., Shen, X., Sato, S.-I., Satoh, T., and Kakuchi, T. Thermoresponsive property controlled by end-functionalization of poly(N-isopropylacrylamide) with phenyl, biphenyl, and triphenyl groups. *Polym. J.* **2006**, *38*, 306–310

[97] Akimoto, J., Nakayama, M., Sakai, K., and Okano, T. Temperature-induced intracellular uptake of thermoresponsive polymeric micelles. *Biomacromolecules* 2009, *10*, 1331–1336

[98] Patenaude, M., and Hoare, T. Injectable, Degradable Thermoresponsive Poly(N -

isopropylacrylamide) Hydrogels. *ACS Macro Lett.* **2012**, *1*, 409–4

[99] Cheng, R., Meng, F., Ma, S., Xu, H., Liu, H., Jing, X., and Zhong, Z. Reduction and temperature dual-responsive crosslinked polymersomes for targeted intracellular protein delivery. *J. Mater. Chem.* **2011**, *21*, 19013.

[100] Gao, X., Cao, Y., Song, X., Zhang, Z., Xiao, C., He, C., and Chen, X. pH- and thermo-responsive poly(N-isopropylacrylamide-co-acrylic acid derivative) copolymers and hydrogels with LCST dependent on pH and alkyl side groups. *J. Mater. Chem. B* **2013**, *1*, 5578.

[101] Hiruta, Y., Funatsu, T., Matsuura, M., Wang, J., Ayano, E., and Kanazawa, H. PH/temperature-responsive fluorescence polymer probe with pH-controlled cellular uptake. *Sensors Actuators, B Chem.* **2015**, *207*, 724–731.

[102] Stayton, P. S., Shimoboji, T., Long, C., Chilkoti, A., Chen, G., Harris, J. M., Hoffman, A. S. Control of protein-ligand recognition using a stimuli-responsive polymer Nature **1995**, *378*, 472-474.

[103] Bulmus, V., Ding, Z., Long, C. J., Stayton, P. S., and Hoffman, A. S. Site-specific polymer - Streptavidin bioconjugate for pH-controlled binding and triggered release of biotin. *Bioconjug. Chem.* **2000**, *11*, 78–83.

Chapter 2. Synthesis of thermoresponsive polymer conjugated with an siRNA molecule (PNIPAAm-siRNA)

2.1. Abstract

In this chapter, the preparation of a new class of polymer having phase transition behavior, poly(*N*-isopropylacrylamide) (PNIPAAm)-conjugated with siRNA, is discussed. To obtain PNIPAAm with controlled molecular weight and a narrow molecular weight distribution, NIPAAm was polymerized through two major techniques of living radical polymerization: atom transfers radical polymerization (ATRP) and reversible addition-fragmentation chain-transfer agent (RAFT) polymerization. The polymerization procedure of PNIPAAm through both living radical polymerizations was discussed. In addition, the end group modification of PNIPAAm was investigated, and eventually, thermoresponsive polymer, PNIPAAm-conjugated with siRNA was successfully synthesized through Copper-free Click Chemistry. Furthermore, in the present study, in a similar manner, non-thermoresponsive polymer, poly (ethylene glycol) (PEG) conjugated-siRNA series were also successfully synthesized as a control system.

2.2. Introduction

Stimuli-responsive polymers have become very popular due to their interesting property, i.e., they induce phase transition behavior responding to the environment they are in. In general, stimuli-responsive polymers can be divided into three major classes, i.e., chemical, physical, and biological stimuli-responsive polymers. pH-responsive polymer such as poly (ethylene imine) (PEI) one of the chemically-dependent stimuli polymers has widely been used as a vector for gene delivery [1-3]. Biological stimuli-dependent polymers such as polymer contain disulfide linker, i.e., glutathione-responsive polymer has been also intensely studied in biotechnology applications field [4,5].

PNIPAAm is one of the most promising candidates in thermoresponsive polymer and has been extensively studied in various applications due to its property, which can change the

structure from coil to globule below and above LCST. The controlled structure of PNIPAAm can be prepared through living radical polymerization. Living radical polymerization enables precisely controlled polymer structures, including molecular weight, molecular weight distribution, end-group functionality and composition. In living radical polymerization, the active polymer chain end is in free radical form and the occurrence of premature termination of the active polymer chain end can be minimized.

Living radical polymerization is divided into three major fundamental techniques: atom transfer radical polymerization (ATRP), reversible addition/fragmentation chain transfer polymerization (RAFT) and nitroxide-mediated polymerization (NMP). In this chapter, the preparation of PNIPAAm was investigated through two major fundamental techniques, i.e., atom transfer radical polymerization (ATRP) and reversible addition/ fragmentation chain transfer polymerization (RAFT). In general, ATRP process uses complexes of transition metals in conjunction with alkyl halides, while in RAFT process uses dithioesters chain transfer agent (CTA) and a free radical initiator for the polymerization in a controlled manner [6, 7-9].

ATRP has proven to be versatile and effective in providing a controlled polymerization environment for a wide range of vinyl monomers, such as styrene, (meth)acrylates, and dienes [10, 12]. The ATRP equilibrium can be proposed in Scheme 2-1. Briefly, in an ATRP, alkyl halide initiator/dormant species (R-X) react with activators, the transition-metal complexes at low-oxidation state of Mt^n/L, to reversibly form propagating radical R* and deactivators, the transition-metal complexes at high-oxidation state of $X\text{-}Mt^{n+1}/L$ [610-12]. The illustration of ATRP equilibrium also can be explained in three situations: a polymer sitting dormant on the left side of the equilibrium, a polymer reacting with monomer on the right side of the equilibrium, and two radical end-groups combining to terminate and kill the reaction.

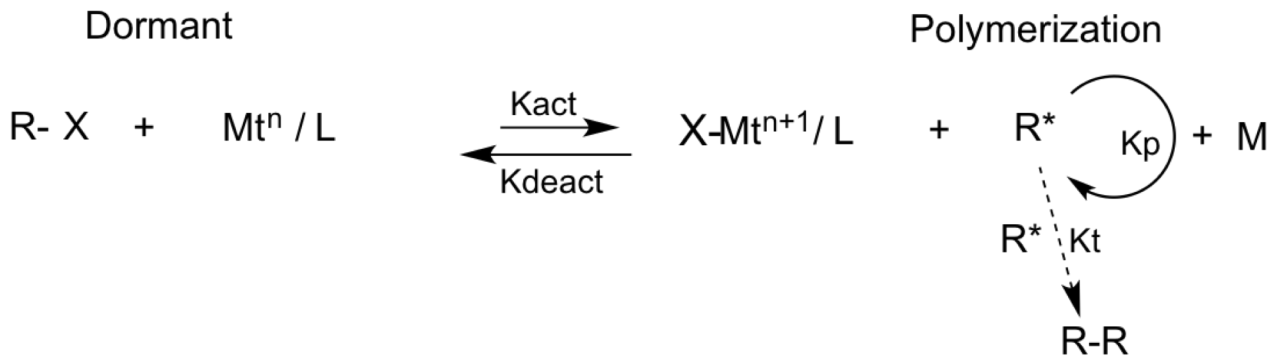

Scheme 2-1. Scheme of ATRP equilibrium. R-X represents alkyl halide initiator/dormant species, Mt^n/L for transition metal complexes with ligand (L), X-Mt^{n+1}/L for oxidized catalyst, R* for active initiator, M for monomer and R-R for terminated polymer. The reaction rates are labeled with K_x, where K_{act} is the rate of activation, K_{deact} is the rate of deactivation, K_p is the rate of monomer addition and K_t is the rate of termination.

In addition, ATRP is a catalytic process and only produces one radical upon activation. In ATRP, the reaction resides on the dormant side most of the time, thereby, minimizes two radical to exist near each other, and thus, minimizes the termination. Through these features, ATRP has emerged as a promising technique for the preparation of controlled polymer. Hence, in the present study, in order to obtain controlled PNIPAAm polymer, the polymerization of NIPAAm through ATRP technique was demonstrated using several approaches.

Furthermore, in the present study, PNIPAAm also was synthesized through RAFT polymerization technique. RAFT polymerization is another well-known technique in living radical polymerization and pioneered by CSIRO [6, 13]. The mechanism of RAFT polymerization can be described as illustrated in Scheme 2-2. In brief, the RAFT polymerization started when the free radical polymerization in the initiation step, followed by

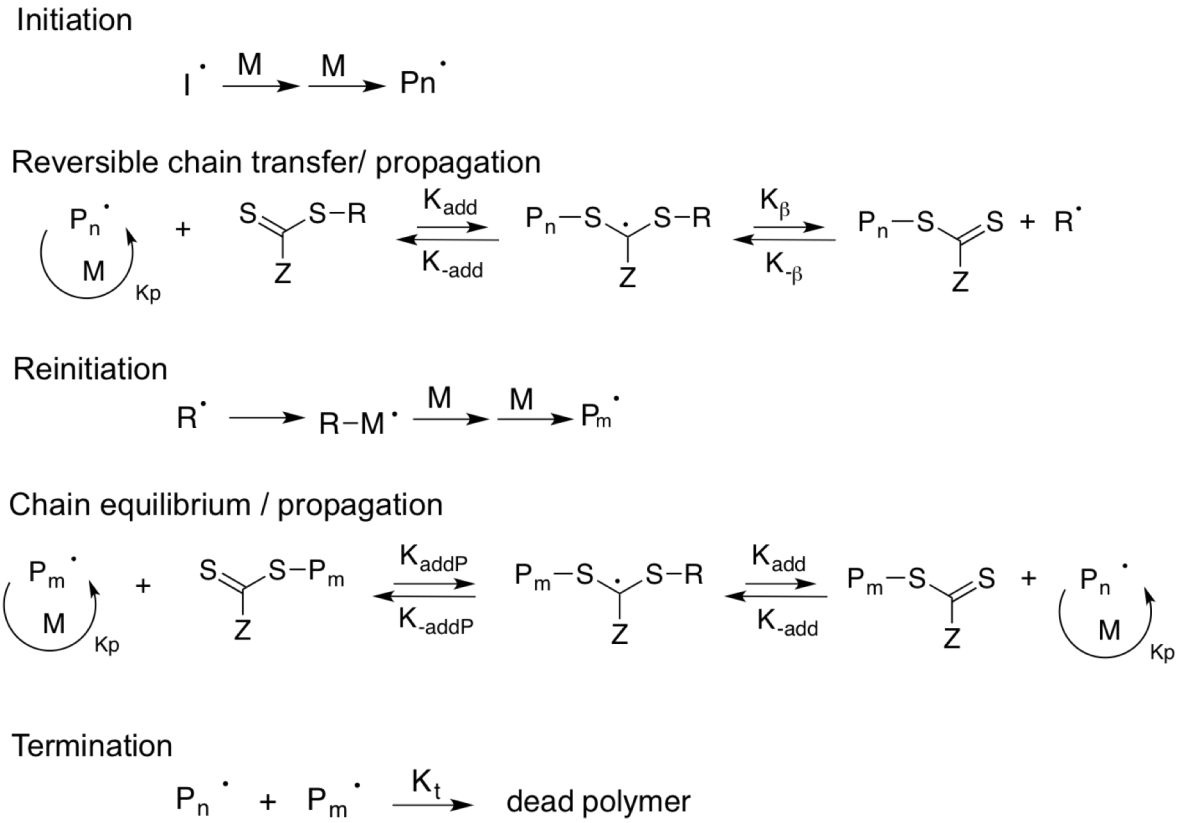

Scheme 2-2. Mechanism of RAFT polymerization.

the reversible addition of the radical onto the chain transfer agent (**1**) to form an intermediate radical (**2**), which can fragment to liberate a reinitiating group and form a new dormant chain (**3**), and subsequently, the new radical reinitiates polymerization by reaction on monomers. Following the re-initiation, polymer chains grow by adding monomer, and they rapidly exchange between existing growing radicals and the species capped with a thiocarbonylthio group. The rapid interchange in the chain-transfer step through the formation of intermediate

limits the termination reaction. The termination reactions still occur through combination or disproportionation mechanism, mainly due to the free radical introduced initially to initiate the polymerization.

Moreover, styrene derivatives, acrylate and acrylamide, as well as methacrylates and methacrylamides are among monomers that have been used in RAFT polymerization [13]. In addition, for an ideal RAFT process, the retention of the thiocarbonylthio groups in polymer, which derives from RAFT agent is important for the living character of RAFT polymerization as well as for end group modifications. Thus, the selection of the RAFT agent to the monomers is important in RAFT process, and in the present study, two types of radical initiators had been used for the RAFT polymerization of NIPAAm to obtain PNIPAAm with desired molecular weight.

Furthermore, in the present study, the conjugation between PNIPAAm and siRNA was prepared through Copper-free Click Chemistry reaction and utilizing a freeze-thaw cycles technique [14]. The gradual freezing of the PNIPAAm contains strained alkyne of DBCO group solution and azide-siRNA solution allows for the enrichment of the solute concentration, and thereby, the freeze-thaw treatment could facilitate the reaction. In a similar manner, PEG-siRNA was also synthesized. In summary, a series of thermoresponsive polymer-conjugated with siRNA, PNIPAAm-siRNA, with precisely controlled structure were successfully synthesized through living radical polymerization and Copper-free Click Chemistry reaction.

2.3. Materials

N-isopropylacrylamide (NIPAAm), tris[2-(dimethylamino)ethyl]amine (Me_6TREN), tributylphosphine (PBu_3), 1-(3-dimethylaminopropyl)-3-ethylcarbodiimide hydrochloride (EDC·HCl), *N*-hydroxybenzotriazole monohydrate (HOBt·H_2O), and 1,2-bis(2-

aminoethoxy)ethane were purchased from Tokyo Chemical Industry Co., Ltd. (Tokyo, Japan). NIPAAm was recrystallized for two times from *n*-hexane before use. CuCl, CuBr, 2-(dodecylthiocarbonothioyltho)-2-methylpropanoic acid (DDMAT) was purchased from Sigma Aldrich (St. Louis, MO, USA). 2,2'-Azobisisobutyronitrile (AIBN) and 2,2'-Azobis(4-methoxy-2-4-dimethylvaleronitrile) (V-70), dichloromethane, 1,4-dioxane, *N*,*N*-dimethylformamide (DMF), tetrahydrofuran (THF), diethyl ether, and triethylamine were purchased from Wako Pure Chemical Indusries, Ltd. (Osaka, Japan). AIBN was purified through precipitated into cold methanol for two times before use. 1,4- Dioxane and DMF were purified by distillation under reduced pressure before use. Series of α-methoxy-ω-amino-poly(ethylene glycol) (PEG-NH_2) were purchased from NOF Co., Ltd. (Tokyo, Japan). Dibenzocyclooctyne-*N*-hydroxysuccinimidyl (DBCO-NHS) ester was purchased from Click Chemistry Tools, Ltd. (Scottsdale, AZ). 4-(2-Hydroxyethyl)-1-piperazineethanesulfonic acid (HEPES) solution (1 M, pH 7.3) was purchased from AMRESCO Inc. (Solon, OH). Series of RNA were synthesized by Hokkaido System Science Co. Ltd. (Hokkaido, Japan). The RNA sequences are as follows:

siGL3 (azide-modified): 5'-(N_3-)-CUU ACG CUG AGU UCG AdTdT-3' (sense strand), 5'-UCG AAG UAG UCA GCG UAA GdTdT(-TAMRA)-3' (antisense strand).

siScramble (azide-modified and TAMRA-labeled) : 5'-(N_3-)- UUC UCC GAA CGU GUC ACG UdTdT-3' (sense strand), 5'-ACG UGA CAC GUU CGG AGA AdTdT-3' (antisense strand).

2.4. Experimental procedures

2.4.1. Synthesis of PNIPAAm through ATRP and end-chain modification

2.4.1.1. Synthesis of PNIPAAm-Br

The polymerization behavior of PNIPAAm was investigated using CuBr/Me_6TREN catalyst/ligand complex system as shown in Scheme 2-3. Briefly, NIPAAm (565 mg, 5

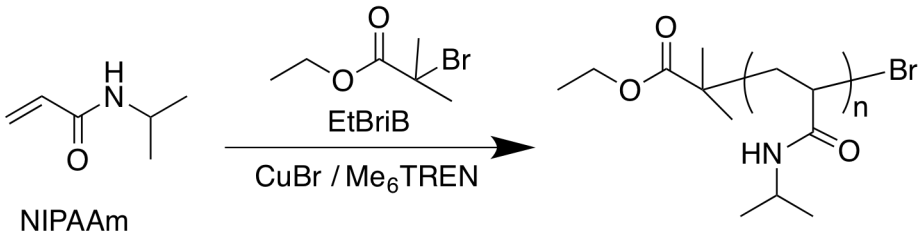

Scheme 2-3. Synthetic scheme of PNIPAAm-Br through ATRP using CuBr/Me_6TREN catalyst/ligand complex system.

mmol), CuBr (7.2 mg, 0.05 mmol) and Me_6TREN (13.6 μL, 0.05 mmol) were dissolved in isopropanol (5 mL) at room temperature for 10 minutes to form Copper (I) bromide/ tris[2-(dimethylamino)ethyl]amine (CuBr/Me_6TREN) complexes and to obtain a homogenous mixture under an argon atmosphere. The reaction solution was frozen and degassed three times via consecutive standard freeze-pump-thaw cycles. Then, the reaction solution was placed at room temperature. Then, ethyl-2-bromoisobutyrate (EtBriB) (7.3 μL, 0.05 mmol) was added under an argon atmosphere to begin the polymerization. The reaction solution was stirred for 24 h at room temperature, and subsequently, the reaction solution was exposed to air. The reaction solution was dialyzed against de-ionized water (molecular weight cut off: 3,500 da) and lyophilized to obtain bromide-terminated polymer, PNIPAAm-Br as white powder. The polymerization of PNIPAAm-Br was determined using matrix-assisted laser desorption/ionization mass spectrometry (MALDI-TOF MS) (ultrafleXtreme, Bruker Corporation). The target degree of polymerization (DPn) for PNIPAAm-Br was set for 100.

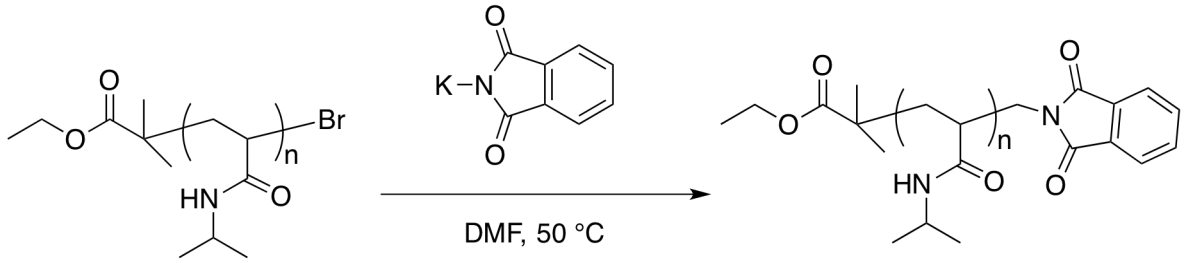

Scheme 2-4. Synthetic scheme of PNIPAAm-Phthalimide

2.4.1.2. The introduction of phthalimide group to PNIPAAm-Br

The synthesis followed Scheme 2-4. PNIPAAm-Br (27.9 mg, 13.53 μmol), potassium phthalimide (12.9 mg, 67.65 μmol) were dissolved in DMF (2 mL) at room temperature. Then, the reaction solution was stirred for 5 h at 50 °C. Subsequently, the reaction solution was dialyzed against de-ionized water (molecular weight cut off: 3,500 Da), followed by lyophilization to obtain white powder of polymer. The chemical structure of obtained white powder of polymer was characterized using proton nuclear magnetic resonance (^{1}H-NMR) (AVANCE III 400, Bruker Corporation) analysis in deuterated chloroform ($CDCl_3$) at room temperature.

2.4.1.3. Synthesis of PNIPAAm-Cl

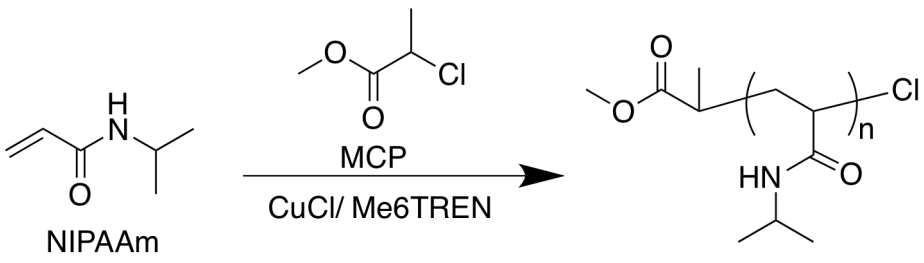

Scheme 2-5. Synthetic scheme of PNIPAAm-Cl using CuCl/Me_6TREN catalyst/ligand complex system

The synthesis of PNIPAAm-Cl using copper (I) chloride/ tris[2-(dimethylamino)ethyl]amine (CuCl/ Me_6TREN) catalyst/ligand complex system followed Scheme 2-5. NIPAAm (453 mg, 4 mmol), CuCl (3.9 mg, 0.04 mmol) and Me_6TREN (10.8 μL, 0.05 mmol) were dissolved in isopropanol (2 mL) at room temperature for 10 minutes to form CuCl/Me_6TREN complexes and to obtain a homogenous mixture under an argon atmosphere. The reaction solution was frozen and degassed three times via consecutive standard freeze-pump-thaw cycles. Then, the reaction solution was placed at room temperature. Then, methyl 2-chloropropionate (MCP) (4.56 μL, 0.04 mmol) was added under an argon atmosphere to begin the polymerization. The reaction solution was stirred for 24 h at room temperature, and subsequently, the reaction solution was exposed to air. The reaction solution was dialyzed against de-ionized water (molecular weight cut off: 3,500 da) and lyophilized to obtain chloride-terminated polymer, PNIPAAm-Cl as white powder. The polymerization of PNIPAAm-Cl was determined using MALDI-TOF MS (ultrafleXtreme, Bruker Corporation) (Data not shown). The target degree of polymerization was set for 100.

2.4.1.4. Synthesis of PNIPAAm-Cl in the presence of water

The synthesis followed Scheme 2-5. NIPAAm (453 mg, 4 mmol), CuCl (3.9 mg, 0.04 mmol) and Me_6TREN (10.8 μL, 0.05 mmol) were dissolved in mixed isopropanol and water (4/1) (v/v) at room temperature for 10 minutes to form CuCl/Me_6TREN complexes and to obtain a homogenous mixture under an argon atmosphere. The reaction solution was frozen and degassed three times via consecutive standard freeze-pump-thaw cycles. Then, the reaction solution was placed at room temperature. Then, MCP (4.56 μL, 0.04 mmol) was added under an argon atmosphere to begin the polymerization. The reaction solution was stirred for 24 h at room temperature, and subsequently, the reaction solution was exposed to air. The reaction solution was dialyzed against de-ionized water (molecular weight cut off:

3,500 da) and lyophilized to obtain chloride-terminated polymer, PNIPAAm-Cl as white powder. PNIPAAm-Cl was characterized using MALDI-TOF MS (ultrafleXtreme, Bruker Corporation). The target degree of polymerization was 100.

2.4.1.5. The introduction of phthalimide group into PNIPAAm-Cl

The synthesis followed Scheme 2-6. PNIPAAm-Cl (306 mg, 7.6 μmol), phthalimide potassium (142 mg, 76 μmol) were dissolved in DMF (4 mL). The reaction solution was

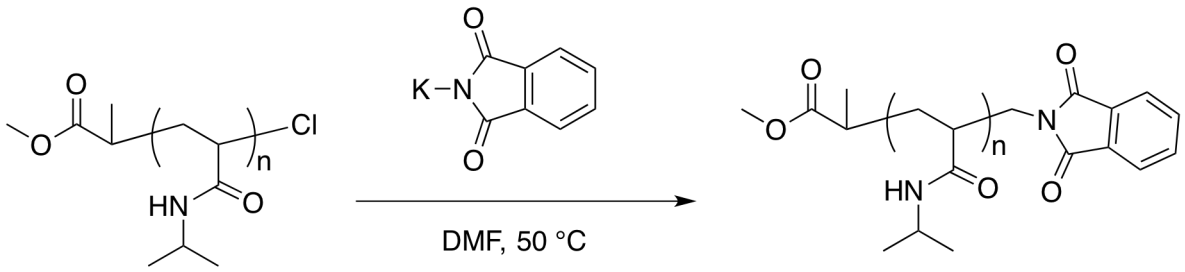

Scheme 2-6. Synthetic scheme of PNIPAAm-Phtalimide

stirred for 5 h at 50 °C, and subsequently dialyzed against de-ionized water (molecular weight cut off: 3,500 Da). Then, the dialyzed solution was lyophilized to obtain white powder of polymer. The chemical structure of obtained white powder of polymer was characterized using ^{1}H-NMR (AVANCE III 400, Bruker Corporation) analysis in $CDCl_3$ at room temperature.

2.4.2. Synthesis of PNIPAAm through RAFT polymerization and end-modification of PNIPAAm

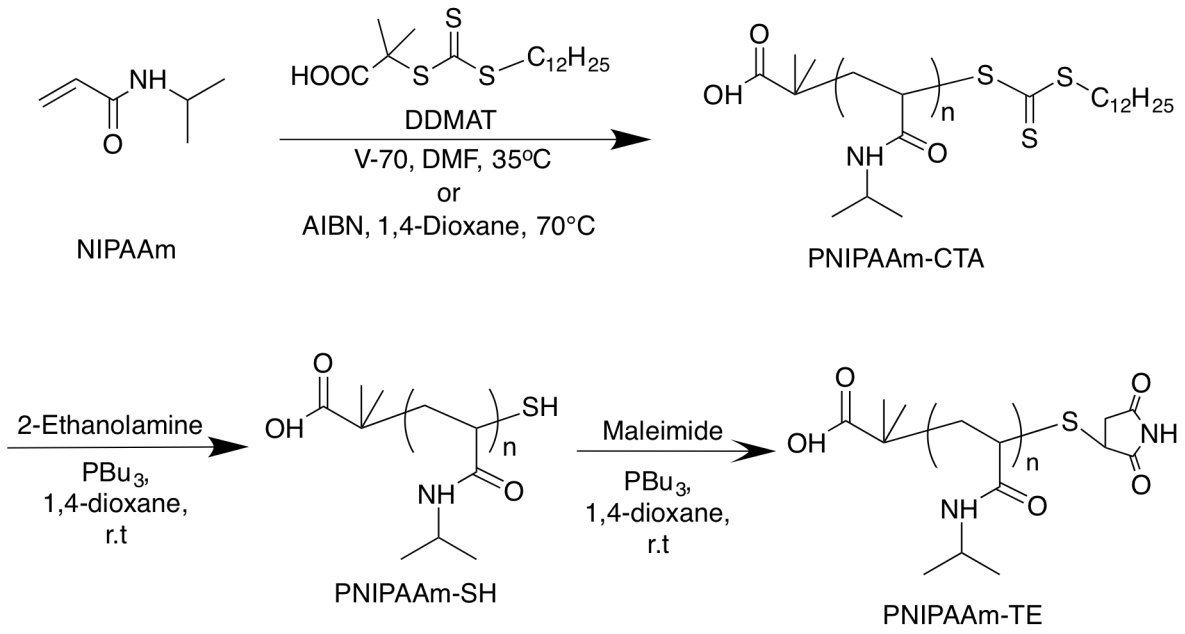

Scheme 2-7. Synthetic procedure of PNIPAAm-TE

2.4.2.1. Synthesis of PNIPAAm with trithiocarbonate terminus (PNIPAAm-CTA) for molecular weight 10,000 g/mol ($PNIPAAm_{10K}$ -CTA)

PNIPAAm was synthesized through RAFT polymerization method [15, 16], as shown in Scheme 2-7. In brief, NIPAAm (3.3 g, 54.8 mmol), DDMAT (195 mg, 0.53 mmol), and AIBN (4.4 mg, 0.027 mmol) were dissolved in 1,4-dioxane (15 mL) at room temperature to obtain a homogenous mixture under an argon atmosphere. Then, the reaction solution was degassed via consecutive standard freeze-pump-thaw cycles for three times. After the reaction solution was stirred at 70 °C for 12 h, the polymerization was stopped by cooling to room temperature and exposure to air. The reaction solution was diluted with arbitrary amount of THF and poured into excess amount of diethyl ether. The obtained crude precipitate was dissolved in THF and further precipitated into diethyl ether to completely remove unreacted monomer. The obtained precipitate was dialyzed against de-ionized water (molecular weight cut off: 3,500 Da) and lyophilized to obtain yellowish powder of trithiocarbonate-terminated

polymer, PNIPAAm-CTA (2.02 g, 61 %). PNIPAAm-CTA was characterized using size exclusion chromatography equipped with RI detector (RI 2075, JASCO, Tokyo, Japan) [column: superAW3000, super AW4000, and superAWL-guard column (TOSOH, Tokyo, Japan), eluent: NMP with 0.05 M LiBr at 40 °C, flow rate 0.3 mL/min] and ^{1}H-NMR. Molecular weight and polydispersity index (Mw/Mn) of polymer were calculated based on standard curve of poly(ethylene glycol). The chemical structure of PNIPAAm-CTA was confirmed using ^{1}H-NMR analysis in deuterated methanol (MeOD).

2.4.2.2. Synthesis of PNIPAAm with trithiocarbonate terminus (PNIPAAm-CTA) for molecular weight 20,000 g/mol (PNIPAAm$_{20K}$-CTA

PNIPAAm$_{20K}$-CTA was also synthesized through RAFT polymerization according to Scheme 2-7. NIPAAm (3.3 g, 54.8 mmol), and DDMAT (44.31 mg, 0.122 mmol) were dissolved in DMF (10 mL) at room temperature to obtain a homogenous mixture under an argon atmosphere. In a separate flask, V-70 (7.50 mg, 0.024 mmol) was diluted in 4 mL of DMF. Both of the mixtures were degassed via consecutive standard freeze-pump-thaw cycles for three times. After the reaction solution was stirred at 35 °C for 12 h, the polymerization was stopped by cooling to room temperature and exposure to air. The reaction solution was diluted with arbitrary amount of THF and poured into excess amount of diethyl ether. The obtained crude precipitate was dissolved in THF and further precipitated into diethyl ether to completely remove unreacted monomer. The obtained precipitate was dialyzed against de-ionized water (molecular weight cut off: 3,500 Da) and lyophilized to obtain yellowish powder of trithiocarbonate-terminated polymer, PNIPAAm$_{20K}$-CTA (2.7 g, 82 %). PNIPAAm$_{20K}$-CTA was characterized using size exclusion chromatography equipped with RI detector (RI 2075, JASCO, Tokyo, Japan) [column: superAW3000, super AW4000, and superAWL-guard column (TOSOH, Tokyo, Japan), eluent: DMF with 0.05 M LiCl at 40 °C,

flow rate 0.3 mL/min] and ^{1}H-NMR.Molecular weight and polydispersity index (Mw/Mn) of polymer were calculated based on standard curve of poly(ethylene glycol). The chemical structure of PNIPAAm$_{20K}$-CTA was confirmed using ^{1}H-NMR analysis in MeOD.

2.4.2.3. Synthesis of PNIPAAm with trithiocarbonate terminus (PNIPAAm-CTA) for molecular weight 40,000 g/mol (PNIPAAm$_{40K}$-CTA)

PNIPAAm$_{40K}$ -CTA was also synthesized in a similar manner to the synthesis of PNIPAAm$_{20K}$ -CTA according to Scheme 2-7. Briefly, the solution of NIPAAm (3.3 g, 54.8 mmol), and DDMAT (22.87 mg, 0.063 mmol) in DMF (10 mL) was homogenously stirred under an argon atmosphere at room temperature. In a separate flask, V-70 (3.87, 0.013 mmol) was diluted in 4 mL of DMF. Subsequently, both of the mixtures were degassed via consecutive standard freeze-pump-thaw cycles for three times. Next, 1 mL of V-70 solution was added into NIPAAm containing reaction solution and the reaction solution was further stirred at 35 °C for 12 h. Next, the polymerization was stopped by cooling to room temperature and exposure to air. Subsequently, the reaction solution was diluted with arbitrary amount of THF and poured into excess amount of diethyl ether. The obtained crude precipitate was dissolved in THF and further precipitated into diethyl ether to completely remove unreacted monomer. The obtained precipitate was dialyzed against de-ionized water (molecular weight cut off: 3,500 Da) and lyophilized to obtain yellowish powder of trithiocarbonate-terminated polymer, PNIPAAm$_{40K}$ -CTA (2.5 g, 76 %). Molecular weight and polydispersity index (Mw/Mn) of polymer were calculated based on standard curve of poly(ethylene glycol) with similar condition to the PNIPAAm$_{20K}$-CTA. The chemical structure of PNIPAAm$_{40K}$ -CTA was confirmed using ^{1}H-NMR analysis in MeOD.

2.4.2.4. Synthesis of PNIPAAm-SH and PNIPAAm-TE

Trithiocarbonate terminus of PNIPAAm-CTA was deprotected into thiol group, followed by a conversion into an unreactive thioether to circumvent unexpected side reactions in the following synthesis steps (Scheme 2-7). PNIPAAm-CTA (Mw: 39,000 g/mol) (0.41 g, 0.01 mmol) was dissolved in 1,4-dioxane (5 mL) and stirred for 6 h under an argon atmosphere in the presence of 2-ethanolamine (6.1 μL, 0.1 mmol) and tributylphosphine (2.5 μL, 0.01 mmol). Then, the reaction solution was poured into excess amount of diethyl ether and the obtained precipitate was washed twice with diethyl ether, followed by drying under vacuum to obtain thiol terminated-polymer, PNIPAAm-SH as white powder (0.3 g, 75%). The complete removal of dodecyl trithiocarbonate terminus was confirmed by ^{1}H NMR analysis in MeOD, as suggested by the disappearance of methyl protons in dodecyl trithiocarbonate terminus at 0.88 ppm (Figure 2-5). In a similar manner, PNIPAAm-SH with Mw of 10,000 (g/mol) and 20,000 (g/mol) were synthesized (Data not shown). Subsequently, PNIPAAm-SH (0.3 g, 0.008 mmol), tributylphosphine (2.2 μL, 0. 0.009 mmol), and maleimide (0.013 g, 0. 0.08 mmol) were dissolved in 1,4-dioxane (5 mL), and the mixture was stirred at room temperature for 12 h. The unreacted maleimide and tributylphosphine were removed by precipitation into diethyl ether twice, and the precipitated polymer was dialyzed against de-ionized water (molecular weight cut off: 3,500 Da). The dialyzed solution was lyophilized to obtain thioether terminated-polymer, PNIPAAm-TE (0.27 g, 90%) as white powder. PNIPAAm-TE with Mw of 10,000 (g/mol) and 22,000 (g/mol) were synthesized in a similar manner.

2.4.2.5. Synthesis of PNIPAAm-DBCO

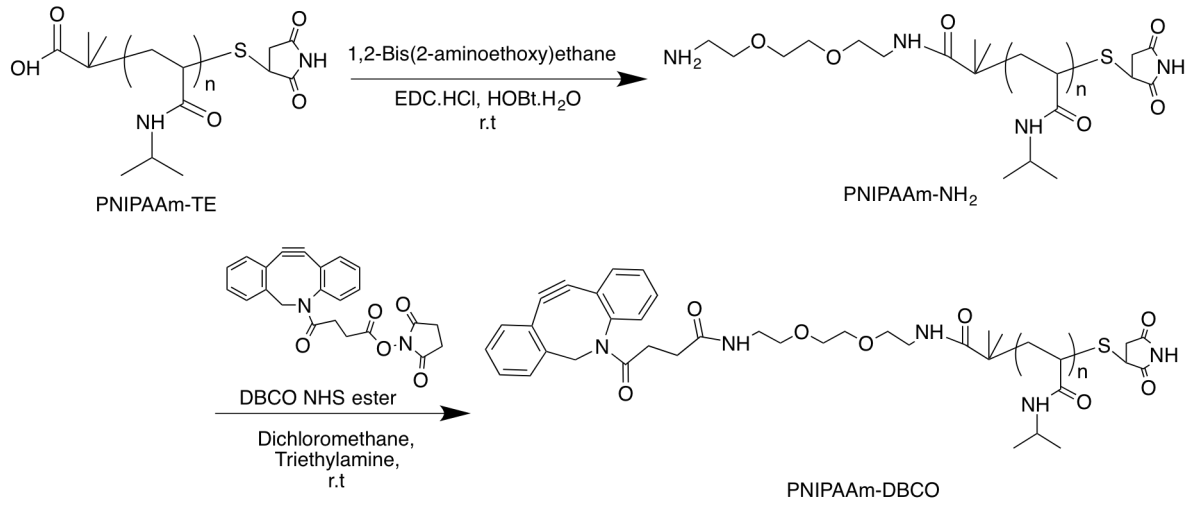

Scheme 2-8. Synthetic procedure of PNIPAAm-DBCO.

The synthesis followed Scheme 2-8. Firstly, PNIPAAm-TE (0.2 g, 0.005 mmol, Mw= 39,000 g/mol), 1,2-bis(2-aminoethoxy)ethane (71 μL, 0.5 mmol), EDC·HCl (0.009 g, 0.05 mmol), and HOBt·H_2O (0.007 g, 0.05 mmol) were dissolved in dichloromethane (2 mL). The reaction solution was stirred at room temperature for 6 h. Subsequently, the reaction solution was poured into excess amount of diethyl ether and the resulting precipitate was dialyzed against de-ionized water (molecular weight cut off: 3,500 Da). The dialyzed solution was lyophilized to produce white powder. The crude product was further purified by ion-exchange chromatography (CM-Sephadex C-50 and QAE-Sephadex A-50) to remove unreacted PNIPAAm-TE, followed by dialysis against de-ionized water (molecular weight cut off: 3,500 Da) and lyophilization to obtain PNIPAAm-NH_2 (0.1 g, 50%) as white powder. The obtained white powder of PNIPAAm-NH_2 was characterized using ion-exchange chromatography [column: SP-5PW (TOSOH, Tokyo, Japan), eluent: 2 mM PB pH 6.5 at r.t., flow rate 0. 5 mL/min]. Subsequently, PNIPAAm-NH_2 (50 mg, 1.28 μmol) and DBCO-NHS-ester (5.16 mg, 1.28 μmol) were dissolved in dichloromethane (2 mL). After an addition of catalytic amount of triethylamine, the reaction mixture was stirred at room temperature in a

dark room for 12 h. Then, the reaction solution was dialyzed against methanol for 24 h, followed by dialysis against de-ionized water for 48 h (molecular weight cut off: 3,500 Da). The dialyzed solution was filtered through a 0.22 μm syringe driven filter and lyophilized to obtain PNIPAAm$_{40K}$-DBCO (41.3 mg, 82.6%) as white powder and the chemical structure was characterized using ^{1}H-NMR measurement in D_2O at room temperature. In a similar manner, PNIPAAm-DBCO with Mw of 10,000 g/mol and 22,000 g/mol were also synthesized.

2.4.2.6. Synthesis of PEG-DBCO

PEG-NH_2 for Mw= 40,000 g/mol (50 mg, 1.25 μmol) and DBCO-NHS ester (2.52 mg, 6.25 μmol) were dissolved in 2 mL of dichloromethane with catalytic amount of triethylamine for 12 h at room temperature in a dark room. Next, the reaction solution was subsequently dialyzed against methanol for 24 h and de-ionized water for 48 h (molecular weight cut off: 3,500 Da). Then, the dialyzed solution was filtered through a 0.22 μm syringe driven filter and lyophilized to obtain PEG-DBCO (43 mg, 86 %) as white powder. Obtained white powder was analyzed by ^{1}H NMR in DMSO-d_6 at 80 °C. PEG-DBCO with Mw of 10,000 g/mol and 20,000 g/mol were also synthesized in a similar manner.

2.4.3. Synthesis of PNIPAAm-siRNA and PEG-siRNA

2.4.3.1. Synthesis of PNIPAAm-siRNA

Series of azide-siRNA solutions in 10 mM HEPES buffer (pH 7.3) (10 μL, 25 μM) and PNIPAAm-DBCO solution in 10 mM HEPES buffer (pH 7.3) (4 μL, 50 μM) were mixed in a 1.5 mL microtube, and 10 mM HEPES buffer (pH 7.3) (64 μL) was added into the solutions. The reaction solutions were frozen at - 20 °C overnight, and then, thawed at 4 °C for 1 h. The crude products were purified by ion-exchange HPLC to obtain series of PNIPAAm-siRNA

conjugates [Column: SuperQ-5PW (TOSOH), eluent: 10 mM HEPES pH 7.4 with gradient concentration of NaCl (from 0 mM to 1 M), flow rate: 0.8 mL/min, detector: UV absorbance at 260 nm]. The purified PNIPAAm-siRNA was analyzed using size-exclusion chromatography equipped with UV detector (absorbance at 260 nm) [Column: Superdex 75 10/300GL (GE Healthcare) at flow rate 0.75 mL/min in eluent 10 mM HEPES pH 7.4 with 500 mM NaCl]. In a similar manner, siRNA conjugated PNIPAAm with Mw of 9,500 g/mol and 22,000 g/mol were synthesized.

2.4.3.2. Synthesis of PEG-siRNA

Series of PEG-siRNAs were also synthesized in a similar manner to the synthesis of PNIPAAm-siRNA (Scheme 2-11), except for the HPLC condition for purification. The solutions of series of siRNA azide in 10 mM HEPES buffer (pH 7.3) (10 μL, 25 μM) and solutions of PEG-DBCO in 10 mM HEPES buffer (pH 7.3) (4 μL, 50 μM) were mixed in a 1.5 mL microtube, and 10 mM HEPES buffer (pH 7.3) was added into the solutions. The reaction solutions were frozen at -20 ^{o}C for overnight and followed by thawing for 1 h at 4 ^{o}C. The crude products of PEG-siRNA were purified using ion-exchange HPLC equipped with UV detector (absorbance at 260 nm) [Column: MonoQ 5/50GL (GE Healthcare) at flow rate 2.0 mL/min in eluent 10 mM HEPES pH 7.4 with gradient concentration of NaCl (from 0 mM to 1 M)]. The purified PEG-siRNA was analyzed using size-exclusion chromatography equipped with UV absorbance at 260 nm. [Column: Superdex 75 10/300GL (GE Healthcare) at flow rate 0.75 mL/min in eluent 10 mM HEPES pH 7.4 with 500 mM NaCl]. In a similar manner, siRNA conjugated PEG with Mw of 10,000 g/mol and 20,000 g/mol were synthesized.

2.4.3.3. Agarose gel electrophoresis

The obtained siRNA-conjugates with PNIPAAm and PEG polymers were further analyzed by agarose gel electrophoresis. Unconjugated siRNA, PNIPAAm-siRNA, and PEG-siRNA (100 ng of siRNA for each sample) were loaded onto agarose gel (2.5% agarose, 1 × TBE) including SYBR safe (Thermo Fisher Scientific Inc., Waltham, MA, USA) and treated at 100 V for 60 min. Next, the band from siRNA and its polymer conjugates were visualized using ChemiDoc XRS Plus Image Lab System (BIO-RAD, California, USA).

2.5. Results

2.5.1. Synthesis of PNIPAAm through ATRP using different catalyst/ligand complexes system

Herein, several ATRP conditions were investigated in order to obtain PNIPAAm with controlled structure: controlled molecular weight and narrow molecular weight distribution. Stover et al. demonstrated the ATRP of PNIPAAm using several alcohols as polymerization solvent, and prepared PNIPAAm using isopropanol solvent exhibited a narrow molecular weight distribution with controlled molecular weight [17]. Based on their results, in the present study, PNIPAAm was first polymerized in isopropanol solvent using ethyl-2-bromoisobutyrate (EtBriB)/CuBr/Me6TREN (1:1:1) as initiating system (Scheme 2-3). Isopropanol was chosen in this study because of the basic premise that a hydrogen-bonding solvent could bind to the amide groups of both monomer and polymer, and thus, reduce the interaction with both catalyst and propagating chain.

However, through MALDI-TOF MS measurement (Figure 2-1), the obtained molecular weight of PNIPAAm was almost 2,000 g/mol, which is not in good agreement with targeted molecular weight (~11,300 g/mol). Although the molecular weight of obtained PNIPAAm was not in control, the livingness of PNIPAAm was investigated by introduced a phthalimide

group to the halide terminus of PNIPAAm (Scheme 2-4). The chemical structure of white powder polymer was characterized by ^{1}H-NMR measurement, and no peaks of phthalimide group could be observed in ^{1}H-NMR spectrum (~7.58 ppm) (Figure 2-2).

Next, ATRP of PNIPAAm was investigated using methyl 2-chloropropionate (MCP)/CuCl/ Me6TREN (1:1:1) as initiating system. The polymerization of NIPAAm in this system followed the Scheme 2-5. The procedure of ATRP in this system is similar to the previous polymerization. However, also the molecular weight of obtained PNIPAAm was not in good agreement with the targeted molecular weight at the early stage of polymerization as determined by MALDI-TOF-MS (data not shown). In addition, no peaks of phthalimide group present in ^{1}H-NMR chart as determined by ^{1}H-NMR measurement (Figure 2-3).

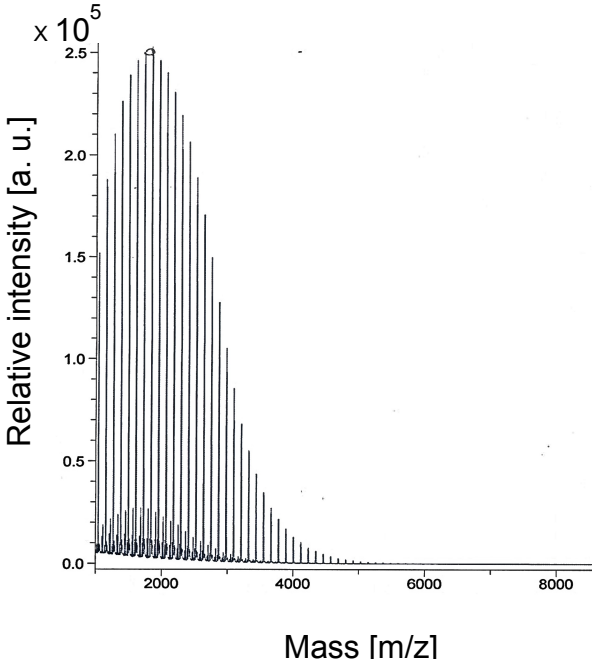

Figure 2-1. MALDI-TOF MS spectrum of PNIPAAm-Br

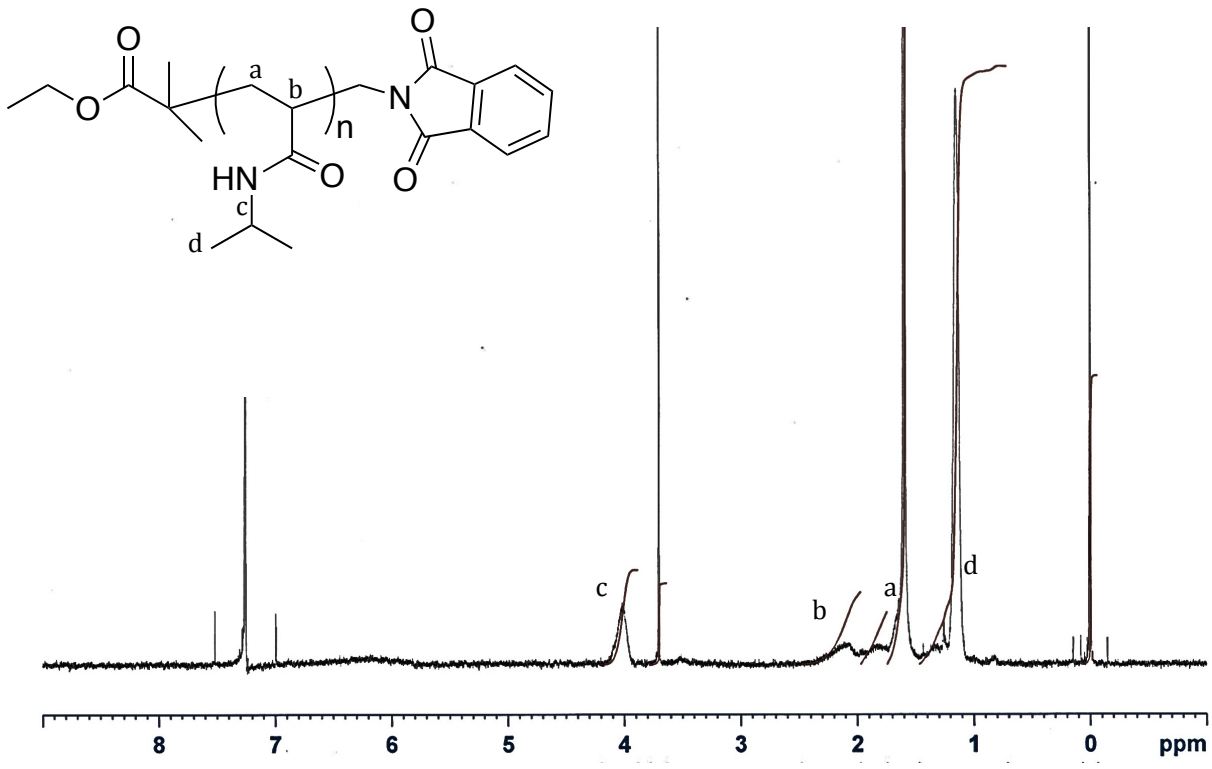

Figure 2-2. ^{1}H-NMR spectrum after the introduction a phthalimide group to the terminus of PNIPAAm-Br.

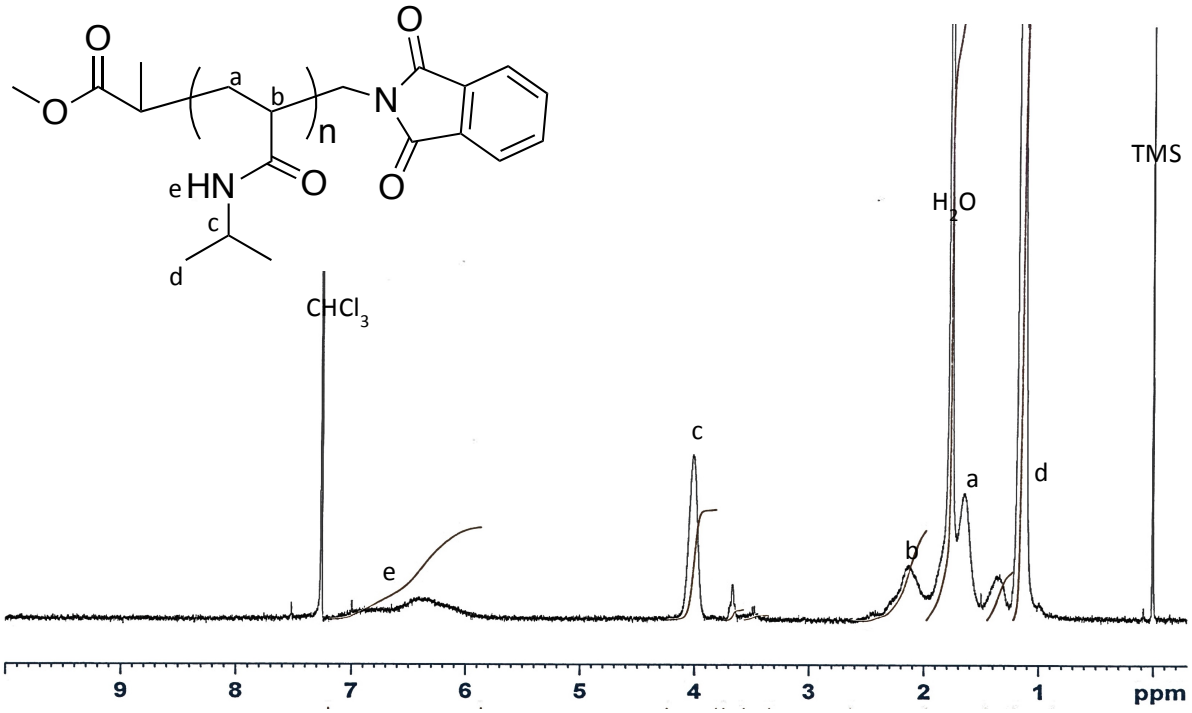

Figure 2-3. ^{1}H-NMR spectrum of PNIPAAm-Phthalimide

2.5.2. Synthesis of PNIPAAm through ATRP in the presence of water

It was reported that a successful polymerization of 2-hydroxyethyl acrylate in the presence of water through ATRP [18], and thus, in the present study, the polymerization of NIPAAm using mixed alcohol and water solvent was also investigated. The polymerization of NIPAAm was initiated using MCP/CuCl/Me_6TREN [1:1:1] system in mixed isopropanol and water (4/1) (v/v) under an argon atmosphere at room temperature (Scheme 2-5). And subsequently I determined the polymerization behavior of the reaction solution by MALDI-TOF MS measurement (Figure 2-4), resulting a polymerization of PNIPAAm with the molecular weight of almost 6,000 (g/mol). Moreover, the expanded spectrum (Figure 2-5) reveals a repeating set of four peaks separated from neighboring sets by NIPAAm monomer molecular weight (113 g/mol). The four peaks are attributed to PNIPAAm backbone bearing an -H, an -OH, an -Cl or a lactone, and the chemical structures were shown in figure 2-6. Those were corresponded to the peaks, as summarized in Table 2-1.

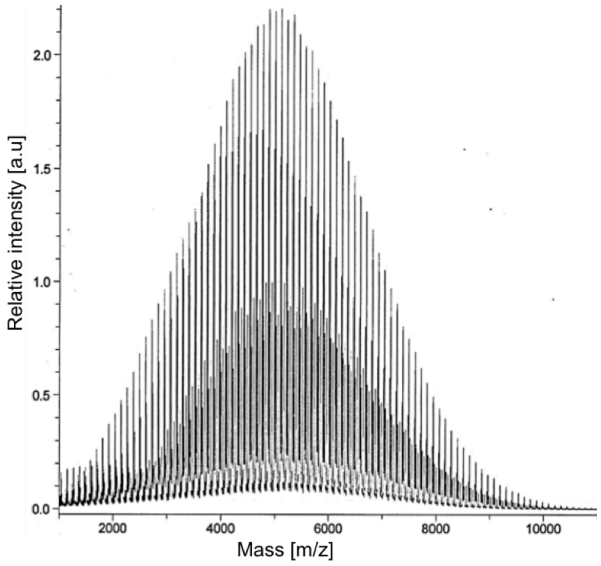

Figure 2-4. MALDI TOF-MS spectrum for ATRP of PNIPAAm

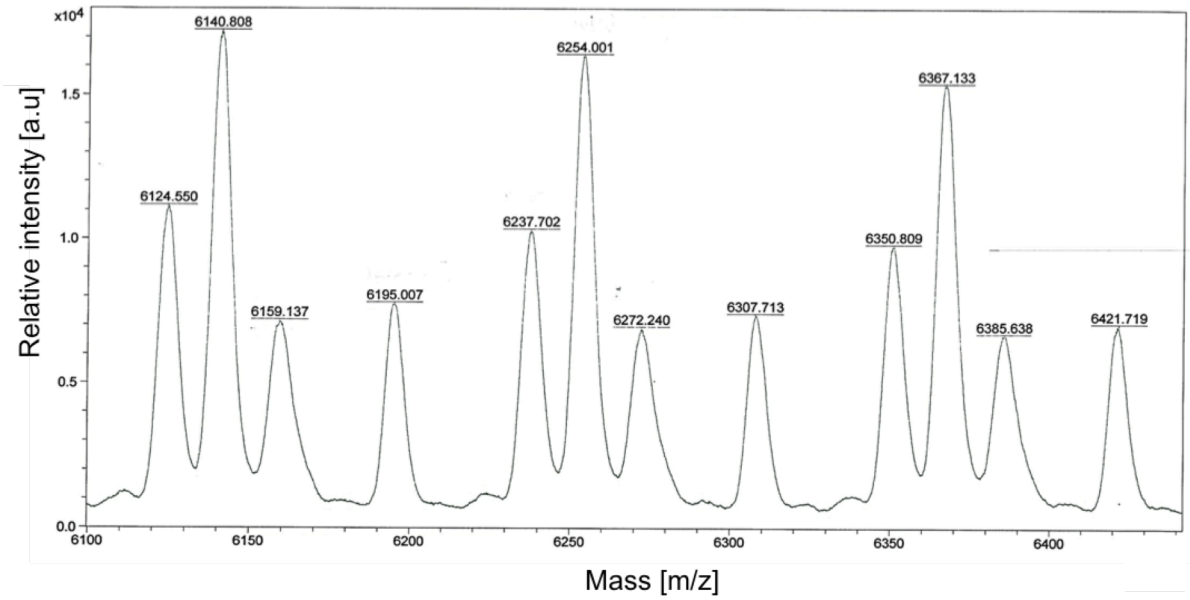

Figure 2-5. Expansion spectrum for Figure 2-4

Table 2-1. MALDI-TOF MS of 55-mer of PNIPAAm prepared in the presence of water

	PNIPAAm-Cl/Na^+	PNIPAAm-H/Na^+	PNIPAAm-OH/Na^+	PNIPAAm-Lactone/Na^+
Mn, theor.	6272.19	6238.19	6254.19	6195.19
Mn, calcd.	6272.24	6237.70	6254.00	6195..01

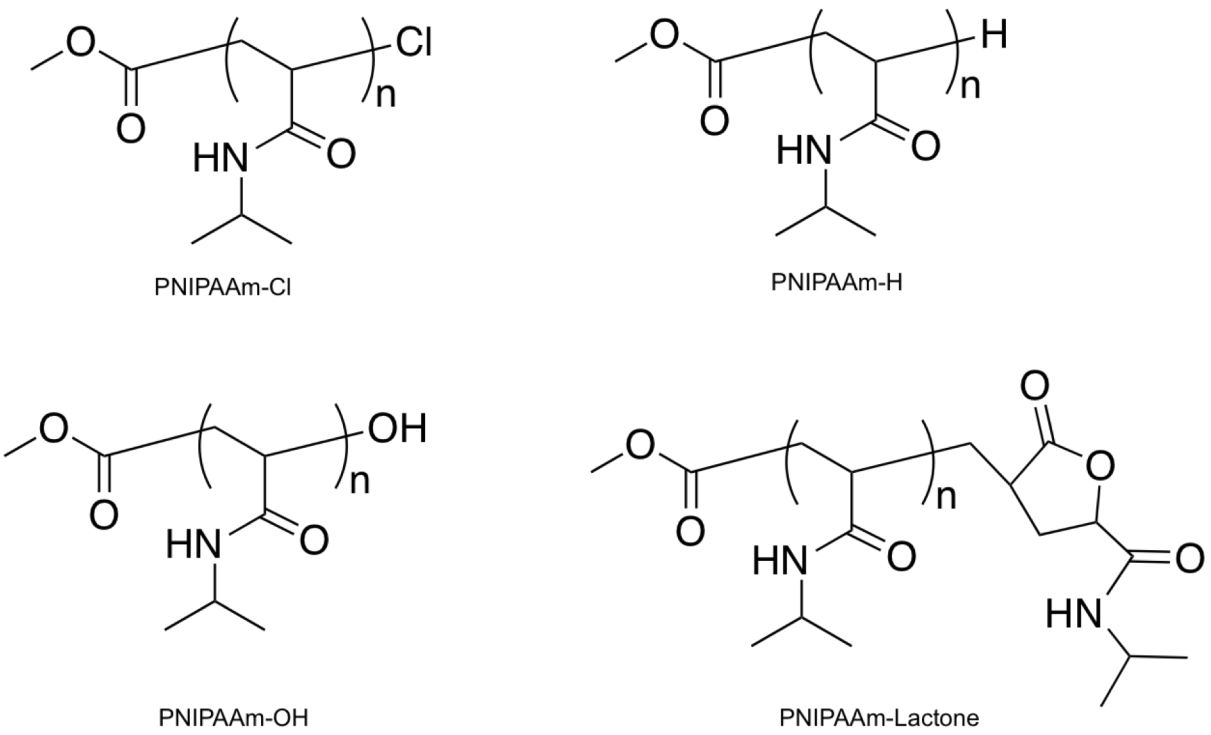

Figure 2-6. Suggestion of chemical structure for PNIPAAm with different terminus group obtained after ATRP in the presence of water.

2.5.3. Synthesis of PNIPAAm through RAFT polymerization and subsequent end groups modification.

Trithiocarbonate-terminated polymers, PNIPAAm-CTAs were prepared through RAFT polymerization method as shown in Scheme 2-7 with targeted molecular weight of 10,000 g/mol, 20,000 g/mol and 40,000 g/mol. The RAFT polymerization of NIPAAm was initiated utilizing two types of azo-initiators, which are AIBN and V-70 and trithiocarbonate group, DDMAT as chain-transfer agent. The number-average molecular weight (Mn), weight-

Table 2-2. Summarized of PNIPAAm-CTA obtained by RAFT polymerization.

	Initiator	Mn, g/mol[a]	Mw, g/mol[a]	Mw/Mn
$PNIPAAm_{10K}$-CTA	AIBN	7,600	9,500	1.24
$PNIPAAm_{20K}$-CTA	V-70	18,700	22,000	1.18
$PNIPAAm_{40K}$-CTA	V-70	31,500	39,000	1.24

[a]Mn, Mw and Mw/Mn obtained by GPC measurement, which were calculated based on standard curve of poly(ethylene glycol).

average molecular weight (Mw) and molecular weight distribution (Mw/Mn) of obtained PNIPAAm-CTAs were characterized using size exclusion chromatography equipped with RI detector and calculated based on standard poly(ethylene glycol) and summarized in Table 2-2. The RAFT polymerization of NIPAAm that used AIBN initiator produced PNIPAAm-CTA with about 9,500 g/mol, which is close to the targeted molecular weight. In addition, the RAFT polymerization that utilized V-70 initiator produced PNIPAAm-CTAs with higher molecular weight, 22,000 g/mol and 39,000 g/mol. All of the PNIPAAm-CTAs possess a narrow molecular weight distribution ranging from Mw/Mn = 1.18 to 1.24 (Table 2-2, Figure 2-7). The resulting PNIPAAm-CTA having a terminal dodecyl trithiocarbonate moeity, which resulted in characteristic ^{1}H-NMR resonances at 0.88 ppm attributed to the terminal –C$\boldsymbol{H_3}$ protons (Figure 2-8).

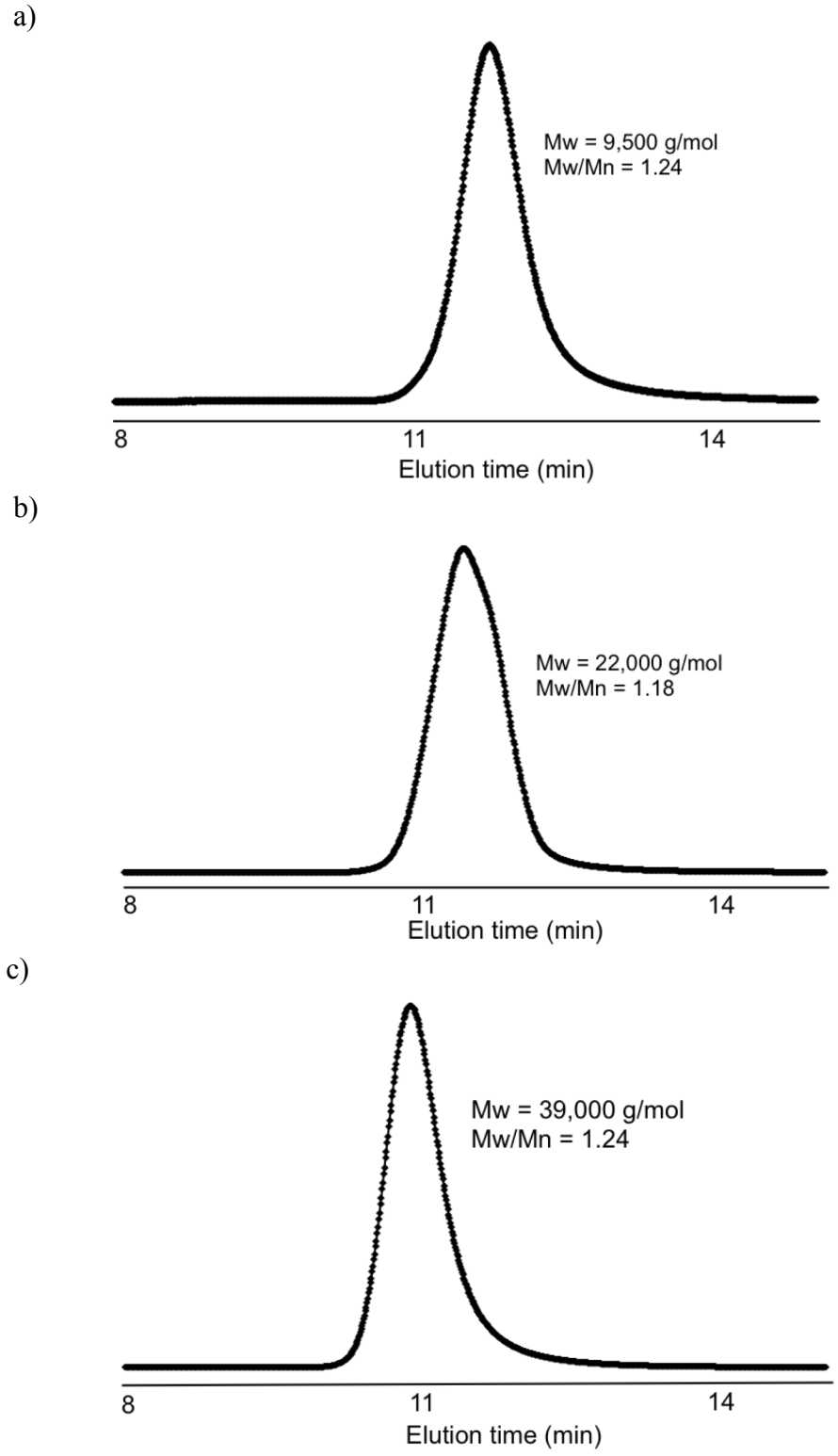

Figure 2-7. SEC-GPC charts of a) PNIPAAm$_{10K}$-CTA, b) PNIPAAm$_{20K}$-CTA, and c) PNIPAAm$_{40K}$-CTA using DMF contains 50 mM LiCl as eluent at 40 °C and the flow-rate was 0.3 mL/min.

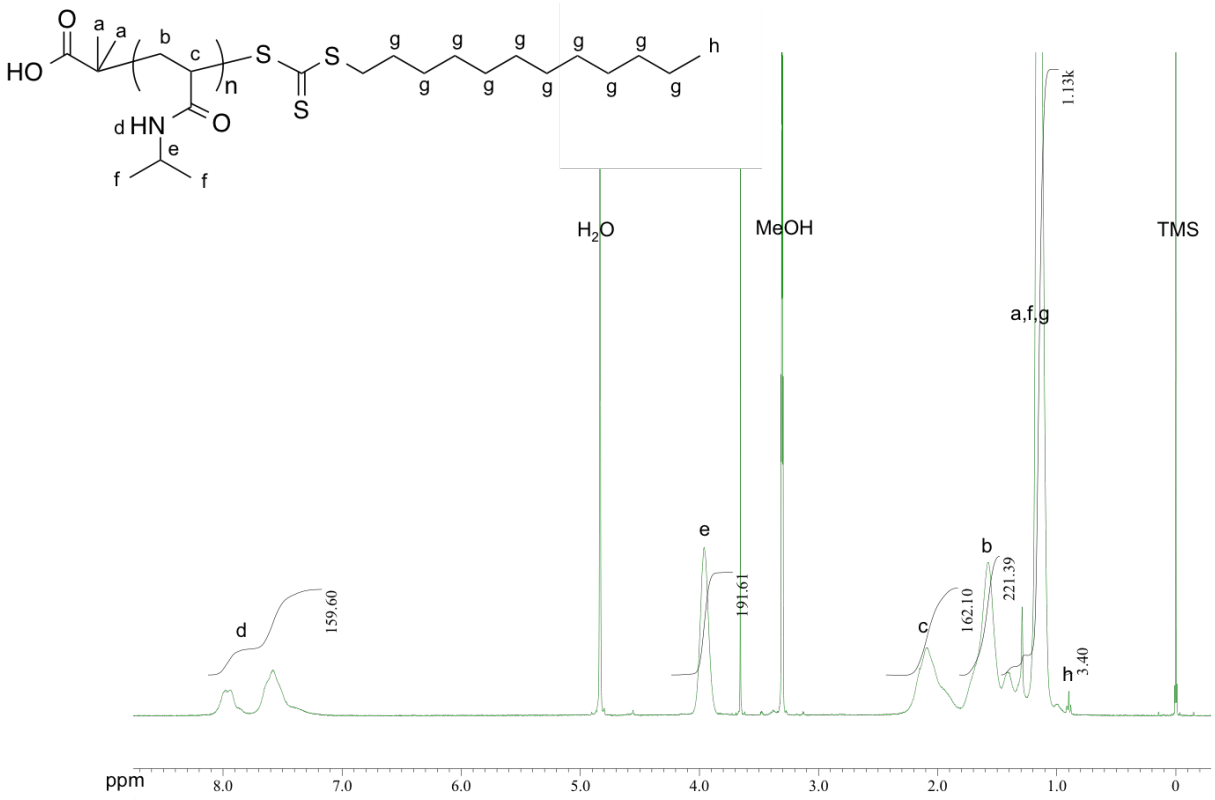

Figure 2-8. ^{1}H-NMR spectrum of PNIPAAm$_{20K}$-CTA in MeOD at room temperature

Then, the terminal trithiocarbonate end groups derived from the CTA were converted to thiol groups through aminolysis (Scheme 2-7) in the presence of a reducing agent to limit disulfide formation. Upon addition of the amine, the yellow color of the reaction solution rapidly disappeared, and I characterized their chemical structure using ^{1}H-NMR in MeOD solvent after purification by precipitation, followed by drying under vacuum. As a result, the -C*H*$_3$ protons in dodecyl trithiocarbonate moeity for ^{1}H-NMR resonances at 0.88 ppm disappeared, indicating that trithiocarbonate end groups were successfully converted into thiol groups, PNIPAAm-SH (Figure 2-9).

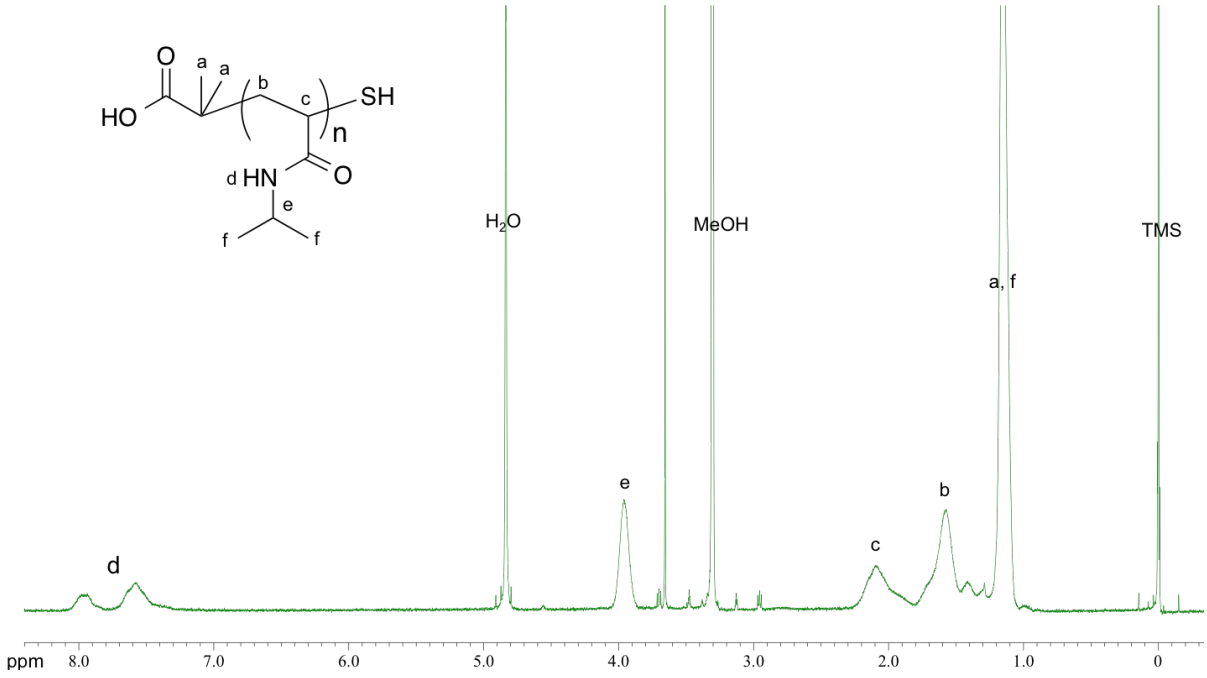

Figure 2-9. ^{1}H-NMR spectrum of PNIPAAm-SH in MeOD at room temperature.

Subsequently, PNIPAAm-SH was converted into maleimide group, an unreactive thioether group in order to circumvent unexpected side reaction. The reaction solutions were stirred at room temperature in 1,4-dioxane, and subsequently dialyzed against de-ionized water, followed by freeze-drying to obtain PNIPAAm-TE. Subsequently, a primary amine group was introduced into a carboxylic group at the terminus of PNIPAAm-TE via amide bond formation in the presence of EDC as a condensation reagent. The products were purified by precipitation into diethyl ether and dialysis against de-ionized water, followed by freeze-dry to obtain white powder. In order to remove unreacted PNIPAAm-TE, the crude products were purified through ion-exchange chromatography (CM-Sephadex C-50 and QAE-Sephadex A-50). The successful removal of unreacted PNIPAAm-TE was confirmed by ion-exchange HPLC as shown in Figure 2-10.

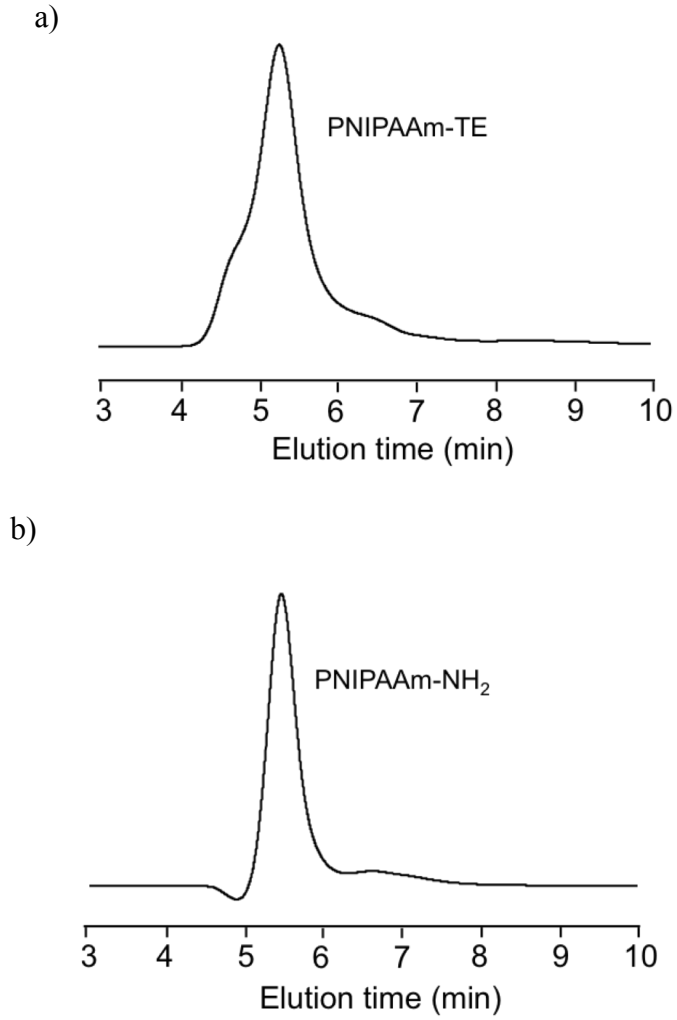

Figure 2-10. Ion-exchange chromatography charts of a) PNIPAAm-TE and b) PNIPAAm-NH_2

In order to conduct Copper-free Click Chemistry, a strained alkyne of dibenzocyclooctyne (DBCO) group was introduced into amine terminus of PNIPAAm through amide bond formation (Scheme 2-8). PNIPAAm-NH_2 and DBCO-NHS ester were dissolved in dichloromethane and stirred in a dark for overnight. The product was purified through dialysis, followed by freeze-dry to obtain PNIPAAm-DBCO as white powder. A quantitative introduction of DBCO moiety into the polymer was confirmed by ^{1}H NMR analysis in D_2O, as calculated from the peak intensity ratio of phenyl protons in DBCO at 7.2- 7.8 ppm (-C_6H_4-) and PNIPAAm at 3.6 – 4.1 ppm (-CONHCH(CH_3)$_2$) (Figure 2-11).

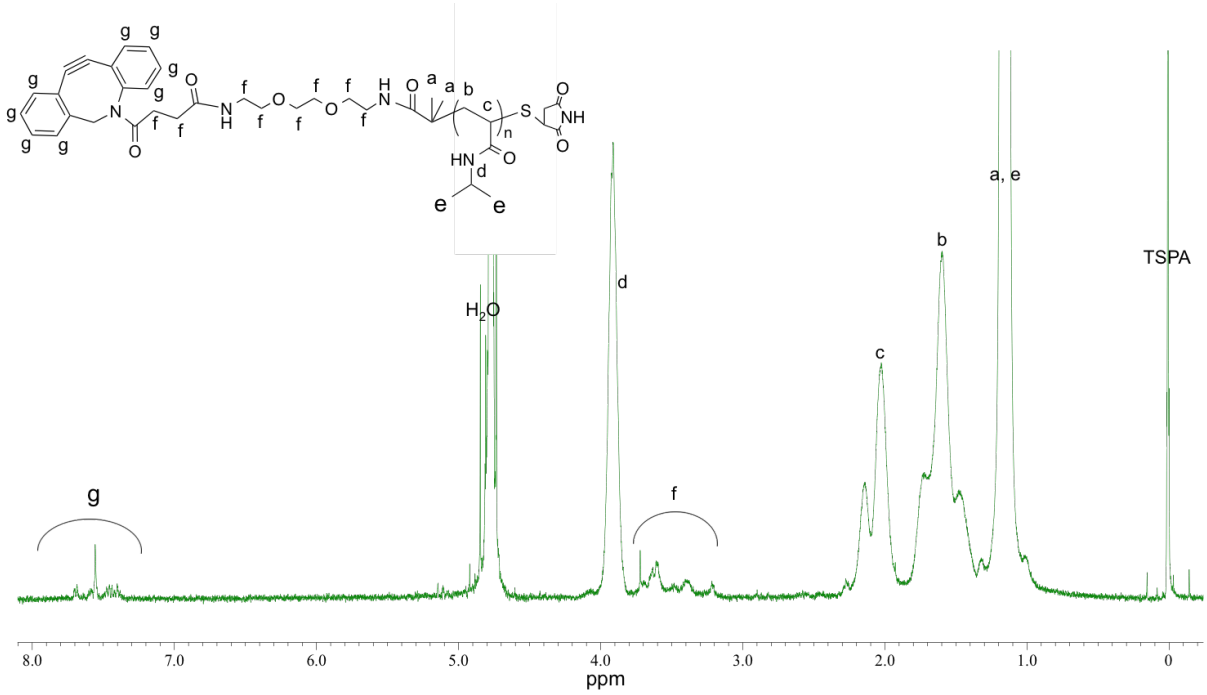

Figure 2-11. ^{1}H-NMR spectrum of PNIPAAm-DBCO in MeOD at room temperature.

2.5.4. Synthesis of PEG-DBCO

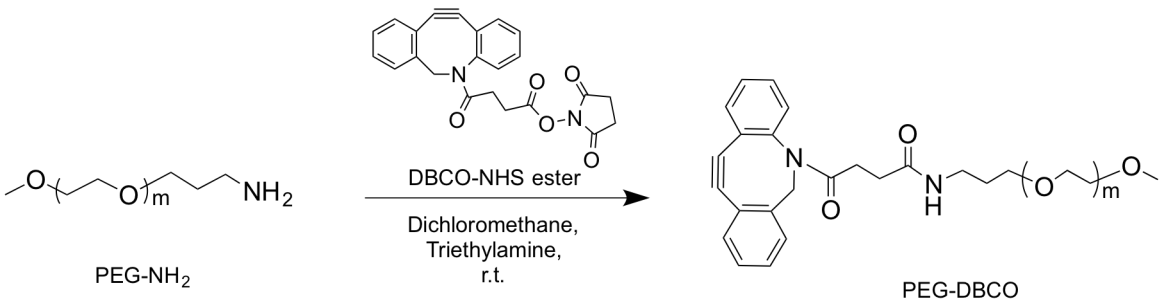

Scheme 2-9. Synthetic procedure of PEG-DBCO

As a control system, non-thermoresponsive poly(ethylene glycol) (PEG) systems with molecular weight 10,000 g/mol, 20,000 g/mol and 40,000 g/mol were used. A DBCO group was introduced into amine terminus of PEG as shown in the Scheme 2-9. The synthetic procedures were in a similar manner with the procedure for the PNIPAAm-DBCO. The chemical structure of obtained PEG-DBCO was characterized by ^{1}H-NMR measurement. The

peak intensity ratio of phenyl protons in DBCO (-C_6H_4-, δ 7.2 – 7.6 ppm) and PEG protons (-C_2H_4O-, δ = 3.5 – 3.6 ppm) confirms a successful introduction of DBCO into the PEG terminus (Figure 2-12).

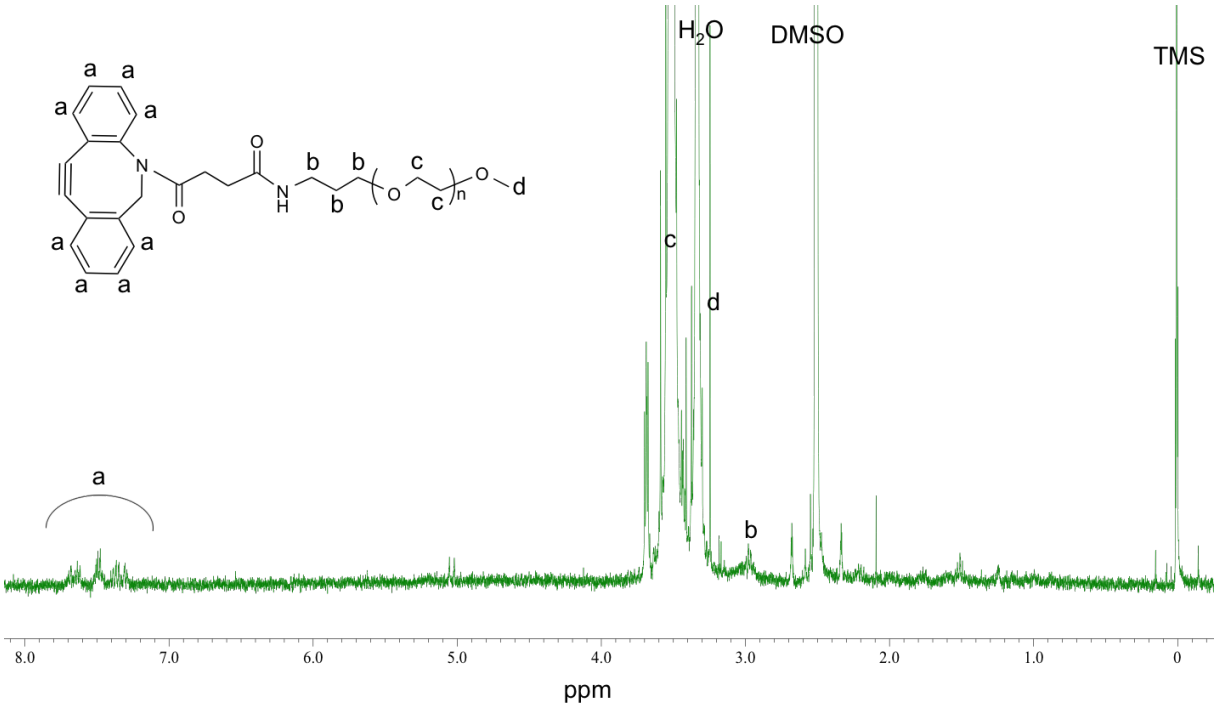

Figure 2-12. ^{1}H-NMR spectrum of PEG-DBCO in DMSO-d6 at 80 °C.

2.5.5. Synthesis of PNIPAAm-siRNA and PEG-siRNA

PNIPAAm-siRNA was synthesized as shown in Scheme 2-10 following the reported method [14]. The reaction solution of PNIPAAm-DBCO and azide-siRNA in 10 mM HEPES

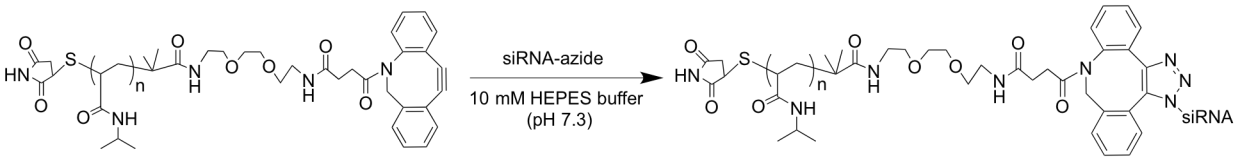

Scheme 2-10. Synthetic procedure of PNIPAAm-siRNA.

pH 7.4 was gradually frozen at -20 °C for overnight and thawed at 4 °C, and subsequently purified using ion-exchange chromatography. Figure 2-13 shows the ion-exchange

chromatography chart of the reaction solution, exhibiting that the desired PNIPAAm-siRNA was successfully separated from unreacted PNIPAAm-DBCO and azide-siRNA.

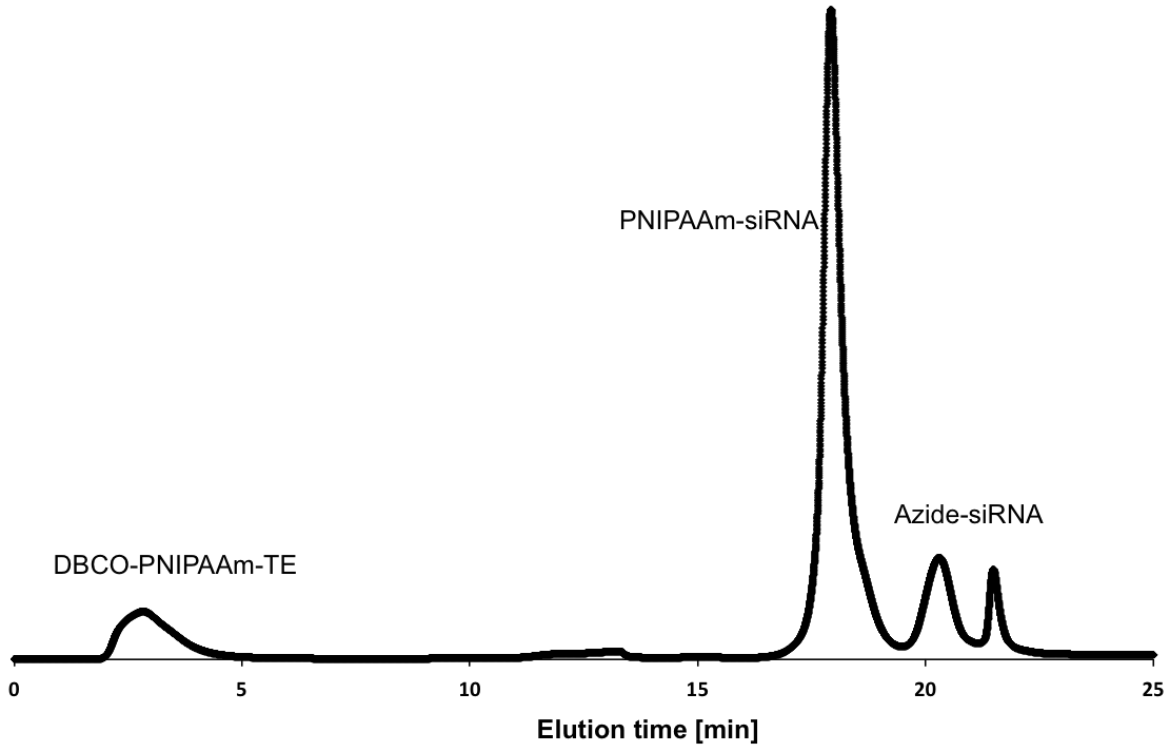

Figure 2-13. Ion exchange chromatography chart of the reaction solution of PNIPAAm-DBCO and azide-siRNA.

Also, in a similar manner, PEG-siRNA was synthesized. The synthesis followed Scheme 2-

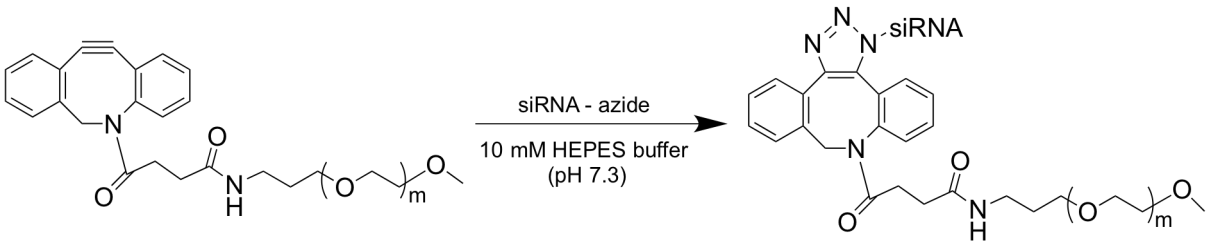

Scheme 2-11. Synthetic procedure of PEG-siRNA

11 and also PEG-siRNA was purified using ion-exchange chromatography. The ion-exchange chromatography chart of PEG-siRNA as shown in Figure 2-14, exhibits that PEG-siRNA was successfully prepared through click chemistry reaction and the unreacted PEG-DBCO as well as azide-siRNA were successfully excluded through fraction using ion-exchange chromatography.

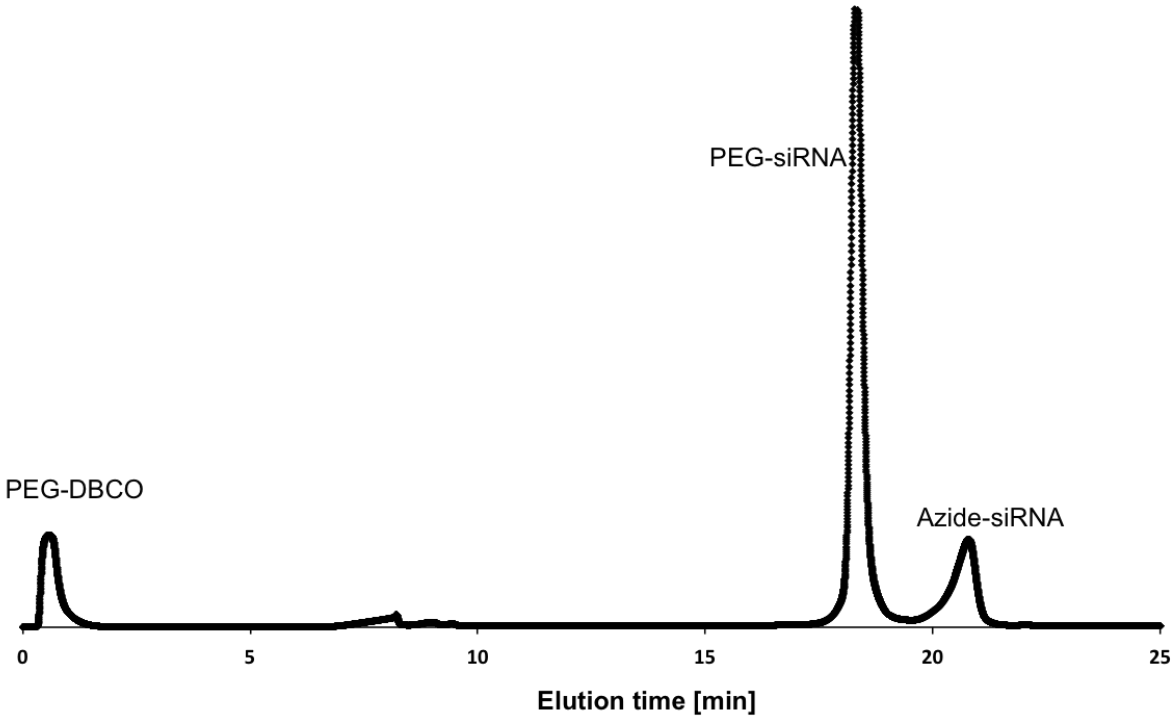

Figure 2-14. Ion exchange chromatography chart of the reaction solution of PEG-DBCO and azide-siRNA.

The obtained PNIPAAm-siRNA and PEG-siRNA were further analyzed through agarose gel electrophoresis and size-exclusion chromatography using SEC column for further confirmation. The shorter migrations of the polymer-conjugated siRNAs, compared to unconjugated siRNA, without the presence of the unconjugated siRNA-related band, confirm the higher molecular weights as a result of polymer conjugation and the successful synthesis as shown in Figure 2-15. Further successful purification of polymers-conjugated siRNA was also characterized by size-exclusion chromatography (Figure 2-16).

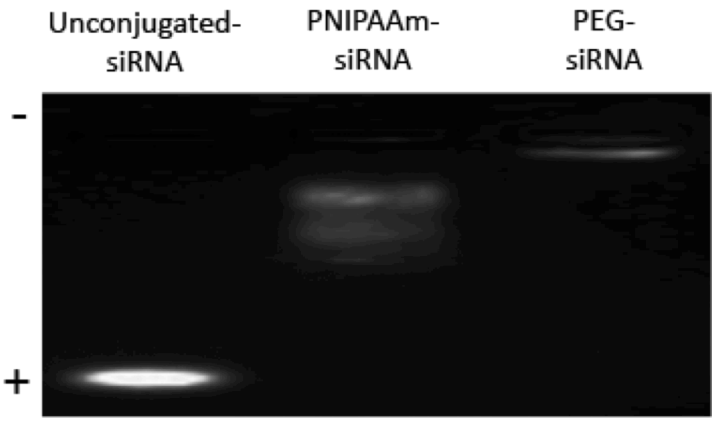

Figure 2-15. Agarose gel electrophoresis of unconjugated-siRNA, PNIPAAm-siRNA and PEG-siRNA

a)

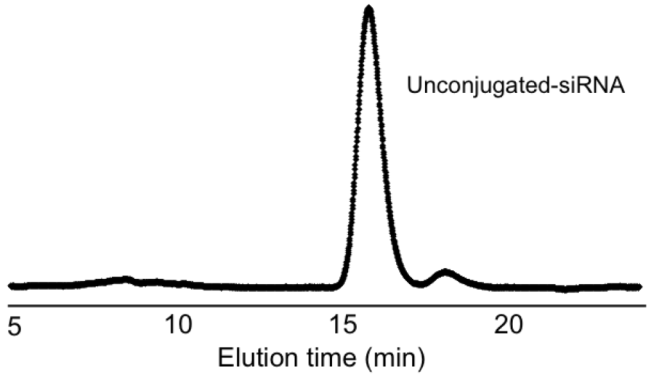

b)

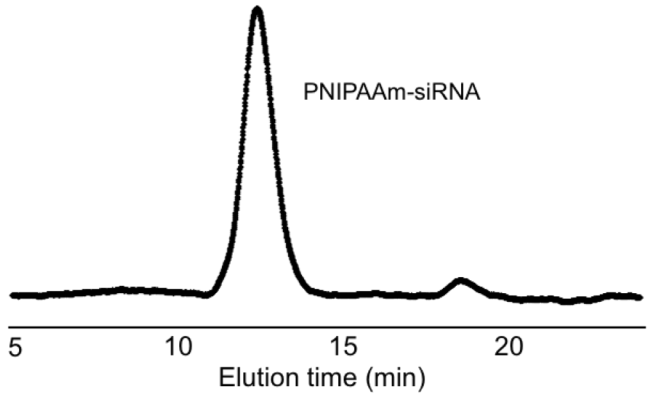

c)

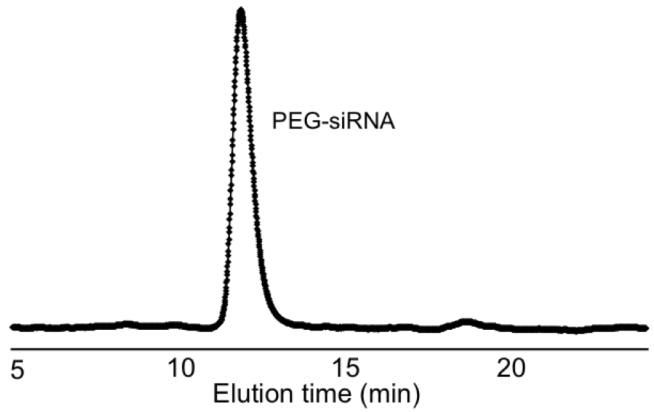

Figure 2-16. SEC charts of a) unconjugated-siRNA, b) PNIPAAm-siRNA and c) PEG-siRNA after fractionation using 10 mM HEPES pH 7.4 with 500 mM NaCl at room temperature and the flow-rate at 0.75 mL/min.

2.6. Discussion

Since the conjugation between polymer and biomolecule was successfully demonstrated several decades ago, the development of conjugating siRNA with functional polymer has attracted a great attention for a successful siRNA-based therapy. In the present study, a new class of polymer-conjugated siRNA was developed, i.e., conjugating a stimuli-responsive polymer to an siRNA molecule. In recent years, a great number of literatures discussing on the polymerization behavior of those controlled radical polymerization of NIPAAm [10, 19-23]. Therefore in this study, PNIPAAm was synthesized through two techniques of living radical polymerization in order to obtain precisely controlled structure of polymer, i.e., narrow molecular weight distribution with desired molecular weight. Those two techniques were atom transfer radical polymerization (ATRP) and reversible addition-fragmentation chain-transfer (RAFT) polymerization. Eventually, obtained PNIPAAm with end group modification was successfully conjugated with an siRNA through Copper-free click chemistry.

Firstly, the ATRP of NIPAAm was investigated using two types of catalysts, i.e., CuBr and CuCl. Me_6TREN was used as a ligand in this study because it gives high rate of polymerization and shows a good control of the molecular weight and polydispersity, as reported in the literature [10]. Although two catalyst/ligand systems were investigated in polymerization of NIPAAm, it could be observed that the absence of bromide group at the terminus of obtained PNIPAAm (Figure 2-1). It was probably due to the nucleophilic displacement of terminal halide by amide group of NIPAAm structure [22, 23]. The nucleophilic displacement leads to the loss of livingness of PNIPAAm. After a phthalimide group was introduced to the PNIPAAm terminus, no peak of phthalimide group could be observed in ^{1}H-NMR spectrum (Figure 2-3), suggesting the difficulty in control of the livingness of ATRP method using CuBr for PNIPAAm synthesis.

Then, NIPAAm was polymerized using CuCl/Me_6TREN catalyst/ligand system in the presence of water. As the same results with the previous investigations, obtained portion of PNIPAAm molecules bear chloride terminus (Figure 2-4). Moreover, using water as assistance solvent produced several types of PNIPAAm bearing different terminus as suggested in Figure 2-5 (Table 2-1), probably due to a cyclization had proceeded during the polymerization, as illustrated in Scheme 2-12, a PNIPAAm chain had undergone cyclization to form a lactone end group. According to these results, the ATRP of NIPAAm is not suitable for end-functionalization in the following steps.

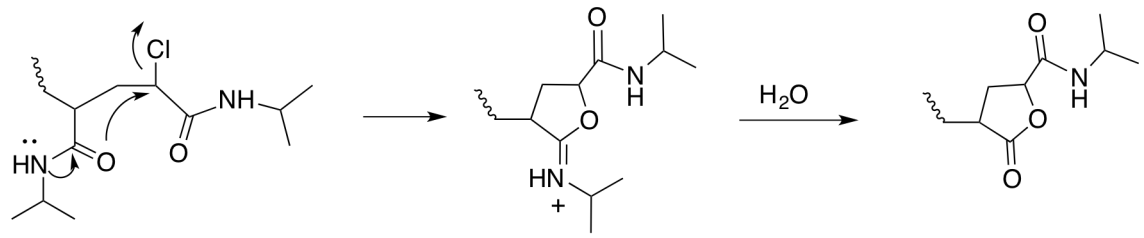

Scheme 2-12. A PNIPAAm chain had undergone a cyclization to form a lactone end group

Then, NIPAAm synthesis was investigated through RAFT polymerization technique using trithiocarbonate group as chain transfer agent, and summarized in Table 2-2. Through RAFT polymerization, PNIPAAm with controlled molecular weight and having narrow molecular weight distribution (Mw/Mn) ranging from 1.18 to 1.24, was obtained, indicating the controlled polymerization over the process. Moreover, an end modification was successful, where the end group was converted to obtained PNIPAAm-DBCO towards siRNA conjugation at the later stage. In addition, both end groups of PNIPAAm had been modified, no changes in the chemical structure of PNIPAAm backbone was observed, suggesting a successful end group modification.

Subsequently, PNIPAAm-DBCO was successfully conjugated with an azide-siRNA through Copper-free Click Chemistry. The successful conjugation of PNIPAAm-siRNA, as

well as PEG-siRNA, utilized reported freeze-thaw technique [14]. PNIPAAm-siRNA and PEG-siRNA was produced with a good yield (> 80%) through this technique, followed by purification and characterization by ion-exchange chromatography and agarose gel electrophoresis, respectively.

2.7. Conclusion

In conclusion, thermoresponsive polymer, PNIPAAm with a controlled molecular weight and a narrow molecular weight distribution was successfully synthesized through RAFT polymerization. A DBCO group was also successfully introduced at the end group of carboxylic terminus of PNIPAAm-TE. The PNIPAAm-siRNA and PEG-siRNA were successfully synthesized through Copper-free Click Chemistry using freeze-thaw method.

2.8. References

[1] Neu, M., Fischer, D., and Kissel, T. Recent advances in rational gene transfer vector design based on poly(ethylene imine) and its derivatives. *J. Gene Med.* **2005,** *7*,992–1009.

[2] C.de Las Heras Alarcon, C., Pennadam, S., and Alexander, C. Stimuli responsive polymers for biomedical applications. *Chem. Soc. Rev.* **2015**, 34, 276–285.

[3] Ganas, C., Weiß, A., Nazarenus, M., Rösler, S., Kissel, T., Rivera Gil, P., and Parak, W. J. Biodegradable capsules as non-viral vectors for in vitro delivery of PEI/siRNA polyplexes for efficient gene silencing. *J. Control. Release* **2014**, *196*, 132–138

[4] Chang, C., Nguyen, T. H., and Maynard, H. D. Thermoprecipitation of Glutathione S-Transferase by Glutathione-Poly(N-isopropylacrylamide) Prepared by RAFT Polymerization. *Macromol. Rapid Commun.* **2010**, *31*, 1691–1695.

[5] Matyjaszewski, K. Atom Transfer Radical Polymerization (ATRP): Current Status and Future Perspectives. *Macromolecules* **2012**, *45*, 4015–4039

[6] Moad, G., Rizzardo, E., and Thang, S. H. Living radical polymerization by the RAFT process A second update. *Aust. J. Chem.* **2009**, *62*, 1402–1472.

[7] Barner-Kowollik, C., Buback, M., Charleux, B., Coote, M. L., Drache, M., Fukuda, T., Goto, A., Klumperman, B., Lowe, A. B., Mcleary, J. B., Moad, G., Monteiro, M. J., Sanderson, R. D., Tonge, M. P., and Vana, P. Mechanism and kinetics of dithiobenzoate-mediated RAFT polymerization. I. The current situation. *J. Polym. Sci. Part A Polym. Chem.* **2006**, *44*, 5809–5831.

[8] Chong, Y. K., Moad, G., Rizzardo, E., and Thang, S. H. Thiocarbonylthio End Group Removal from RAFT-Synthesized Polymers by Radical-Induced Reduction. *Macromolecules* **2007**, *40*, 4446–4455

[9] Masci, G., Giacomelli, L., and Crescenzi, V. Atom Transfer Radical Polymerization of N-isopropylacrylamide *Macromol. Rapid. Commun.* **2004**, *32*, 559–564.

[10] Matyjaszewski, K., and Xia, J. Atom transfer radical polymerization. *Chem. Rev.* **2001**, *101*, 2921–2990.

[11] Kato, M., Kamigaito, M., Sawamoto, M., and Higashimuras, T. Polymerization of Methyl Methacrylate with the Carbon TetrachloridelDichlorotris-(triphenylphosphine)ruthedum(II)/ Methylaluminum Bis(2,6-di-tert-butylphenoxide) Initiating System: Possibility of Living Radical Polymerization1. *Macromolecules* **1996**, *28*, 1721–1723.

[12] Jakubowski, W., Min, K., and Matyjaszewski, K. Activators regenerated by electron transfer for atom transfer radical polymerization of styrene. *Macromolecules* **2006**, *39*, 39–45.

[13] Barner-Kowollik, C., Buback, M., Charleux, B., Coote, M. L., Drache, M., Fukuda, T., Goto, A., Klumperman, B., Lowe, A. B., Mcleary, J. B., Moad, G., Monteiro, M. J., Sanderson, R. D., Tonge, M. P., and Vana, P. Mechanism and kinetics of dithiobenzoate-mediated RAFT polymerization. I. The current situation. *J. Polym. Sci. Part A Polym. Chem.*

2006, *44*, 5809–5831.

[14] Takemoto, H., Miyata, K., Ishii, T., Hattori, S., Osawa, S., Nishiyama, N., and Kataoka, K. Accelerated Polymer–Polymer Click Conjugation by Freeze–Thaw Treatment. *Bioconjug. Chem.* **2012**, *23*, 1503–1506.

[15] Convertine, A. J., Ayres, N., Scales, C. W., Lowe, A. B., and McCormick, C. L. Facile, Controlled, Room-Temperature RAFT Polymerization of N -Isopropylacrylamide †. *Biomacromolecules* **2004**, *5*, 1177–1180.

[16] Scales, C. W., Convertine, A. J., and McCormick, C. L. Fluorescent labelling of RAFT-generated poly(N-isopropylacrylamide) via a facile maleimide-thiol coupling reaction. *Biomacromolecules* **2006**, *7*, 1389–1392.

[17] Xia, Y., Yin, X., Burke, N. A. D., and Stöver, H. D. H. Thermal Response of Narrow-Disperse Poly(N -isopropylacrylamide) Prepared by Atom Transfer Radical Polymerization. *Macromolecules* **2005**, *38*, 5937–5943.

[18] Coca, S., Jasieczek, C. B., Beers, K. L., and Matyjaszewski, K. Polymerization of acrylates by atom transfer radical polymerization. Homopolymerization of 2-hydroxyethyl acrylate. *J. Polym. Sci. Part a-Polymer Chem.* **1998**, *36*, 1417–1424.

[19] Xia, Y., Yin, X., Burke, N. A. D., and Sto, H. D. H. Thermal Response of Narrow-Disperse Poly (N-isopropylacrylamide) Prepared by Atom Transfer Radical Polymerization. *Macromolecules* **2005**, 5937–5943.

[20]Xia, Y., Burke, N. A. D., and Stöver, H. D. H. End group effect on the thermal response of narrow-disperse poly(N-isopropylacrylamide) prepared by atom transfer radical polymerization. *Macromolecules* **2006**, *39*, 2275–2283.

[21] Chen, G., and Hoffman, A. S. Preparation and properties of thermoreversible, phase-separating enzyme-oligo(N-isopropylacrylamide) conjugates. *Bioconjug. Chem.* **1993,** *4*, 509–514.

[22] Teodorescu, M., and Matyjaszewski, K. Atom transfer radical polymerization of (meth)acrylamides. *Macromolecules* **1999**, *32*, 4826–4831.

[23] Rademacher, J. T., Baum, M., Pallack, M. E., Brittain, W. J., and Simonsick, W. J. Atom transfer radical polymerization of N,N-dimethylacrylamide. *Macromolecules* **2000**, *33*, 284–288.

Chapter 3. Physicochemical properties of PNIPAAm-siRNA

3.1. Abstract

The physicochemical properties of poly(*N*-isopropylacrylamide) (PNIPAAm)-conjugated siRNA are discussed in this chapter. The LCST related-behavior of PNIPAAm before and after the conjugation with siRNA was investigated. The temperature at 50% optical transmittance for end group modified PNIPAAm in 10 mM HEPES pH 7.4 solution was almost 33 °C, indicating that PNIPAAm exhibited LCST related-behavior even after the structure modification. Through scattering light intensities analysis, PNIPAAm-siRNA in 10 mM HEPES pH 7.4 solution started to aggregate at 35 °C, upon heating the solution from 20 °C to 40 °C, suggesting that the conjugated PNIPAAm segment undergoes the LCST related-behavior even in the vicinal presence of siRNA. In addition, the hydrodynamic diameter of PNIPAAm-siRNA in 100 nM was investigated using fluorescence correlation spectroscopy (FCS) measurement at room temperature and 37 °C. The hydrodynamic diameter of PNIPAAm-siRNA decreased after heating the PNIPAAm-siRNA solution at 37 °C.

3.2. Introduction

Poly (*N*-isopropylacrylamide) (PNIPAAm) is the most commonly and successfully studied polymer among thermoresponsive polymers. PNIPAAm is a polyvinyl polymer and a chemical isomer of polyleucine, but has the polar peptide group in the side chain, rather than in the backbone. The LCST of PNIPAAm is at 33 °C, which is close to the physiological conditions, and thus, PNIPAAm has been applied in biological application including drug delivery and tissue engineering [1-5]. Below LCST, PNIPAAm is in coil form and hydrophilic state, while above LCST, PNIPAAm collapse their conformation into globule form and hydrophobic state. The LCST of PNIPAAm can be raised or lowered by introduction of hydrophilic or hydrophobic vinyl comonomers, respectively [6,7].

A great number of studies have been devoted to investigate the behavior of temperature responsive PNIPAAm, and many techniques have been used to determine its LCST. For example, the coil-to-globule transition as well as the changes in hydrodynamic diameter of PNIPAAm and its copolymer has been widely investigated through UV-vis measurement, light scattering, fluorescence, infrared spectroscopy as well as differential scanning calorimetry [8-12]. In addition, PNIPAAm microhydrogel particle suspended in water also has been determined their phase transition through photon density wave spectroscopy, focused beam reflectance measurement, and particle vision microscope measurement [13, 14]. These studies exhibit the phase transition of PNIPAAm at around 33 °C.

In the present study, the LCST related-behaviors of PNIPAAm solutions before and after the conjugation with an siRNA molecule were determined through UV-vis measurement, light scattering intensity analysis, and fluorescence correlation spectroscopy. Before conjugation with an siRNA molecule, thioether terminus PNIPAAm, PNIPAAm-TE and DBCO terminus PNIPAAm, PNIPAAm-DBCO in 10 mM HEPES pH 7.4 solutions were investigated from the view of the temperature at 50% of optical transmittance upon heating.

Moreover, because my designed PNIPAAm-siRNA conjugate is not nanoparticle, the determination of coil-to-globule form is impossible to be visualized using high beam instrument such as transmission electron microscopy. In addition, siRNA is very small molecule and such high energy beam may break the siRNA structure. Therefore, the coil-to-globule transition behavior of my newly conjugated PNIPAAm-siRNA was investigated by light scattering intensity analysis. For this experiment, I investigated the scattering intensity of PNIPAAm-siRNA solution at two concentrations: 15 μM and 5 μM of siRNA.

I also investigated the coil-to-globule transition behavior of PNIPAAm-siRNA using fluorescence correlation spectroscopy (FCS). The measurement was performed in 10 mM HEPES pH 7.4 buffer solution at low concentration (100 nM siRNA), which is the

concentration similar to concentration in the cell experiments. FCS is a technique to detect single molecule fluorescence to study the molecular dynamics. In FCS, a fluorescent molecule emits photons while moving in a confocal volume. The fluorescent intensity of the moving molecule was recorded and analyzed to obtain their diffusion coefficients and hydrodynamic radius [15, 16]. Owing to a very high sensitivity for single molecule, FCS not only has been used in molecular cell biology, but it also has been applied in polymer and colloid science, such as to investigate stimuli-responsive polymer systems [17]. In this regard, for FCS measurement, I used TAMRA-labeled PNIPAAm-siRNA for the determination of hydrodynamic diameter at different temperature. Carboxytetramethylrhodamine (TAMRA) is one of rhodamine derivatives. TAMRA has fluorescence property of excitation wavelength at 540 nm and emission wavelength at 580 nm, which is often used as a fluorescence probe to study the distribution of molecules such as cell-penetrating peptides (CPPs) and as fluorescence partner in applications such as luminescence resonance energy transfer (LRET) and fluorescence resonance energy transfer (FRET) [18-20]. In the present study, the hydrodynamic diameter of PNIPAAm-siRNA was calculated based on Stokes-Einstein equation derived from the obtained diffusion coefficient and used Rhodamine 6G as a reference sample. The Stokes-Einstein equation as shown in Figure 3-1, where d_H is hydrodynamic diameter, k is stand for Boltzmann's Constant, T is for absolute temperature, η is for the viscosity of solution and D is for diffusion coefficient obtained from FCS measurement.

$$d_H = \frac{k\,T}{3\,\pi\,\eta\,D}$$

Figure 3-1. The Stokes-Einstein equation

3.3. Experimental procedures

3.3.1. Transmittance analysis of PNIPAAm-TE

Solutions of PNIPAAm-TE for molecular weight of 10,000 g/mol, 20, 000 g/mol and 40,000 g/mol for concentration 5 mg/mL in 10 mM HEPES pH 7.4 were prepared at room temperature. The transmittance of the solutions was measured at 500 nm at various temperatures using spectrometer (V-650, JASCO) with heating rate 0.1 °C/min and stirrer speed 350 rpm. The LCST was determined as the temperature shows 50% of the optical transmittance of the samples.

3.3.2. Transmittance analysis of PNIPAAm-DBCO

In a similar manner with the solution of PNIPAAm-TE series, PNIPAAm-DBCO for molecular weight of 10,000 g/mol, 20, 000 g/mol and 40,000 g/mol for concentration 5 mg/mL in 10 mM HEPES pH 7.4 were prepared at room temperature. The transmittance of PNIPAAm-DBCO solutions was measured at 500 nm at various temperatures using spectrometer (V-650, JASCO). The solutions were heated with heating rate 0.1 °C/min and stirred at speed 350 rpm. The LCST was determined as the temperature shows 50% of the optical transmittance of the samples.

3.3.3. Light scattering analysis of PNIPAAm-siRNA

The scattering light intensities of the solutions of siRNA and its polymer conjugates in 10 mM HEPES buffer (pH 7.3) at 15 μM and 5 μM siRNA concentrations (30 μL) were analyzed using a Zetasizer Nano ZS (Malvern Instruments, Worcestershire, UK) at a detection angle of 173 °. The scattering light intensities were measured at various temperatures from 20 to 40 °C. The results are presented as mean value of count rate in kilo counts per second (kcps) and standard deviation obtained from three times repetitions.

3.3.4. Evaluation of reversible thermoresponsiveness of PNIPAAm$_{40K}$-siRNA by light scattering analysis

Reversible thermoresponsiveness of PNIPAAm40K-siRNA in 10 mM HEPES pH 7.4 with 150 mM NaCl at 5 μM siRNA concentration (30 μL) was analyzed using a Zetasizer Nano ZS at a detection angle of 173 °. The scattering light intensities of solution were measured at heating temperature from 25 to 40 °C and cooling temperature from 40 to 25 °C. The temperature of the solution was maintained for 3 min prior to temperature changing. The results are presented as mean value of count rate in kilo counts per second (kcps) and standard deviation obtained from three times repetitions.

3.3.5. Fluorescence correlation spectroscopy (FCS) measurement of PNIPAAm-siRNA

Solutions of TAMRA-labeled siRNA and its polymer conjugates in 10 mM HEPES buffer (pH 7.3) at 100 nM siRNA concentration were prepared at room temperature and were put into an 8-well chamber (Nalge Nunc International, Rochester, NY, USA) for measurements. FCS analysis was performed using a LSM710 confocal laser scanning microscope (CLSM, Carl Zeiss, Oberlochen, Germany) equipped with a Confocor3 module and C-Apochromat 40 × water immersion objective. An argon laser (514 nm) was used for excitation and a 560 – 600 nm band pass filter for emission. The measurements were performed for ten times repetitions at ambient temperature and 37 °C with a sampling time for 10 s. The diffusion coefficients of TAMRA-labeled siRNA and its polymer conjugates were calculated according to the manufacture's protocol and rhodamine6G as a reference, and the obtained diffusion coefficients were further converted into hydrodynamic diameter based on Stokes-Einstein equation.

3.3.6. Evaluation of reversible thermoresponsiveness of PNIPAAm-siRNA by FCS

Solutions of TAMRA-labeled unconjugated siRNA, TAMRA-labeled $PNIPAAm_{40K}$-siRNA and TAMRA-labeled PEG_{40K}-siRNA in 10 mM HEPES buffer (pH 7.3) at 100 nM siRNA concentration were prepared at room temperature and were put into an 8-well chamber for measurements. FCS analysis was performed using a LSM710 confocal laser scanning microscope equipped with a Confocor3 module and C-Apochromat 40 × water immersion objective. An argon laser (514 nm) was used for excitation and a 560 – 600 nm band pass filter was used for emission. The measurements were performed for ten times repetitions at heated temperature (37 °C) and cooled temperature (30 °C) with a sampling time for 10 s. The diffusion coefficients of TAMRA-labeled siRNA and its polymer conjugates were calculated according to the manufacture's protocol and rhodamine6G as a reference, and the obtained diffusion coefficients were further converted into hydrodynamic diameter based on Stokes-Einstein equation.

3.4. Results

3.4.1. Turbidity measurement of PNIPAAm using UV-vis measurement

Both end groups of the obtained PNIPAAm-CTA was modified into two groups: trithiocarbonate group of PNIPAAm-CTA was modified into thioether group (PNIPAAm-TE), and the carbonyl group of the other terminus of PNIPAAm-CTA was converted into a DBCO group (PNPAAm-DBCO). Both modifications end group of PNIPAAm-CTA (PNIPAAm-TE and PNIPAAm-DBCO) were determined their turbidity at 50% optical transmittance. Figure 3-2, Figure 3-3 and Figure 3-4 show the temperature-dependent optical transmittance at 500 nm of PNIPAAm-TE for molecular weight at 10,000 g/mol ($PNIPAAm_{10K}$-TE), 20,000 g/mol ($PNIPAAm_{20K}$-TE) and 40,000 g/mol ($PNIPAAm_{40K}$-TE),

respectively. Upon heating from 25 °C to 40 °C at heating rate 0.1 °C/min while stirring the solutions at 350 rpm, the temperatures at 50% optical transmittance for $PNIPAAm_{10K}$-TE, $PNIPAAm_{20K}$-TE and $PNIPAAm_{40K}$-TE in 10 mM HEPES pH 7.4 solution (5 mg/mL) were ~35 °C, ~36 °C and ~35 °C, respectively.

Furthermore, I also investigated the transmittance behavior of DBCO-modified PNIPAAm (PNIPAAm-DBCO) for different molecular weight in 10 mM HEPES pH 7.4 solutions. The temperature-dependent optical transmittance at 500 nm for $PNIPAAm_{10K}$-DBCO, $PNIPAAm_{20K}$-DBCO and $PNIPAAm_{40K}$-DBCO at 500 nm as shown in Figure 3-5, Figure 3-6 and Figure 3-7, respectively. Upon heating the solution at rate of 0.1°C/min and stirred at 350 rpm for $PNIPAAm_{10K}$-DBCO, $PNIPAAm_{20K}$-DBCO and $PNIPAAm_{40K}$-DBCO showed the temperatures at 50% optical transmittance at ~32 °C, ~34 °C and ~33 °C, respectively.

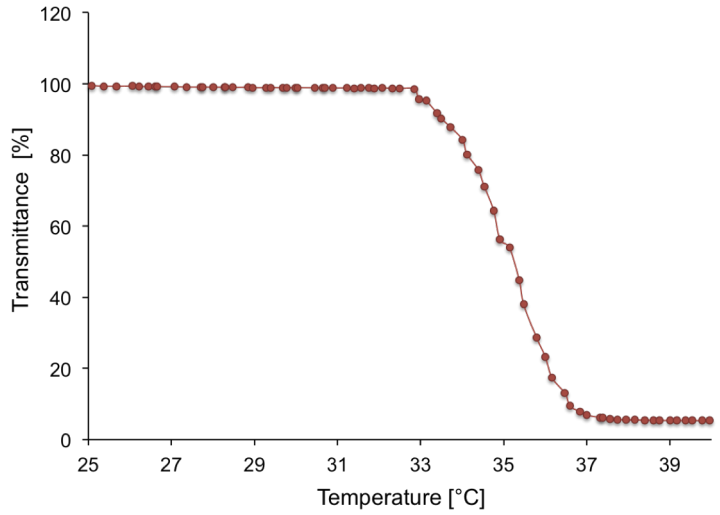

Figure 3-2. Turbidity curve of PNIPAAm$_{10K}$-TE in 10 mM HEPES pH 7.4.

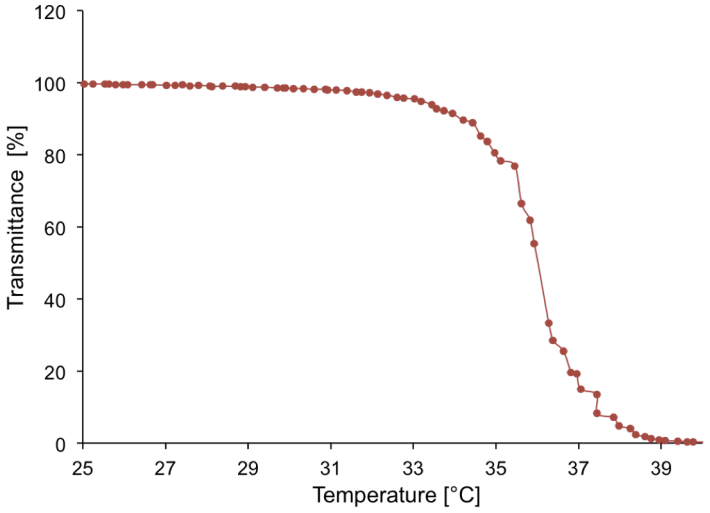

Figure 3-3. Turbidity curve of PNIPAAm$_{20K}$-TE in 10 mM HEPES pH 7.4.

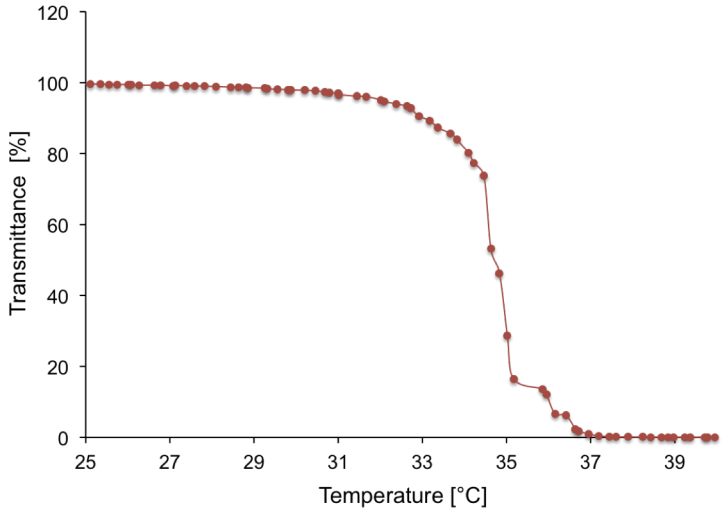

Figure 3-4. Turbidity curves of PNIPAAm$_{40K}$-TE in 10 mM HEPES pH 7.4.

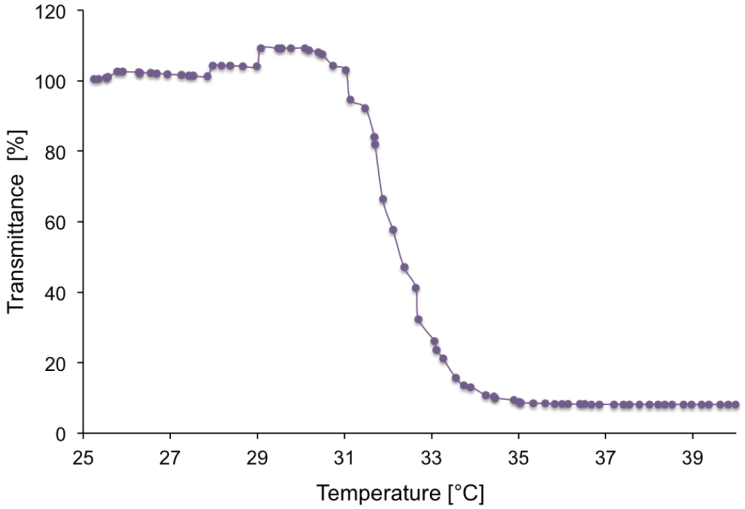

Figure 3-5. Turbidity curve of PNIPAAm$_{10K}$-DBCO in 10 mM HEPES pH 7.4.

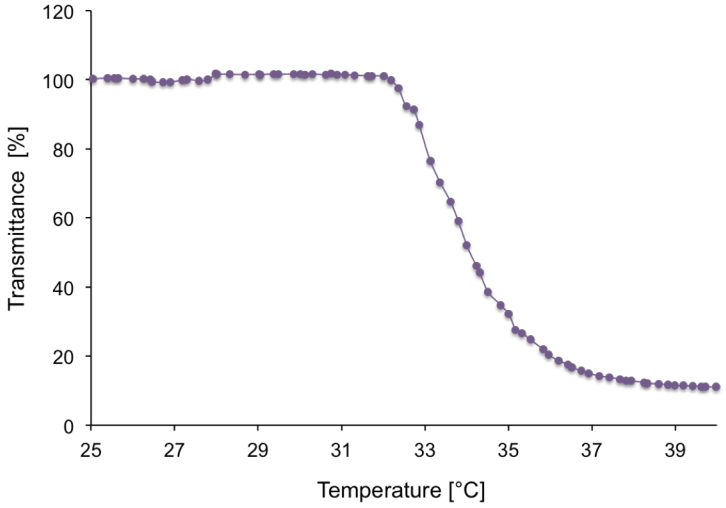

Figure 3-6. Turbidity curve of PNIPAAm$_{20K}$-DBCO in 10 mM HEPES pH 7.4.

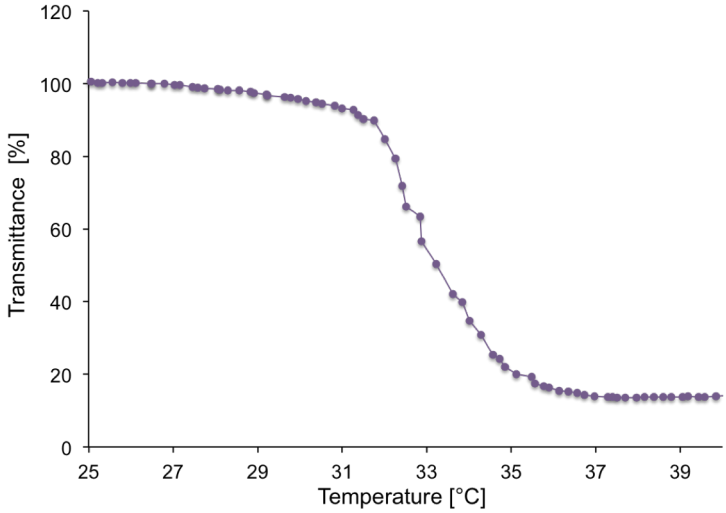

Figure 3-7. Turbidity curve of PNIPAAm$_{40K}$-DBCO in 10 mM HEPES pH 7.4.

3.4.2. Scattering light intensity analysis of PNIPAAm-siRNA

To confirm the coil-to-globule transition behavior of PNIPAAm after the conjugation with an siRNA molecule, as a widely used method, I performed the scattering light intensity analysis for PNIPAAm-siRNA, by changing the temperature of solution at two concentrations: at 15 μM siRNA and 5 μM siRNA. Upon heating from 26 °C to 40 °C of $PNIPAAm_{10K}$-siRNA, $PNIPAAm_{20K}$-siRNA and $PNIPAAm_{40K}$-siRNA solutions in 10 mM

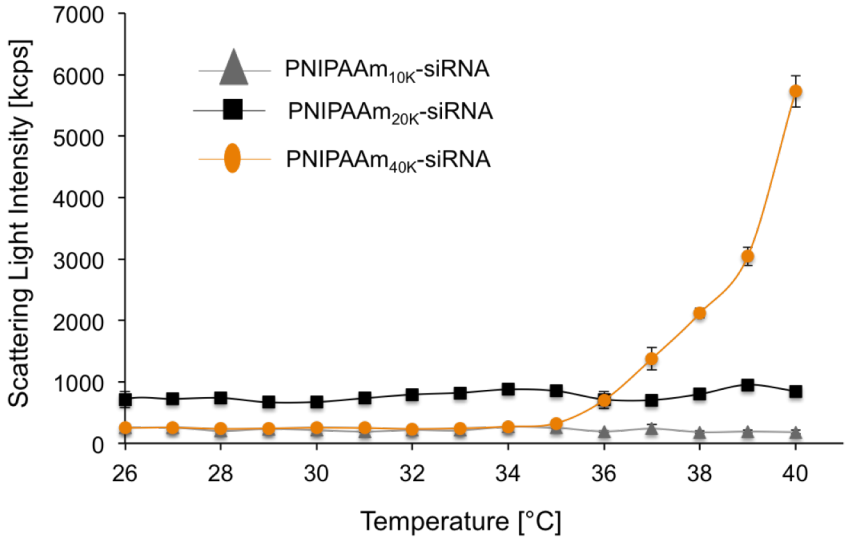

Figure 3-8. Light scattering intensities of $PNIPAAm_{10K}$-siRNA, $PNIPAAm_{20K}$-siRNA and $PNIPAAm_{40K}$-siRNA in 10 mM HEPES pH 7.4 solution at 15 μM siRNA. Results were shown as mean and standard deviation obtained from three measurements.

HEPES pH 7.4, only solution of $PNIPAAm_{40K}$-siRNA showed the increasing of scattering light intensities at 35 °C as shown in Figure 3-7. Meanwhile, the solutions of $PNIPAAm_{10K}$-siRNA and $PNIPAAm_{20K}$-siRNA did not show any changes for scattering light intensity upon heating (Figure 3-8).

Moreover, the scattering light intensity of $PNIPAAm_{40K}$-siRNA was also determined at lower concentration, which is 5 μM siRNA concentration. As a result, upon heating, through scattering light intensities analysis, the intensity of PNIPAAm-siRNA solution in 10 mM HEPES pH 7.4 at 5 μM siRNA started to increase at 35 °C. At the same time, I compared the

scattering light intensity for non-thermoresponsive polymer-conjugated siRNA (PEG_{40K}-siRNA) and unconjugated siRNA solutions at 5 μM siRNA concentration. Upon heating from 20 °C to 40 °C, both PEG-siRNA and unconjugated siRNA solutions maintained their light scattering intensities as shown in Figure 3-9.

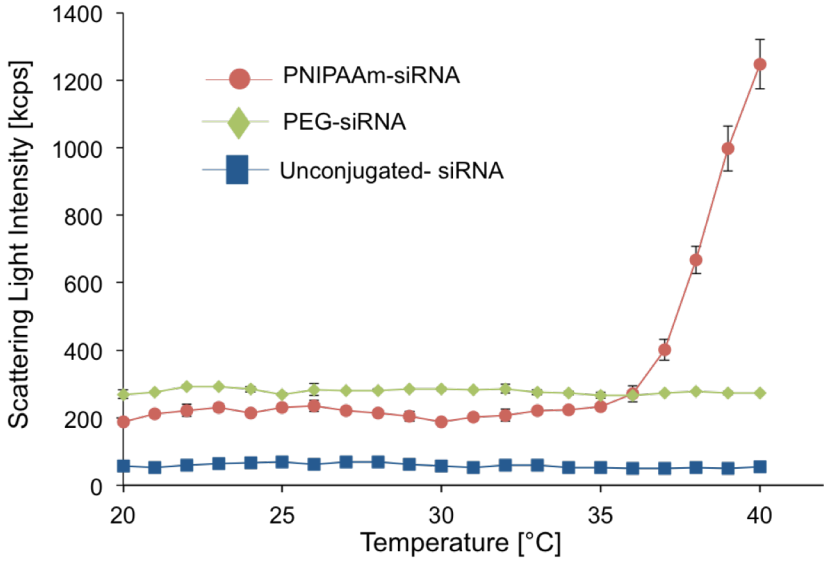

Figure 3-9. Light scattering intensities of $PNIPAAm_{40k}$-siRNA, PEG_{40K}-siRNA and Unconjugated siRNA in 10 mM HEPES pH 7.4 solution at 5 μM siRNA. Results were shown as mean and standard deviation obtained from three measurements.

In addition, I investigated reversible thermoresponsiveness of $PNIPAAm_{40K}$-siRNA through scattering light analysis at 5 μM siRNA concentration in 10 mM HEPES pH 7.4 with 150 mM NaCl solution. As the results, upon heating from 25 to 40 °C, the light scattering intensity started to increase at 33 °C and hysteresis can be observed upon cooling the solution as shown in Figure 3-10.

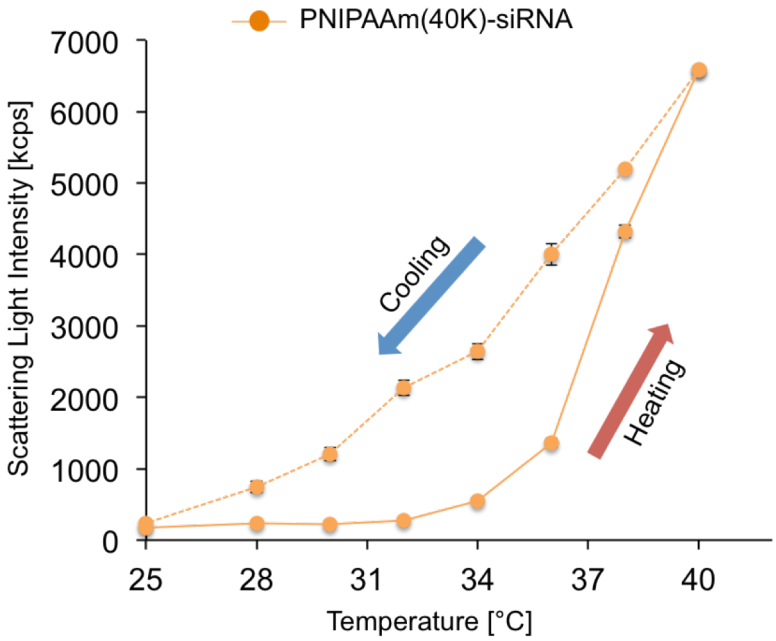

Figure 3-10. Light scattering intensity of PNIPAAm$_{40k}$-siRNA on heating and cooling in 10 mM HEPES pH 7.4 with 150 mM NaCl solution at 5 μM siRNA. Results were shown as mean and standard deviation obtained from three measurements.

3.4.3. Hydrodynamic diameter of PNIPAAm-siRNA

Based on the result of scattering light intensity analysis, I observed that only PNIPAAm-siRNA with molecular weight of 40 000 g/mol showed the increasing of scattering light intensity upon heating the solution. Then, I investigated the hydrodynamic diameter of PNIPAAm$_{40K}$-siRNA at room temperature (below LCST) and at 37 °C (above LCST). As the result, the hydrodynamic diameter of PNIPAAm$_{40K}$-siRNA decreased almost ~1.1 nm in size of diameter from 7.61± 0.23 nm at room temperature to 6.50 ± 0.21 nm at 37 °C. As control samples, the hydrodynamic diameters of non-thermoresponsive polymer, PEG$_{40K}$-siRNA, and unconjugated siRNA were analyzed, showing that both molecules maintained their size even after heating the solution. At room temperature and 37 °C, the size of unconjugated siRNA were 4.14 ± 0.44 nm and 4.10 ± 0.21 nm in diameter, respectively. PEG$_{40K}$-siRNA showed

8.83 ± 0.39 nm and 8.83 ± 0.29 nm of hydrodynamic diameter at room temperature and at 37 °C, respectively. The results are summarized in Table 3-1.

Table 3-1. The hydrodynamic diameters (nm) of TAMRA-labeled unconjugated siRNA, TAMRA-labeled PNIPAAm$_{40K}$-siRNA, and TAMRA-labeled PEG$_{40K}$-siRNA for 100 nM siRNA (10 mM HEPES pH 7.4) at room temperature and 37 °C, determined by FCS measurement. Results were shown as mean and standard deviation obtained from ten measurements.

	Unconjugated-siRNA	PNIPAAm$_{40K}$-siRNA	PEG$_{40K}$-siRNA
r. t.	4.14 ± 0.44	7.61 ± 0.23	8.83 ± 0.39
37 °C	4.10 ± 0.28	6.50 ± 0.21	8.83 ± 0.29

Moreover, I evaluated the reversible thermoresponsiveness of PNIPAAm$_{40K}$-siRNA by FCS measurement. As control samples, the hydrodynamic diameter of TAMRA-labeled PEG$_{40K}$-siRNA and TAMRA-labeled unconjugated siRNA were also evaluated. The calculated hydrodynamic diameter for all of the samples based on obtained diffusion coefficients were illustrated in Figure 3-11. As the results, the hydrodynamic diameter of PNIPAAm$_{40K}$-siRNA showed the reversible decrease and increase cycle upon heating and cooling the solution. Meanwhile, PEG$_{40K}$-siRNA and unconjugated-siRNA maintained their hydrodynamic diameters over the heating and cooling processes.

Although the scattering light intensity of PNIPAAm$_{10K}$-siRNA and PNIPAAm$_{20K}$-siRNA did not show any changes upon heating the solutions, I investigated the hydrodynamic diameter at room temperature and at 37 °C for both of samples along with PEG-siRNA series as a control through FCS measurement. The hydrodynamic diameters calculated based on obtained diffusion coefficient were summarized in Table 3-2. According to the results, the hydrodynamic diameters for PNIPAAm$_{10K}$-siRNA slightly decreased from 5.63 ± 0.37 nm at

room temperature to 5.51 ± 0.29 nm at 37 °C. PNIPAAm$_{20K}$-siRNA also showed slight decrease in size of diameter from 6.02 ± 0.22 nm at room temperature to 5.61 ± 0.49 nm at 37 °C. Meanwhile, the hydrodynamic diameters for PEG$_{10K}$-siRNA and PEG$_{20K}$-siRNA maintained their size even when heated the solutions at 37 °C.

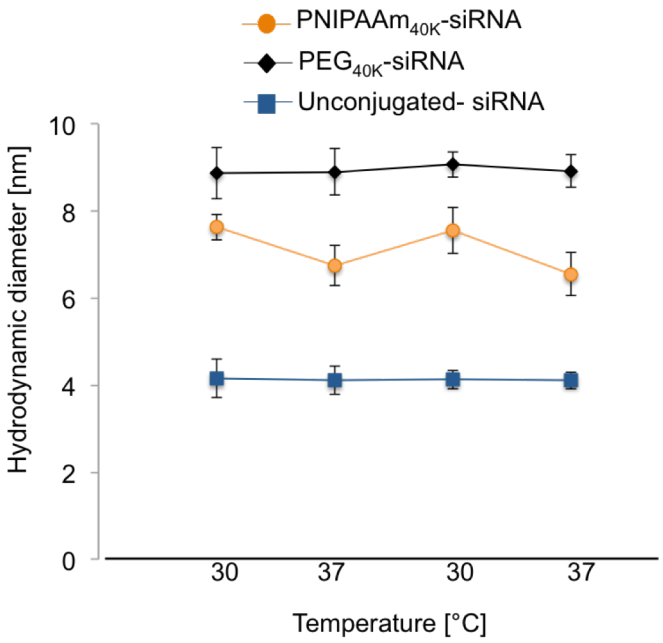

Figure 3-11. The hydrodynamic diameters (nm) of TAMRA-labeled unconjugated siRNA, TAMRA-labeled PNIPAAm$_{40K}$-siRNA, and TAMRA-labeled PEG$_{40K}$-siRNA for 100 nM siRNA (10 mM HEPES pH 7.4) at cycle 30 and 37 °C, determined by FCS measurement. Results were shown as mean and standard deviation obtained from ten measurements.

Table 3-2. The list of hydrodynamic diameters (nm) of TAMRA-labeled unconjugated siRNA and TAMRA-labeled siRNA conjugated polymers with various molecular weights (100 nM siRNA, 10 mM HEPES pH 7.4) at room temperature and 37 °C, determined by FCS measurement. Results were shown as mean and standard deviation obtained from ten measurements.

	Hydrodynamic diameter, d_H (nm)	
	r. t.	37 °C
Unconjugated-siRNA	4.14 ± 0.44	4.10 ± 0.28
$PNIPAAm_{10K}$-siRNA	5.63 ± 0.37	5.51 ± 0.29
$PNIPAAm_{20K}$-siRNA	6.02 ± 0.22	5.61 ± 0.49
$PNIPAAm_{40K}$-siRNA	7.61 ± 0.23	6.50 ± 0.21
PEG_{10K}-siRNA	6.04 ± 0.31	6.09 ± 0.18
PEG_{20K}-siRNA	7.09 ± 0.29	7.02 ± 0.34
PEG_{40K}-siRNA	8.83 ± 0.29	8.83 ± 0.29

3.5. Discussion

The LCST-related behavior of newly synthesized PNIPAAm with end group modification as well as PNIPAAm-siRNA was evaluated though transmittance, scattering light intensity and FCS measurements. After the modification of the end group into PNIPAAm-TE, the temperature at 50% optical transmittance were ~35 °C, whereas after the introduction of DBCO group into carbonyl group terminus, the temperature at 50% optical transmittance slightly decreased to ~33 °C. The slight decrease of the temperature at 50% optical transmittance is possibly because of a hydrophobic phenyl group of DBCO structure, and it is consistent with report that hydrophobic materials decreased the LCST of PNIPAAm [21]. The chemical structures of PNIPAAm-TE and PNIPAAm-DBCO are as shown in Figure 3-10.

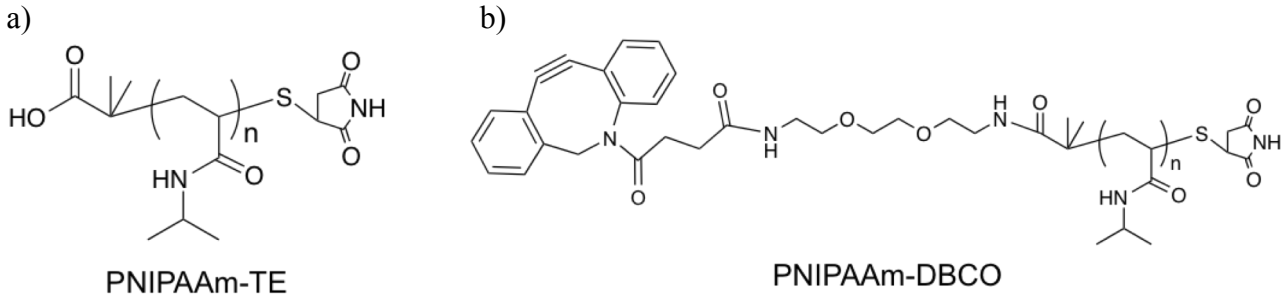

Figure 3-12. Chemical structures of a) PNIPAAm-TE and b) PNIPAAm-DBCO

Moreover, the LCST of end group modified PNIPAAm-CTA showed LCST close to the reported PNIPAAm, which is 33 °C.

According to the scattering light intensity analysis, PNIPAAm$_{40K}$-siRNA at both 15 μM and 5 μM siRNA concentrations in 10 mM HEPES pH 7.4 showed that the solution started to increase their scattering light intensity at 35 °C, indicating that the conjugated PNIPAAm segment undergoes phase transition behavior from coil form to globule form. Globule form of the conjugated PNIPAAm would aggregate each other through hydrophobic interaction, and thus resulting in increased intensity of scattering light. The increasing of scattering light intensity of PNIPAAm-siRNA solution indicates that the conjugated PNIPAAm segment undergoes coil-globule transition behavior even in the vicinal presence of siRNA. Moreover, hysteresis was observed after the heated solution was cooled, possibly because the additional interchain hydrogen bond was formed in the aggregated form above LCST, which can not be completely removed at the near LCST upon cooling process [22].

Moreover, the hydrodynamic diameter of TAMRA-labeled PNIPAAm$_{40K}$-siRNA (100 nM) in 10 mM HEPES pH 7.4 solution decreased almost ~1.1 nm in diameter after heating the solution from room temperature to 37 °C as calculated based on obtained diffusion coefficient from FCS measurement using Stokes-Einstein equation, indicating that conjugated

PNIPAAm-segment underwent coil-to-globule transition behavior upon changing the environment temperature. Meanwhile, TAMRA-labeled unconjugated siRNA and TAMRA-labeled PEG-siRNA maintained their hydrodynamic diameters even when changing the temperature. These results suggest a high potential for the conjugated PNIPAAm segment for thermoresponsive exposure of conjugates siRNA and associated artificial control of the vicinal siRNA toward manipulative induction of gene silencing activity in the cell.

3.6. Conclusion

In summary, the LCST-related behaviors of PNIPAAm and PNIPAAm-siRNA were successfully confirmed through optical transmittance measurement, temperature-dependent scattering light intensity analysis and fluorescence correlation spectroscopy analysis. As the results, PNIPAAm polymers with end group modification maintained their thermoresponsive behavior with the LCST closely to the report (33 °C). Moreover, the increasing in scattering light intensity of PNIPAAm-siRNA solution at 35 °C upon heating the solution, indicating the thermoresponsive behavior of PNIPAAm segment even in the presence of vicinal siRNA. Furthermore, decreasing in hydrodynamic diameter of PNIPAAm-siRNA upon heating the solution at 37 °C suggests that conjugated PNIPAAm segment undergoes coil-globule transition behavior for thermoresponsive exposure of siRNA.

3.7. References

[1] Ward, M. A., and Georgiou, T. K. Thermoresponsive Polymers for Biomedical Applications **2011**, 1215–1242.

[2] Roy, D., Cambre, J. N., and Sumerlin, B. S. Future perspectives and recent advances in stimuli-responsive materials. *Prog. Polym. Sci.* **2010**, *35*, 278–301.

[3] Stuart, M. A. C., Huck, W. T. S., Genzer, J., Müller, M., Ober, C., Stamm, M.,

Sukhorukov, G. B., Szleifer, I., Tsukruk, V. V., Urban, M., Winnik, F., Zauscher, S., Luzinov, I., and Minko, S. Emerging applications of stimuli-responsive polymer materials. *Nat. Mater.* **2010**, *9*, 101–113.

[4] Ayano, E., Karaki, M., Ishihara, T., Kanazawa, H., and Okano, T. Poly (N-isopropylacrylamide)-PLA and PLA blend nanoparticles for temperature-controllable drug release and intracellular uptake. *Colloids Surfaces B Biointerfaces* **2012**, *99*, 67–73.

[5] Matsuzaka, N., Nakayama, M., Takahashi, H., Yamato, M., Kikuchi, A., and Okano, T. Terminal-functionality effect of poly (N-isopropylacrylamide) brush surfaces on temperature-controlled cell adhesion/detachment. *Biomacromolecules* **2013**, 14, 9, 3164-3171.

[6] Feil, H., Bae, Y. H., Feijen, J., and Kim, S. W. Effect of comonomer hydrophilicity and ionization on the lower critical solution temperature of N-isopropylacrylamide copolymers. *Macromolecules* **1993**, *26*, 2496–2500.

[7] López-Pérez, P. M., Da Silva, R. M. P., Pashkuleva, I., Parra, F., Reis, R. L., and San Roman, J. Hydrophobic-electrostatic balance driving the LCST offset aggregation-redissolution behavior of N -Alkylacrylamide-based ionic terpolymers. *Langmuir* **2010**, *26*, 5934–5941.

[8] Wu, C., and Zhou, S. Laser Light Scattering Study of the Phase Transition of Poly(N-isopropylacrylamide) in Water. *Macromolecules* **1995**, *28*, 8387.

[9] Piçarra, S., Relógio, P., Afonso, C. A. M., Martinho, J. M. G., and Farinha, J. P. S. Coil-Globule Transition of Poly(Dimethylacrylamide): Fluorescence and Light Scattering Study. *Macromolecules* **2003**, *36*, 8119–8129.

[10] Boutris, C., Chatzi, E. G., and Kiparissides, C. Characterization of the LCST behaviour of aqueous poly(N-isopropylacrylamide) solutions by thermal and cloud point techniques. *Polymer (Guildf).* **1997**, *38*, 2567–2570.

[11] Cheng, H., Shen, L., and Wu, C. LLS and FTIR studies on the hysteresis in association

and dissociation of poly(N-isopropylacrylamide) chains in water. *Macromolecules* **2006**, *39*, 2325–2329.

[12] Cho, E. C., Lee, J., and Cho, K. Role of bound water and hydrophobic interaction in phase transition of poly(N-isopropylacrylamide) aqueous solution. *Macromolecules* **2003**, *36*, 9929–9934.

[13] Ooi, H. W., Jack, K. S., Peng, H., and Whittaker, A. K. "Click" PNIPAAm hydrogels – a comprehensive study of structure and properties. *Polym. Chem.* **2013**, *4*, 4788-4800.

[14] Werner, P., Münzberg, M., Hass, R., and Reich, O. Process analytical approaches for the coil-to-globule transition of poly(N-isopropylacrylamide) in a concentrated aqueous suspension. *Anal. Bioanal. Chem.* **2016***,* 1-13

[15] Xie, J., Nakai, K., Ohno, S., Butt, H. J., Koynov, K., and Yusa, S. I. Fluorescence Correlation Spectroscopy Monitors the Hydrophobic Collapse of pH-Responsive Hairy Nanoparticles at the Individual Particle Level. *Macromolecules* **2015**, *48*, 7237–7244.

[16] Berberan-Santos, M. N., and Valeur, B. *Molecular Fluorescence; Principles and Application*, Second Edition, Wiley-VCH. **2012**.

[17] Woll, D. Fluorescence correlation spectroscopy in polymer science. *Rsc Adv.* **2014**, *4*, 2447–2465.

[18] Liu, J., Cheng, J., and Zhang, Y. Upconversion nanoparticle based LRET system for sensitive detection of MRSA DNA sequence. *Biosens. Bioelectron.* **2013**, *43*, 252–256.

[19] Renčiuk, D., Zhou, J., Beaurepaire, L., Guédin, A., Bourdoncle, A., and Mergny, J.-L. A FRET-based screening assay for nucleic acid ligands. *Methods* **2012**, *57*, 122–128.

[20] Bahnsen, J. S., Franzyk, H., Sayers, E. J., Jones, A. T., and Nielsen, H. M. Cell-Penetrating Antimicrobial Peptides - Prospectives for Targeting Intracellular Infections. *Pharm. Res.* **2015**, *32*, 1546–1556.

[21] Duan, Q., Narumi, A., Miura, Y., Shen, X., Sato, S.-I., Satoh, T., and Kakuchi, T.

Thermoresponsive property controlled by end-functionalization of poly(N-isopropylacrylamide) with phenyl, biphenyl, and triphenyl groups. *Polym. J.* **2006**, *38*, 306–310.

[22] Lu, Y., Zhou, K., Ding, Y., Zhang, G., and Wu, C. Origin of hysteresis observed in association and dissociation of polymer chains in water. *Phy. Chem. Chem. Phys.*, **2010**, 12, 3188-3194.

Chapter 4. *In vitro* evaluation of the biological properties of PNIPAAm-siRNA

4.1. Abstract

In this chapter, biological properties of new class of PNIPAAm-siRNA were investigated using luciferase-expressing human cervical cancer cell line, HeLa-Luc and Lipofectamine RNAiMAX as a delivery carrier. Gene silencing activity and interaction with gene silencing related protein, Ago2, for PNIPAAm-siRNA was investigated at two different temperatures (30 °C and 37 °C). The coil form of PNIPAAm segment below LCST inhibits gene silencing activity. Meanwhile, the globule form of PNIPAAm segment above LCST offers a ready access for siRNA to the proteins, and leads to efficient gene silencing. As the results, the treatment with $PNIPAAm_{40K}$-siRNA system at 10 nM siRNA suppressed ~80% of gene silencing at 37 °C (T > LCST), which is close to the treatment with unconjugated siRNA system. In contrast, the treatment with $PNIPAAm_{40K}$-siRNA (10 nM siRNA) at 30 °C (T < LCST) suppressed 20% of luciferase expression, indicating the controlled gene silencing induction by coil-globule transition of conjugated PNIPAAm.

4.2. Introduction

siRNA has a great therapeutic potential due to its strong gene silencing ability in a sequence specific manner [1, 2]. Cationic lipid is one of promising delivery carriers and many studies designed cationic lipids to facilitate and enhance the delivery of DNA or siRNA into the cells [3-7]. Lipofectamine RNAiMAX is one of cationic lipid and has shown high efficiency in delivering siRNA in several types of cancer cells [8-10]. Hence, due to high performance transfection for nucleic acid, Lipofectamine RNAiMAX was used in this study for in vitro evaluation of the biological performance of PNIPAAm-siRNA, i. e., endogenous gene-silencing assay, cellular viability, cellular uptake assay and the association with Ago2 proteins in the cultured human cervical cancer cells stably expressing luciferase (HeLa-Luc). Basic structure of cationic lipid consists of a positively charged head group and one or two

hydrocarbon chains group. The positive charge of cationic lipid will interact with negative charged phosphate backbone of DNA or siRNA and form lipoplex. The positive charges of cationic lipid also interact with negative charged cell membrane, allowing for DNA or siRNA to cross the cellular membrane into the cytoplasm. Once in the cytosol, siRNA is recognized by the proteins to initiate RNAi process.

The temperatures for biological performances were set at 37 °C as above LCST and 30 °C as below LCST. As I described in the previous chapter, through scattering light intensity analysis, PNIPAAm-siRNA solution started to aggregate at 35 °C due to thermoresponsive behavior of the conjugated PNIPAAm segment, and thus, at 37 °C, the conjugated PNIPAAm segment would be in globule form. On the other hand, PNIPAAm segment would be in coil form at 30 °C. The globule form of the conjugated PNIPAAm would offer siRNA molecule for a ready access to the gene silencing related-proteins (e.g., Ago2) in the cytosol, thereby, leads to the efficient gene silencing. Meanwhile, the coil form of the conjugated PNIPAAm would inhibit siRNA molecule recognition by proteins, and thus, inhibits the activity of siRNA. Although the overall rate of metabolism slightly reduces at 30 °C, the energy charge of cells do not decrease [11]. Thus, it would be sufficient to demonstrate biological performances at 30 °C for below LCST. Meanwhile, it is known that the optimum temperature of cell growth is near to body temperature, which is 37 °C.

Immunoprecipitation is one of the most widely used methods for isolation of proteins and other biomolecules from cell or tissue lysates. Immunoprecipitation is the small-scale affinity purification of antigens using a specific antibody that is immobilized to a solid support such as magnetic beads or agarose resin. Many researchers have identified the endogenous RNA induced silencing complex (RISC)-associated RNAs for understanding the RNAi process in the cell by isolating RISC-associated mRNA using immunoprecipitation method [12-14]. Magnetic beads are solid and spherical, which gives sufficient surface area for high-capacity

antibody binding. Moreover, antibody binding of magnetic beads is limited to the surface of each bead. In this study, TAMRA-labeled asRNA, which is recognized by Ago2 and incorporated into endogenous RISC complexes, is collected by immunoprecipitation using magnetic beads containing anti-human Ago2 monoclonal antibody. TAMRA-labeled asRNA was used in this study in order to easily detecting the incorporated amount of asRNA into RISC complexes, i.e., it can easily be calculated based on the fluorescence intensity.

4.3. Materials

A luciferase-expressing human cervical cancer cell line, HeLa-Luc, was purchased from Caliper LifeScience (Hopkinton, MA, USA). Dulbecco's modified eagle's medium (DMEM) was purchased from Sigma Aldrich (St. Louis, MO, USA). Fetal bovine serum (FBS) was purchased from Dainippon Sumitomo Pharma Co., Ltd. (Osaka, Japan). Lipofectamine RNAiMAX was purchased from Invitrogen (Carlsbad, CA). Luciferase Assay System Kit was purchased from Promega Co. (Madison, WI). MagCapture^{TM} microRNA Isolation Kit (Human Ago2) were purchased from Wako Pure Chemical Industries, Ltd. (Osaka, Japan).

4.4. Experimental procedures

4.4.1. Endogenous gene-silencing analysis

HeLa-Luc cells were seeded on a 96-well plate at a density of 2,500 cells per well in 100 μL of DMEM containing 10% FBS, followed by 24 h incubation at 37 °C. Lipoplexes of siRNA and its polymer conjugates were prepared with Lipofectamine RNAiMAX according to the manufacturer's protocol, and were applied to each well at the final siRNA concentration of 0.1 nM, 1 nM, 5 nM, and 10 nM. Gene silencing analysis was performed for different molecular weight of the conjugated polymers (Mw = 10, 000 g/mol, 20,000 g/mol and 40,000 g/mol) and the luciferase-targeting sequence (siLuc) and scrambled sequence

(siScr) were utilized to confirm the sequence-specific gene silencing effect. After another incubation at 37 °C and 30 °C for 48 h, the cells were washed with 100 μL of PBS and lysed with 20 μL of cell culture lysis buffer (Promega, Fitchburg, WI, USA). Luminescence intensities of cell lysates were measured using Luciferase Assay System (Promega) and a luminometer (Glomax 96, Promega). The relative luminescence unit (RLU) value was calculated from the obtained luminescence intensity as a relative value to non-treated wells. The results are presented as mean and standard error of the mean obtained from six samples.

4.4.2. Cellular viability assay

Cells were seeded at a density of 2,500 cells per well in 96-well plates and incubated at 37 °C for 24 h. Lipoplexes of siRNA and its polymer conjugates were prepared in a similar manner to that for gene silencing assay, and were applied to each well at the final siRNA concentrations of 0.1 nM, 1 nM, 5 nM, 10 nM. The cells were further incubated at 37 °C and 30 °C for 48 h. Next, 10 μL of Cell Counting Kit-8 (DOJINDO laboratories, Kumamoto, Japan) solution was added following the manufacturer's protocol. The cellular viability was analyzed by measuring absorbance at 450 nm in each well using a microplate reader (iMark, BIO-RAD). The cellular viability in each well was calculated from the obtained values as a percentage to untreated control wells. The results were expressed as mean and standard error of the mean obtained from six samples.

4.4.3. Cellular uptake analysis using flow cytometry

HeLa-luc cells were seeded onto 12-well plates at a density of 50,000 cells per well in 1 mL of DMEM containing 10% FBS and incubated for 24 h. Next, the culture medium was replaced with fresh culture medium, and lipoplexes prepared from TAMRA-labeled siRNA and its polymer conjugates were applied to each well at the final siRNA concentration of 10

nM. The cells were further incubated at 37 °C and 30 °C for 24 and 48 hours. After the incubation, the cells were washed two times with PBS and collected by trypsinization. Then, the fluorescence intensity of TAMRA from the collected cells was measured by flow cytometric analysis using a Guava easyCyte 6-2L (Merck Millipore, Germany). The results are expressed as mean and standard deviation obtained from three samples.

4.4.4. Counting of Ago2-associated asRNA

HeLa-Luc cells were seeded on a cell culture flask at a density of 1,250,000 cells in 10 mL of DMEM containing 10% FBS, followed by incubation at 37 °C for 24 h. Lipoplexes prepared from TAMRA-labeled siRNA, or its polymer conjugates were applied to cells in a flask at the final siRNA concentration of 100 nM. After another incubation at 37 °C or 30 °C for 48 h, the culture medium was removed and the cells were rinsed twice with PBS, then, collected by trypsinization. The Ago2-associated TAMRA-labeled asRNA was extracted from the collected cells using MagCapture microRNA Isolation Kit (Wako) according to the manufacture's protocol. The fluorescence intensity of the extracted RNA solution was measured by a spectrofluorometer (JASCO, Tokyo, Japan). The amount of collected TAMRA-labeled asRNA and populations of TAMRA-labeled asRNA per cell were calculated based on a standard curve of TAMRA-labeled asRNA. The results were presented as mean and standard error of the mean obtained from three samples.

4.5. Results

4.5.1. Endogenous gene silencing after the treatment with siRNA conjugated polymer at different temperatures

In order to investigate thermoresponsive behavior of the newly conjugated PNIPAAm-siRNA, gene silencing assay was demonstrated in two different temperatures. For the treatment with unconjugated siRNA and its PNIPAAm conjugates of the molecular weight at 10,000 g/mol abbreviated as $PNIPAAm_{10K}$-siLuc and PEG_{10K}-siLuc, at both temperatures, 37 °C and 30 °C, almost no silencing could be observed at 0.1 nM siRNA and gene silencing efficacy increased with increasing the siRNA concentration. The treatment with $PNIPAAm_{10K}$-siLuc and PEG_{10K}-siLuc at 10 nM siRNA at 37 °C dramatically suppressed ~80% and ~70% of luciferase expression, respectively. Gene silencing efficacy for the treatment with PNIPAAm-siLuc and PEG-siLuc at 10 nM siRNA decreased to ~40% for the treatment at 30 °C. Meanwhile, for the treatment with unconjugated siLuc at 30 °C gene silencing showed slightly decreased to ~70% of luciferase expression (Figure 4-1a and Figure 4-1b). The sequence specific silencing by siLuc was confirmed by no luciferase silencing at indicated concentrations after the treatment with scrambled-sequence of siRNA and its siRNA polymer conjugates.

Gene silencing activity for HeLa-Luc cells was also investigated for the treatment with higher molecular weight of the conjugated polymer at 37 °C and 30 °C. Figure 4-2 and figure 4-3 show gene silencing activity of the conjugated polymer with molecular weight for 20,000 g/mol and 40,000 g/mol, respectively. The conjugated polymer for molecular weight of 20,000 g/mol; $PNIPAAm_{20K}$-siLuc and PEG_{20K}-siLuc, and for molecular weight of 40,000 g/mol; $PNIPAAm_{40K}$-siLuc and PEG_{40K}-siLuc. The treatment with $PNIPAAm_{20K}$-siLuc and $PNIPAAm_{40K}$-siLuc at 10 nM siRNA at 37 °C suppressed ~80% of luciferase expression (Figure 4-2a and Figure 4-3a). In sharp contrast, gene silencing efficacy at 30 °C dramatically

dropped to ~ 40% of luciferase suppression for the treatment with PNIPAAm$_{20K}$-siLuc (Figure 4-2b) and ~20% of luciferase suppression for the treatment with PNIPAAm$_{40K}$-siLuc (Figure 4-3b). Meanwhile, the treatment with PEG$_{20K}$-siLuc and PEG$_{40K}$-siLuc showed ~10% of luciferase suppression at 10 nM siRNA at both temperature. Moreover, at 37 °C and 30 °C, the treatment with scrambled-sequence of unconjugated siRNA and its polymer conjugates at indicated concentrations showed no luciferase silencing and confirmed the sequence-specific silencing by siLuc.

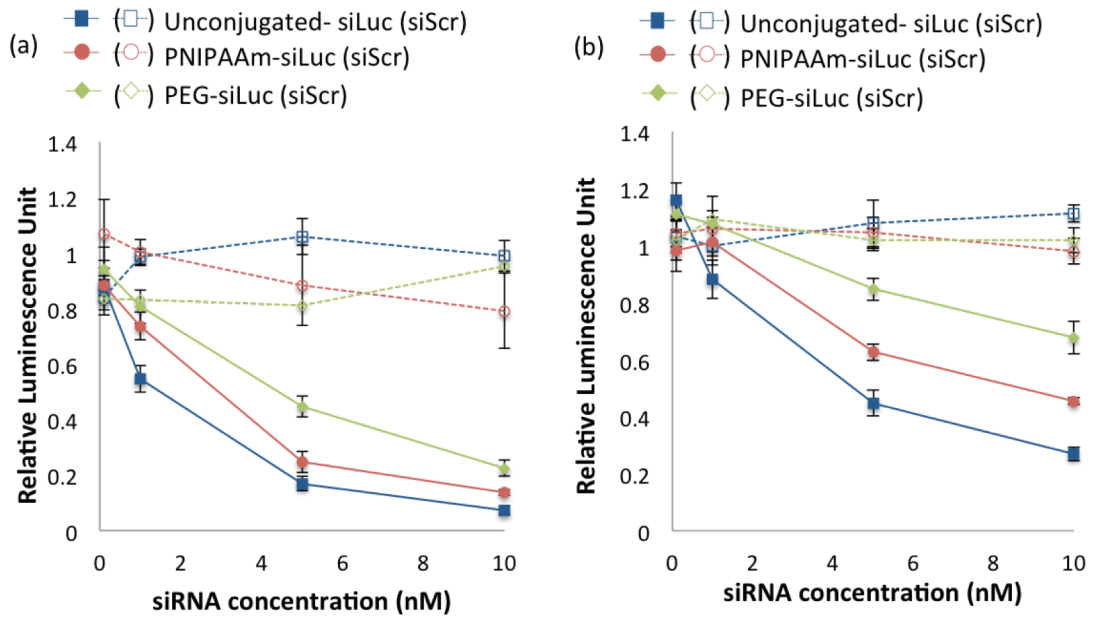

Figure 4-1. Gene silencing efficacies of siRNA series for conjugated polymer with molecular weight 10,000 g/mol at 37 °C (a) and 30 °C (b) for HeLa-Luc cells. Results were shown as mean and standard error of the mean obtained from six samples.

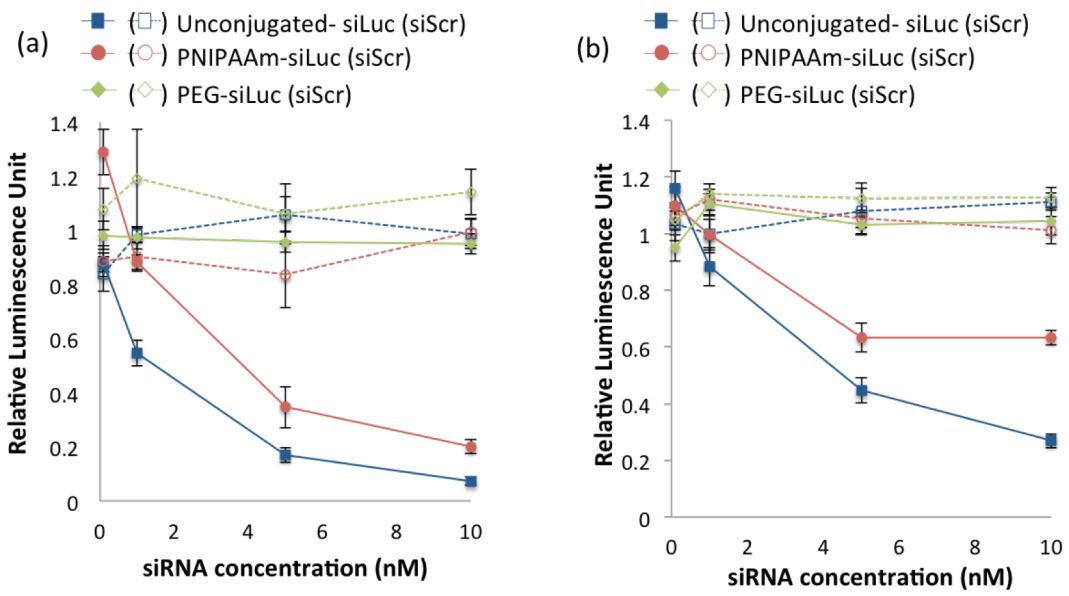

Figure 4-2. Gene silencing efficacies of siRNA series for conjugated polymer with molecular weight 20,000 g/mol at 37 °C (a) and 30 °C (b) for HeLa-Luc cells. Results were shown as mea n and standard error of the mean obtained from six samples.

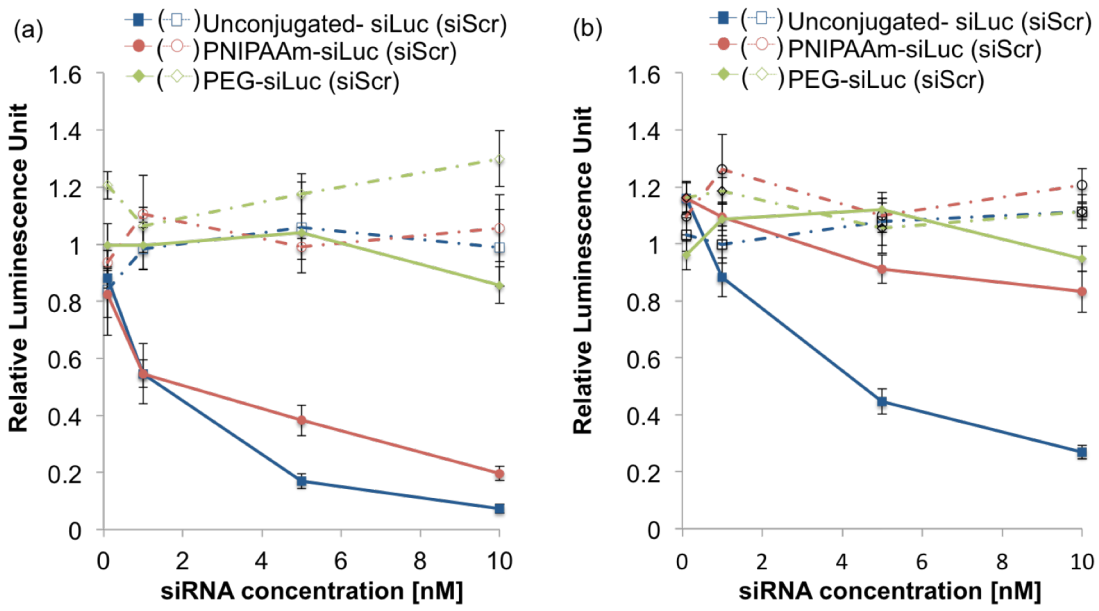

Figure 4-3. Gene silencing efficacies of siRNA series for conjugated polymer with molecular weight 40,000 g/mol at 37 °C (a) and 30 °C (b) for HeLa-Luc cells. Results were shown as mean and standard error of the mean obtained from six samples.

4.5.2. Cellular viability assay of siRNA conjugated polymer at different temperatures

In order to investigate the drop of gene silencing for PNIPAAm-siRNA after changing the temperature, the cellular viability assay using CCK-8 kit was performed. The procedure of cellular viability assay for HeLa-Luc was in a similar manner with gene silencing assay. After the treatment of the cells with siRNA and its conjugates at indicated concentrations and incubation at 30 °C and 37 °C for 48 h, CCK-8 solutions were applied into the cells. The absorbance at 450 nm of obtained solution was determined using microplate reader. As the results, no significant cytotoxicity could be observed for any samples at indicated concentrations after incubating the treated cells at 30 °C and 37 °C as shown in Figure 4-4, Figure 4-5 and Figure 4-6.

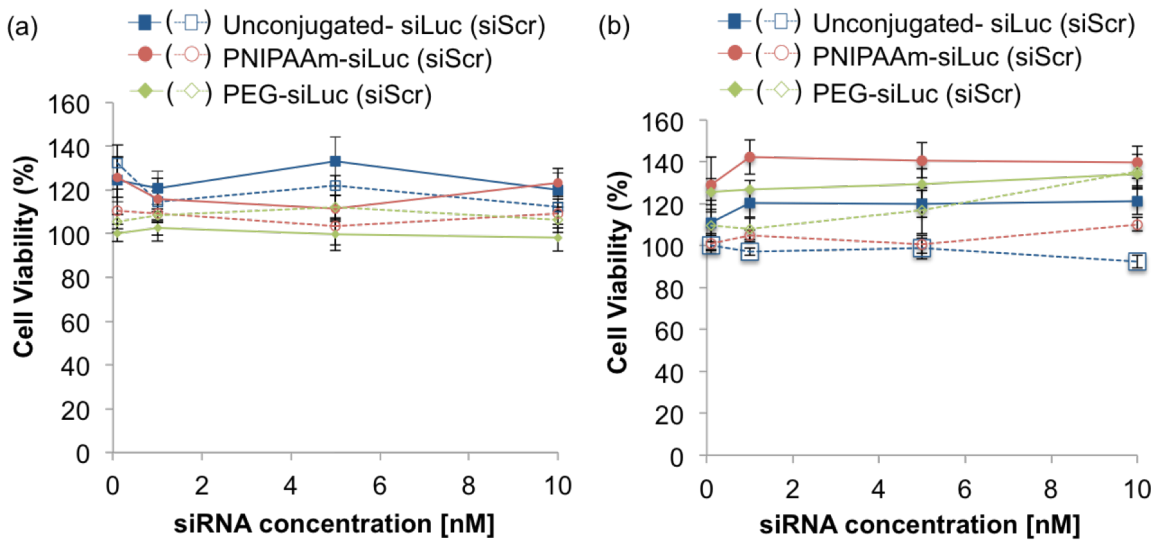

Figure 4-4. Cell viability after the treatment of HeLa-Luc cells with unconjugated siRNA and its conjugates (molecular weight of the conjugated polymer: 10, 000 g/mol) at 37 °C (a) and 30 °C (b) for HeLa-Luc cells. Results were shown as mean and standard error of the mean obtained from six samples.

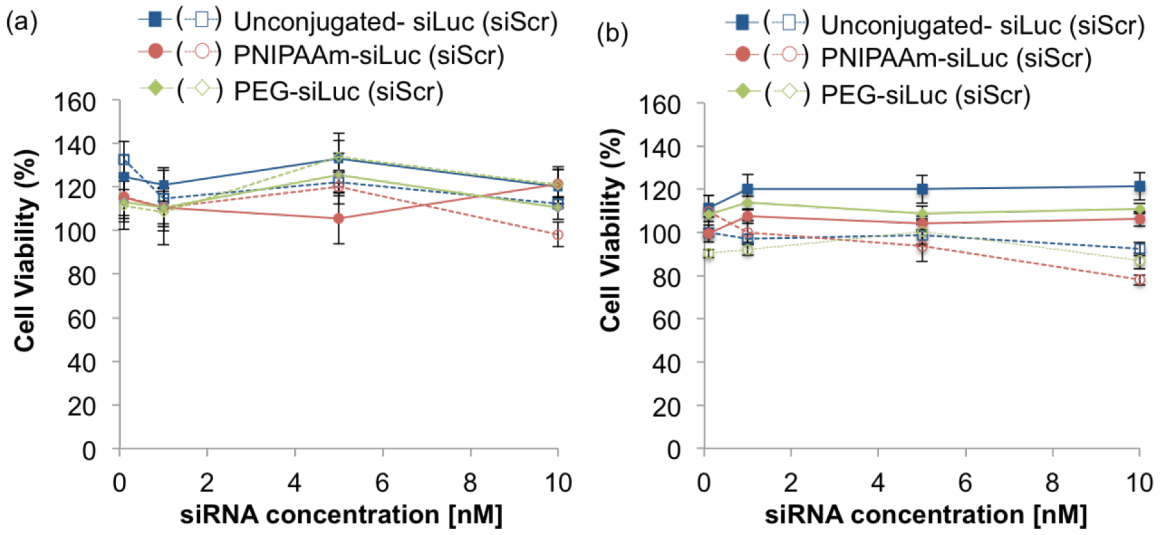

Figure 4-5. Cell viability after the treatment of HeLa-Luc cells with unconjugated siRNA and its conjugates (molecular weight of the conjugated polymer: 20, 000 g/mol) at 37 °C (a) and 30 °C (b) for HeLa-Luc cells. Results were shown as mean and standard error of the mean obtained from six samples.

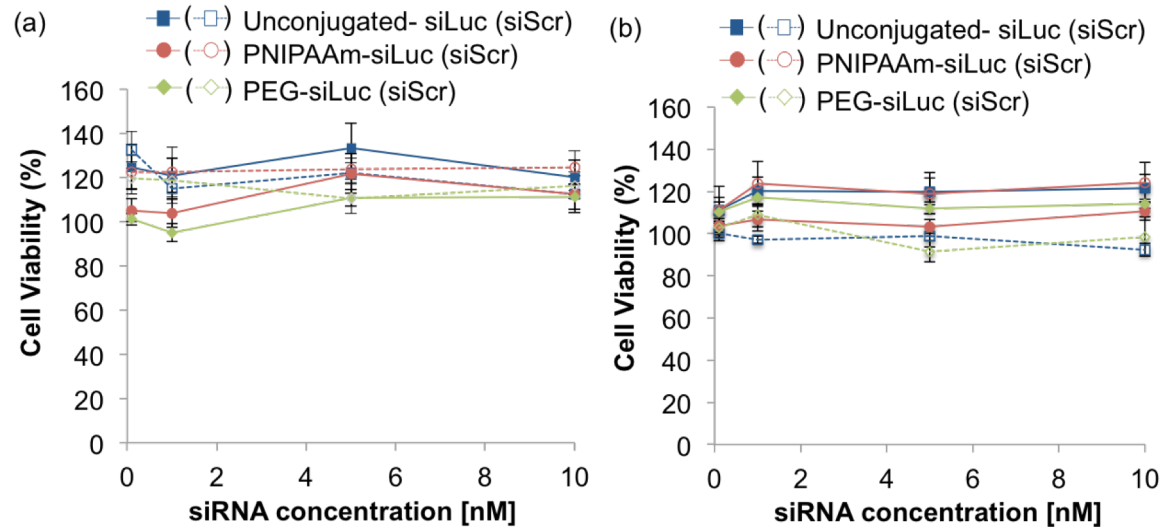

Figure 4-6. Cell viability after the treatment of HeLa-Luc cells with unconjugated siRNA and its conjugates (molecular weight of the conjugated polymer: 40, 000 g/mol) at 37 °C (a) and 30 °C (b) for HeLa-Luc cells. Results were shown as mean and standard error of the mean obtained from six samples.

4.5.3. Cellular uptake analysis of siRNA conjugated polymer

Next, in order to investigate the difference in gene silencing activity at 37 °C and 30 °C between the treatment with PNIPAAm-siRNA system and the treatment with PEG-siRNA system, the transfection amount of unconjugated siRNA and its polymer conjugates were investigated. Cells were treated with lipoplexes containing TAMRA-labeled unconjugated siRNA and TAMRA-labeled PNIPAAm-siRNA as well as PEG-siRNA at 10 nM siRNA and incubated at 37 °C and 30 °C for 24 h and 48 h.

After incubation at indicated time, the trypsinized cells were analyzed by flow cytometer. Results were shown as the relative fluorescence intensities from the treated cells. As the results, the transfection amount for unconjugated siRNA was slightly higher than its polymer conjugates series. Meanwhile, the fluorescence intensities were not significantly different between PNIPAAm-siRNA series and PEG-siRNA series at both temperatures, 30 °C and 37

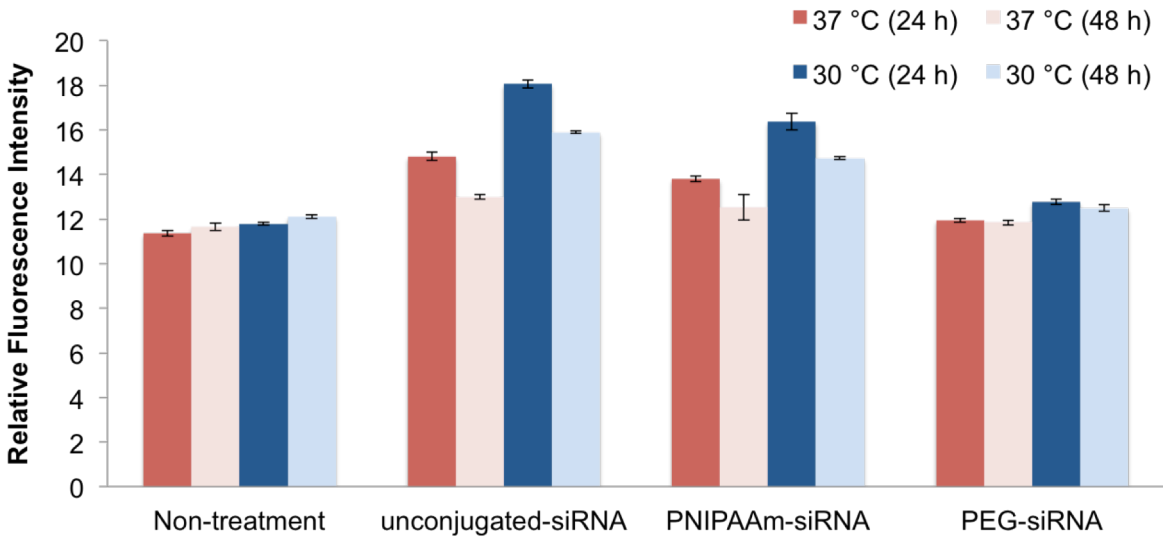

Figure 4-7. Cellular uptake efficacies of unconjugated siRNA and its conjugates (molecular weight of the conjugated polymer: 10,000 g/mol) for HeLa-Luc cells. 24 h and 48 h after the treatment of TAMRA-labeled siRNA series (10 nM of siRNA concentration) at 37 °C (red) or 30 °C (blue). Results were shown as mean and standard deviation obtained from three samples.

°C. Figure 4-7, Figure 4-8 and Figure 4-9 show the siRNA amount uptaken by the cells for the conjugated polymer for 10,000 g/mol series, 20, 000 g/mol series and 40,000 g/mol series, respectively.

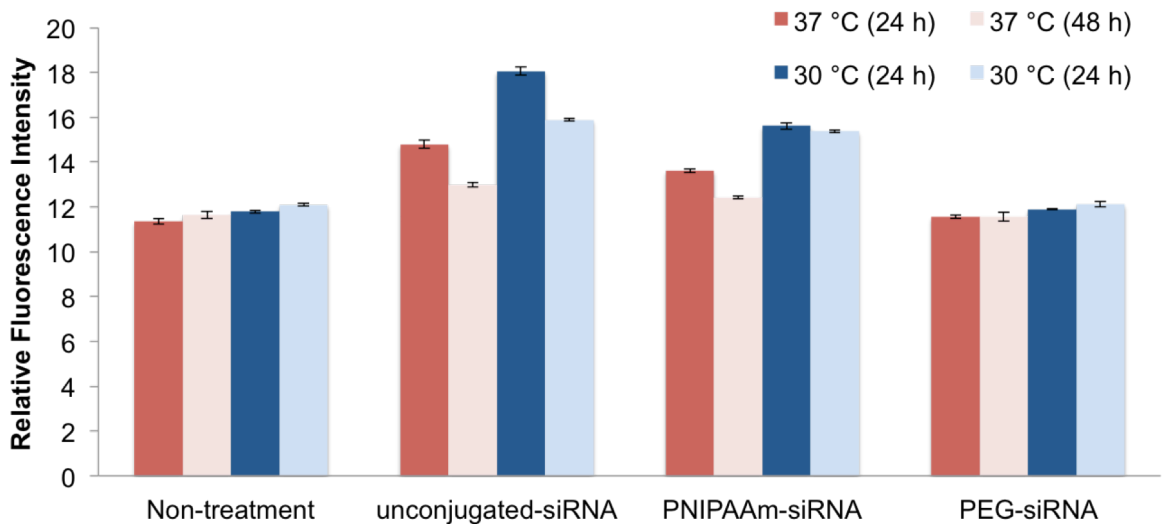

Figure 4-8. Cellular uptake efficacies of unconjugated siRNA and its conjugates (molecular weight of the conjugated polymer: 20,000 g/mol) for HeLa-Luc cells. 24 h and 48 h after the treatment of TAMRA-labeled siRNA series (10 nM of siRNA concentration) at 37 °C (red) or 30 °C (blue). Results were shown as mean and standard deviation obtained from three samples.

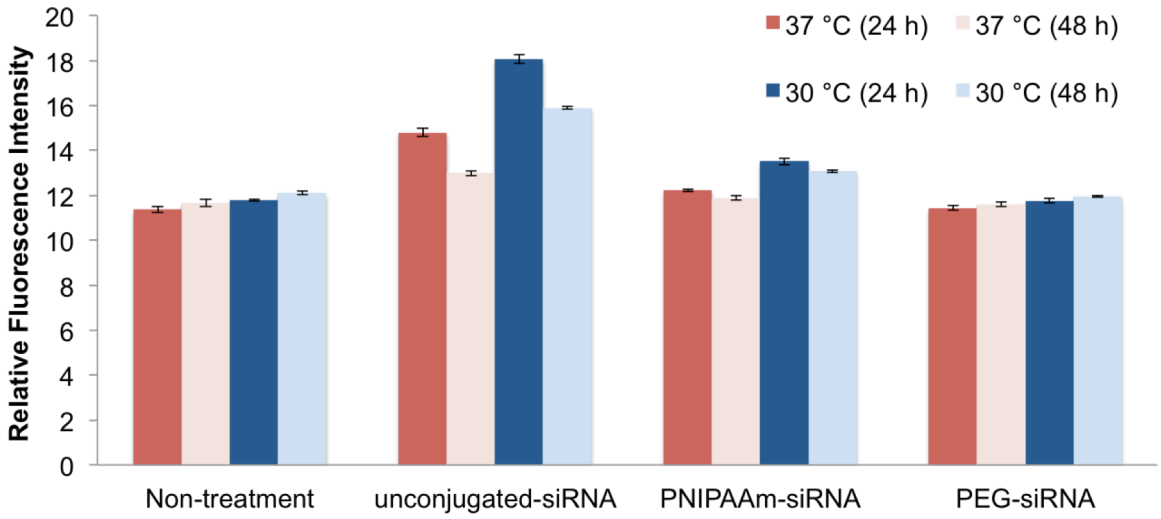

Figure 4-9. Cellular uptake efficacies of unconjugated siRNA and its conjugates (molecular weight of the conjugated polymer: 40,000 g/mol) for HeLa-Luc cells. 24 h and 48 h after the treatment of TAMRA-labeled siRNA series (10 nM of siRNA concentration) at 37 °C (red) or 30 °C (blue). Results were shown as mean and standard deviation obtained from three samples.

4.5.4. Collection of Ago2-associated asRNA

In order to elucidate the underlying mechanism of huge drop in the gene silencing at 30 °C for the treatment of PNIPAAm-siRNA system, the interaction with gene silencing related-protein, Ago2, below and above LCST, in the cytosol were investigated. In this experiment, the conjugated polymer for molecular weight of 40,000 g/mol with TAMRA-labeled $PNIPAAm_{40K}$-siRNA and PEG_{40K}-siRNA as well as TAMRA-labeled unconjugated siRNA were used for final concentration at 100 nM siRNA. Lipofectamine RNAiMAX was used as transfection reagent. The procedure was in a similar manner to the gene silencing assay. I treated the cultured cells at 100 nM siRNA in order to increase signal-to-noise ratio and obtain reliable values. After incubation of the treated cells with TAMRA-labeled unconjugated siRNA and its polymer conjugates at 37 °C and 30 °C for 48 h, the cell lysates

of the treated cells were incubated with magnetic beads for immunoprecipitation at 4 °C. Eventually, Ago2-associated asRNA was collected after heating the magnetic solution at 90 °C. The relative number of Ago2-associated asRNA per cell was calculated based on standard curve of TAMRA-labeled asRNA.

The collected number of Ago2-associated asRNA per cell after the treatment with TAMRA-labeled unconjugated siRNA, TAMRA-labeled PNIPAAm-siRNA and TAMRA-labeled PEG-siRNA at 30 °C and 37 °C were summarized in Table 4-1. As the results, after the treatment at 30 °C, the number of Ago2-associated TAMRA per cell were ca. 190, 000 ± 42,000, 69, 000 ± 10,000 and 11, 000 ± 6,500 for unconjugated siRNA, PNIPAAm-siRNA and PEG-siRNA, respectively. In contrast, after the treatment at 37 °C, the numbers of Ago2-associated TAMRA-asRNA per cell were ca. 340, 000 ± 20,000, 190, 000 ± 13,000 and 7,000 ± 3,000 for unconjugated siRNA, PNIPAAm-siRNA, and PEG-siRNA, respectively.

Table 4-1. The number of Ago2-associated asRNA per cell after the treatment with TAMRA-labeled unconjugated siRNA, TAMRA-labeled PNIPAAm-siRNA, and TAMRA-labeled PEG-siRNA, at 30 °C or 37 °C. Results were shown as mean and stardard error of the mean obtained from three samples.

	Unconjugated-siRNA	PNIPAAm-siRNA	PEG-siRNA
30 °C	190,000 ± 42,000	69,000 ± 10,000	11,000 ± 6,500
37 °C	340,000 ± 20,000	190,000 ± 13,000	7,000 ± 3,000

4.6. Discussion

Gene silencing activity of developed thermoresponsive polymer-conjugated siRNA, PNIPAAm-siRNA, was demonstrated for the cultured HeLa-Luc cells at two different temperatures, 37 °C and 30 °C. As the control systems, unconjugated siRNA and PEG-conjugated siRNA were used. At 37 °C, the treatment with unconjugated siRNA showed an effective gene silencing at almost ~90% of luciferase suppression. Meanwhile, gene silencing efficacy slightly decreased at 30 °C, possibly due to the decreased metabolism of the cell at 30 °C.

Furthermore, the treatment with PNIPAAm-siRNA at 37 °C suppressed ~80% of luciferase expression for all PNIPAAm-siRNA series, which are close to the treatment with unconjugated siRNA. Meanwhile, gene silencing decreased to ~20% suppression of luciferase expression after the treatment at 30 °C. The huge drop of gene silencing efficacy after the treatment with PNIPAAm-siRNA system is possibly due to the coil-globule transition behavior of the conjugated PNIPAAm segment. At 37 °C, the conjugated PNIPAAm segment was in globule form, thereby offering a ready access for siRNA to the proteins, leading to an efficient gene silencing. In this regard, the coil form of the conjugated PNIPAAm-segment below LCST offered 7.6 nm in the hydrodynamic diameter of PNIPAAm-siRNA, which is 1.1 nm larger than the globule form of PNIPAAm-siRNA. Only 1.1 nm difference in the hydrodynamic diameter potentially inhibits the activity of vicinal siRNA. Moreover, the difference in the hydrodynamic diameter for PEG with molecular weight of 10,000 g/mol and PEG with molecular weight of 20,000 g/mol was 1.1 nm, but, showed ~80% of silencing for PEG of 10,000 g/mol, and ~5% of gene silencing after the treatment at 37 °C. These results supported the coil-globule transition associated with the changes in the hydrodynamic diameter of PNIPAAm-segment controlled the activity of siRNA.

It should be noted that no significant cytotoxicity was observed for the treatment from any samples at both temperatures (37 °C and 30 °C) (Figure 4-4, Figure 4-5 and Figure 4-6), as determined in a cell viability assay using a water soluble tetrazolium salt (WST-8). In addition, cellular uptake efficacy as evaluated by flow cytometry, showed no significant difference between the treatment with PNIPAAm-siRNA system and the treatment with PEG-siRNA system at two different temperatures (Figure 4-7, Figure 4-8 and Figure 4-9). According to these results, the efficient gene silencing for the treatment with PNIPAAm-siRNA would be attributed to the event inside the cells, and it strongly suggests that thermoresponsive behavior of the conjugated PNIPAAm segment controlled the recruitment of siRNA into gene silencing pathway. Thus, in order to further elucidate the underlying mechanism for the huge drop of PNIPAAm-siRNA system, I collected and calculated the number Ago2-associated TAMRA-labeled asRNA per cell through immunoprecipitation method.

The number of collected Ago2-associated asRNA per cell for the treatment with unconjugated siRNA obtained 340,000 of Ago2-associated asRNA per cell after treated with 100 nM of siRNA (Table 4-1). According to the result of gene silencing assay, 1 nM of siRNA was sufficient for ~50% silencing for the treatment with unconjugated siRNA at 37 °C and it suggests that almost 3,400 of asRNA would be associated with Ago2 in the cell. Indeed, the value is consistent with the literatures that a few thousands siRNA molecules per cell are sufficient for effective gene silencing [1, 15-18]. Meanwhile, the number of collected Ago2-associated asRNA per cell for the treatment with PNIPAAm-siRNA system at 37 °C was 190,000, i.e., less than that in unconjugated siRNA system, suggesting the globule form of the conjugated PNIPAAm segment still inhibits the association of siRNA to the Ago2 proteins, due to the steric hindrance effect, compared to unconjugated siRNA (Table 4-1). Moreover, the relative number of collected Ago2-associated asRNA after the treatment with

PEG-siRNA system showed no significant difference between the treatment at 37 °C and at 30 °C, and it is possibly due to the steric hindrance effect of the conjugated PEG segment regardless of the treated temperatures.

The collected number of Ago2-associated asRNA after the treatment with PNIPAAm-siRNA at 37 °C was 2.78 times higher compared to the treatment at 30 °C, and it is significantly higher ($p < 0.05$) than the treatment with unconjugated siRNA. In the treatment with unconjugated siRNA system, the collected number of Ago2-asssociated asRNA per cell at 37 °C was led to 1.84 times higher compared to the treatment at 30 °C (Figure 4-10). The multiplied increase in the number of Ago2-associated asRNA, in response to the increase in temperature, is higher for PNIPAAm-siRNA system, compared to unconjugated siRNA system, probably because of the coil-globule transition of the conjugated PNIPAAm segment

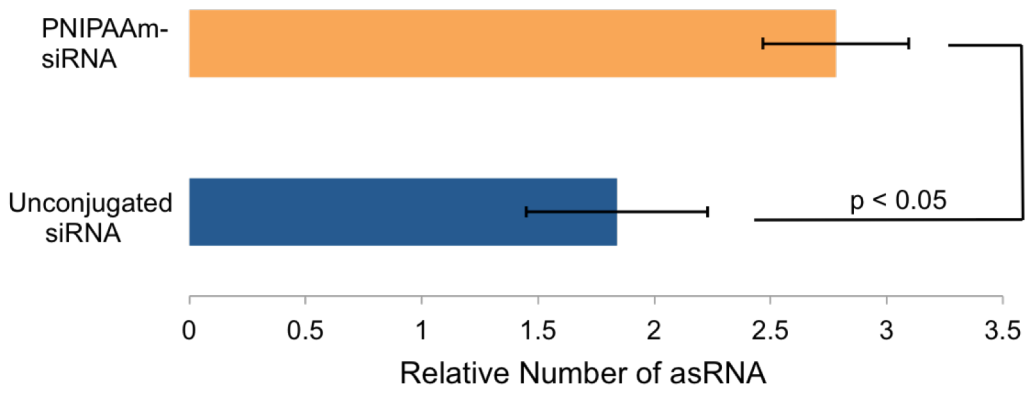

Figure 4-10. The number of the Ago2-associated asRNA per cell after the unconjugated siRNA or PNIPAAm-siRNA treatment at 37 °C was divided by the separately obtained value after the treatment with unconjugated siRNA or PNIPAAm-siRNA at 30 °C. The treatment condition similar to the gene silencing assay. Results were shown as mean and standard error of the mean obtained from three samples. The p value was calculated according to the Student's *t* test.

and associate changes in hydrodynamic diameter as well as steric hindrance effect. This result supports the motivation of my study that coil-globule transition of the conjugated polymer regulates siRNA recognition by Ago2 protein in cell, and leads to artificial control of gene silencing activity.

4.7. Conclusion

The newly developed thermoresponsive polymer, PNIPAAm-siRNA effectively works for an artificial control of the activity of siRNA via interaction with gene silencing-related protein, Ago2 in the cytosol based on coil-globule transition behavior of the conjugated PNIPAAm segment. Interestingly, the molecular weight of the conjugated polymer affected the gene silencing activity of siRNA, i.e., larger hydrodynamic diameter derived from the conjugated polymer for higher molecular weight (40,000 g/mol) works well for an artificial control of the recruitment of siRNA into gene silencing pathway. At 37 °C, the globule state of the conjugated PNIPAAm potentially offers a ready access of siRNA to the proteins, and leads to effective gene silencing (~80 % of luciferase expression), which is close to the treatment with unconjugated siRNA (~90% of luciferase expression); in contrast, at 30 °C, the coil form of PNIPAAm inhibits the access of siRNA, and thus, silencing efficacy decreased to ~20%. Meanwhile, the treatment with PEG_{40k}-siRNA system suppressed only ~10% of silencing due to the steric hindrance effect of the conjugated PEG segment. The multiplied increase in Ago2 associated asRNA in the PNIPAAm-siRNA system compared to the unconjugated siRNA system, strongly suggests that coil-globule transition of the conjugated PNIPAAm potentially control the siRNA bioactivity in the cell.

4.8. Reference

[1] Rana, T. M. Illuminating the silence: understanding the structure and function of small RNAs. *Nat. Rev. Mol. Cell Biol.* **2007**, *8*, 23–36.

[2] Kanasty, R. L., Whitehead, K. A., Vegas, A. J., and Anderson, D. G. Action and reaction: the biological response to siRNA and its delivery vehicles. *Mol. Ther.* **2012**, *20*, 513–24.

[3] Schroeder, A., Levins, C. G., Cortez, C., Langer, R., and Anderson, D. G. Lipid-based nanotherapeutics for siRNA delivery. *J. Intern. Med.* **2010**, *267*, 9–21.

[4] Gomes-Da-Silva, L. C., Fonseca, N. A., Moura, V., Pedroso De Lima, M. C., Simões, S., and Moreira, J. N. Lipid-based nanoparticles for siRNA delivery in cancer therapy: Paradigms and challenges. *Acc. Chem. Res.* **2012**, *45*, 1163–1171.

[5] Zhang, S., Zhao, B., Jiang, H., Wang, B., and Ma, B. Cationic lipids and polymers mediated vectors for delivery of siRNA. *J. Control. Release* **2007**, *123*, 1–10.

[6] Brazas, R. M., and Hagstrom, J. E. Delivery of small interfering RNA to mammalian cells in culture by using cationic lipid/polymer-based transfection reagents. *Methods Enzymol.* **2005**, *392*, 112–24.

[7] Semple, S. C., Akinc, A., Chen, J., Sandhu, A. P., Mui, B. L., Cho, C. K., Sah, D. W. Y., Stebbing, D., Crosley, E. J., Yaworski, E., Hafez, I. M., Dorkin, J. R., Qin, J., Lam, K., Rajeev, K. G., Wong, K. F., Jeffs, L. B., Nechev, L., Eisenhardt, M. L., Jayaraman, M., Kazem, M., Maier, M. A., Srinivasulu, M., Weinstein, M. J., Chen, Q., Alvarez, R., Barros, S. A., De, S., Klimuk, S. K., Borland, T., Kosovrasti, V., Cantley, W. L., Tam, Y. K., Manoharan, M., Ciufolini, M. A., Tracy, M. A., de Fougerolles, A., MacLachlan, I., Cullis, P. R., Madden, T. D., and Hope, M. J.Rational design of cationic lipids for siRNA delivery. *Nat. Biotechnol.* **2010**, *28*, 172–176.

[8] Zhao, M., Yang, H., Jiang, X., Zhou, W., Zhu, B., Zeng, Y., Yao, K., and Ren, C. Lipofectamine RNAiMAX: An efficient siRNA transfection reagent in human embryonic

stem cells. *Mol. Biotechnol.* **2008,** *40*, 19–26.

[9] Dominska, M., and Dykxhoorn, D. M. Breaking down the barriers: siRNA delivery and endosome escape. *J. Cell Sci.* **2010,** *123*, 1183–9.

[10] Felgner, P. L., Gadek, T. R., Holm, M., Roman, R., Chan, H. W., Wenz, M., Northrop, J. P., Ringold, G. M., and Danielsen, M. Lipofection: A Highly Efficient, Lipid-Mediated DNA-Transfection Procedure. *Pnas* **1987**, *84*, 7413–7417.

[11] Moore, A., Mercer, J., Dutina, G., Donahue, C. J., Bauer, K. D., Mather, J. P., Etcheverry, T., and Ryll, T. Effects of temperature shift on cell cycle, apoptosis and nucleotide pools in CHO cell batch cultues. *Cytotechnology* **1997**, *23*, 47–54.

[12] Nelson, J. D., Denisenko, O., and Bomsztyk, K. Protocol for the fast chromatin immunoprecipitation (ChIP) method. *Nat. Protoc.* **2006**, *1*, 179–185.

[13] Iwasaki, S., Sasaki, H. M., Sakaguchi, Y., Suzuki, T., Tadakuma, H., and Tomari, Y. (2015) Defining fundamental steps in the assembly of the Drosophila RNAi enzyme complex. *Nature* **2015**, *521*, 533–536.

[14] Wu, S. Y., Yang, X., Gharpure, K. M., Hatakeyama, H., Egli, M., McGuire, M. H., Nagaraja, A. S., Miyake, T. M., Rupaimoole, R., Pecot, C. V, Taylor, M., Pradeep, S., Sierant, M., Rodriguez-Aguayo, C., Choi, H. J., Previs, R. a, Armaiz-Pena, G. N., Huang, L., Martinez, C., Hassell, T., Ivan, C., Sehgal, V., Singhania, R., Han, H.-D., Su, C., Kim, J. H., Dalton, H. J., Kovvali, C., Keyomarsi, K., McMillan, N. a J., Overwijk, W. W., Liu, J., Lee, J.-S., Baggerly, K. a, Lopez-Berestein, G., Ram, P. T., Nawrot, B., and Sood, A. K. 2'-OMe-phosphorodithioate-modified siRNAs show increased loading into the RISC complex and enhanced anti-tumour activity. *Nat. Commun.* **2014**, *5*, 3459, 1-9.

[15] Wei, J., Jones, J., Kang, J., Card, A., Krimm, M., Hancock, P., Pei, Y., Ason, B., Payson, E., Dubinina, N., Cancilla, M., Stroh, M., Burchard, J., Sachs, A. B., Hochman, J. H., Flanagan, W. M., and Kuklin, N. a. RNA-induced silencing complex-bound small interfering

RNA is a determinant of RNA interference-mediated gene silencing in mice. *Mol. Pharmacol.* **2011**, *79*, 953–963.

[16] Bartlett, D. W., and Davis, M. E. Insights into the kinetics of siRNA-mediated gene silencing from live-cell and live-animal bioluminescent imaging. *Nucleic Acids Res.* **2006**, *34*, 322–333.

[17] Landesman, Y., Svrzikapa, N., Cognetta, A., Zhang, X., Bettencourt, B. R., Kuchimanchi, S., Dufault, K., Shaikh, S., Gioia, M., Akinc, A., Hutabarat, R., and Meyers, R. In vivo quantification of formulated and chemically modified small interfering RNA by heating-in-Triton quantitative reverse transcription polymerase chain reaction (HIT qRT-PCR). *Silence* **2010**, *1*, 16.

[18] Gilleron, J., Querbes, W., Zeigerer, A., Borodovsky, A., Marsico, G., Schubert, U., Manygoats, K., Seifert, S., Andree, C., Stöter, M., Epstein-Barash, H., Zhang, L., Koteliansky, V., Fitzgerald, K., Fava, E., Bickle, M., Kalaidzidis, Y., Akinc, A., Maier, M., and Zerial, M. Image-based analysis of lipid nanoparticle-mediated siRNA delivery, intracellular trafficking and endosomal escape. *Nat. Biotechnol.* **2013**, *31*, 638–46.

Chapter 5. Summary and Future Perspectives

5.1. Summary

To date, tremendous reports have been dedicated to the design of siRNA-based medicine, due to its strong gene silencing ability [1,2]. For example, sophisticatedly created carriers for siRNA delivery to the targeted site, and modified siRNA structure for physiological resistance leading to prolonged bioactivity of siRNA have been developed [3,4,5]. siRNA conjugation with functional polymeric molecule is also one of the attractive approaches, where it not only improves inherent siRNA bioactivity, but also endows siRNA with entirely new functionalities [6]. However, the conjugation with polymeric molecule having steric hindrance effect often suppresses siRNA recruitment into gene silencing pathway in the cells [7,8]. In this regard, I exploited a new methodology for an artificial induction of siRNA bioactivity in the cell, based on the conjugation with stimuli-responsive polymer, and described the significance of the study as well as introduction of general information related to the study in **Chapter 1**. In detail, the conjugated stimuli-responsive polymer would undergo coil-globule transition behavior in response to the environment change. The coil-globule transition behavior of the conjugated polymer would associate with the considerable change of size, thereby, the conjugation would artificially control the vicinal siRNA recognition by the proteins into gene silencing pathway, and would lead to the manipulative gene silencing activity in the cell. In order to realize the methodology, I developed new synthetic roots for the desired siRNA-conjugated polymers, and investigated the steric hindrance effect of the conjugated polymer on vicinal siRNA from physicochemical and biological views.

Chapter 2 introduced the original synthetic roots of siRNA-conjugated polymer. With regard to the conjugated polymer having coil-globule transition behavior, I investigated the preparation of thermoresponsive polymer, PNIPAAm, with controlled polymer structure through ATRP and RAFT living radical polymerization techniques. Eventually, I successfully

synthesized PNIPAAm with narrow molecular weight distribution and desired molecular weight through RAFT polymerization method. The obtained PNIPAAm having narrow molecular weight distributions (Mw/Mn = 1.18 – 1.24) and targeted molecular weights (Mw = 10,000 g/mol, 20,000 g/mol and 40,000 g/mol) which were calculated based on standard poly(ethylene glycol) (PEG) through GPC, and their end group was successfully modified by introducing a DBCO group towards the siRNA conjugation with an azide-siRNA molecule. In a similar manner, non-thermoresponsive polymer, PEG-DBCO was successfully prepared. Subsequently, both PNIPAAm-siRNA and PEG-siRNA were produced at good yields (> 80%) through Copper-free Click Chemistry utilizing freeze-thaw technique, followed by purification and characterization by ion-exchange chromatography and agarose gel electrophoresis, respectively.

Chapter 3 describes the physicochemical properties of the newly designed PNIPAAm-siRNA. Almost all of the physicochemical properties of PNIPAAm-siRNA were discussed on LCST-related behavior studies. The turbidity of PNIPAAm with end group modification through transmittance measurement revealed that the LCST ranging from ~33 °C to ~35°C for 50% optical transmittance, i.e., the temperature close to the original LCST of reported PNIPAAm (33 °C) [9]. Furthermore, thermoresponsive behavior of PNIPAAm-siRNA was examined by light scattering analysis and fluorescence correlation spectroscopic (FCS) study. It was found that, the aggregation temperature of 35 °C for PNIPAAm-siRNA solution in 10 mM HEPES pH 7.4 (5 μM siRNA) indicates that PNIPAAm undergoes coil-globule transition behavior even in the presence of the vicinal siRNA. This result suggests the thermoresponsive exposure of siRNA, owing to coil-globule transition of PNIPAAm segment, when the PNIPAAm-siRNA is in diluted concentration, such as after entering the cell. Indeed, the hydrodynamic diameter of PNIPAAm segment decreased ~1.1 nm of size in diameter from 7.61± 0.23 nm at room temperature to 6.50 ± 0.21 nm at 37 °C, confirmed by

FCS analysis (100 nM siRNA, 10 mM HEPES pH 7.4). In contrast, unconjugated siRNA and PEG-siRNA showed constant values of scattering light intensity as well as hydrodynamic diameters, regardless of a change in temperature. These results suggest the high potential of the PNIPAAm segment for an artificial control of the vicinal siRNA and the induction of gene silencing activity in the cell.

To demonstrate the temperature-dependent gene silencing activity of PNIPAAm-siRNA, biological performances were demonstrated in *in vitro* study and were described in **Chapter 4**. Gene silencing activity of PNIPAAm-siRNA was investigated for cultured human cervical cancer cells stably expressing luciferase (HeLa-Luc) at two different temperatures, at 37 °C (T > LCST) and at 30 °C (T < LCST) using Lipofectamine RNAiMAX. In order to confirm the sequence-specific gene silencing effect, the scrambled siRNA sequence (siScr) was utilized as well as the luciferase-specific sequence (siLuc). As a result, the treatment with PNIPAAm-siLuc at 37 °C for siRNA concentration at 10 nM achieved 80% silencing of luciferase expression, while PNIPAAm-siLuc treatment at 30 °C and PEG-siLuc treatment at 37 °C resulted in 20% and 10% silencing, respectively. According to the flow cytometric analysis, the cellular uptake efficacies of PNIPAAm-siRNA and PEG-siRNA series systems were not significantly different. Hence, the enhanced gene silencing of PNIPAAm-siRNA at 37 °C compared to PEG-siRNA should be attributed to the event inside the cell. To further explore the mechanism of improved gene silencing in PNIPAAm-siRNA system, the Ago2-associated asRNA was counted utilizing TAMRA-labeled asRNA for siRNA preparation. The number of Ago2-asscociated asRNA per cell after the treatment with PNIPAAm-siRNA at 37 °C was 2.78 times higher compared to the treatment at 30 °C. Meanwhile, the treatment with unconjugated siRNA at 37 °C led to 1.84 times increase in Ago2-associated asRNA per cell. The increase in the number of Ago2-associated asRNA with the elevated temperature for unconjugated siRNA system can be explained by the less activity of the cell at lower

temperature. Moreover, the significantly higher multiplied increase ($p < 0.05$) for the PNIPAAm-siRNA system, compared to the unconjugated siRNA system, strongly suggests that the thermoresponsive behavior of the PNIPAAm segment, as well as the thermal effect on the cell activity, affected gene silencing efficacy, i.e., globule form of PNIPAAm offered a ready access for siRNA to gene silencing-related proteins in the cells.

Overall, the conjugation of siRNA with polymer having coil-globule transition behavior successfully controls the efficacy of the siRNA recruitment into gene silencing pathway, leading to the success in the manipulative gene silencing activity.

5.2. Future Perspective

To the best knowledge of the author, this is the first study to represent a successful scientific methodology for an artificial control of gene silencing activity of siRNA in the cell. This methodology showed that the polymer conjugation with an siRNA molecule can regulate siRNA recognition by Ago2 protein and gene silencing activity based on the coil-globule transition behavior of the conjugated polymer. In design, an siRNA was linearly conjugated to the PNIPAAm. Coil form of the conjugated PNIPAAm inhibited the siRNA recognition by the proteins, due to the steric hindrance effect, and thus, compromised gene silencing activity in the cell. On the other hand, the globule form of the conjugated PNIPAAm exposed siRNA for a ready access to the proteins, leading to effective gene silencing pathway.

The main focus on this study is on development and demonstration of a new methodology to control siRNA bioactivity, therefore, PNIPAAm was utilized as the conjugated polymer in the present study due to the simplicity of the responsiveness of PNIPAAm, i.e., responsiveness only to the temperature changes. In order to translate this methodology into therapeutic application with high medicinal potential, the introduction of the responsiveness to site-specific biological stimuli, such as pH, enzyme, and redox should be further

developed. It is known that the responsiveness of PNIPAAm can be tuned by copolymerization with other acrylic monomers having pH-responsive or enzymatic responsibility [10, 11].

The achievement of a newly developed methodology for an artificial control of siRNA bioactivity based on the coil-globule transition behavior of the conjugated polymer in the present study, would provide not only fundamental knowledge for molecular design but also new methodology for siRNA-based therapeutics that can be utilized for enhancing its role in realizing a better lifestyle for the people suffering from intractable diseases.

5.3. References

[1] Elbashir, S. M., Harborth, J., Lendeckel, W., Yalcin, A., Weber, K., and Tuschl, T. Duplexes of 21 ± nucleotide RNAs mediate RNA interference in cultured mammalian cells. *Nature* **2001**, *411*, 494–498.

[2] Whitehead, K. a, Langer, R., and Anderson, D. G. Knocking down barriers: advances in siRNA delivery. *Nat. Rev. Drug Discov.* **2009**, *8*, 129–138.

[3] Nair, J. K., Willoughby, J. L. S., Chan, A., Charisse, K., Alam, M. R., Wang, Q., Hoekstra, M., Kandasamy, P., Kelin, A. V., Milstein, S., Taneja, N., Oshea, J., Shaikh, S., Zhang, L., Van Der Sluis, R. J., Jung, M. E., Akinc, A., Hutabarat, R., Kuchimanchi, S., Fitzgerald, K., Zimmermann, T., Van Berkel, T. J. C., Maier, M. A., Rajeev, K. G., and Manoharan, M. Multivalent N -acetylgalactosamine-conjugated siRNA localizes in hepatocytes and elicits robust RNAi-mediated gene silencing. *J. Am. Chem. Soc.* **2014**, *136*, 16958–16961.

[4] Chiu, Y.-L., Ali, A., Chu, C., Cao, H., and Rana, T. M. Visualizing a Correlation between siRNA Localization, Cellular Uptake, and RNAi in Living Cells. *Chem. Biol.* **2004**, *11*, 1165–1175.

[5] Gilleron, J., Querbes, W., Zeigerer, A., Borodovsky, A., Marsico, G., Schubert, U., Manygoats, K., Seifert, S., Andree, C., Stöter, M., Epstein-Barash, H., Zhang, L., Koteliansky, V., Fitzgerald, K., Fava, E., Bickle, M., Kalaidzidis, Y., Akinc, A., Maier, M., and Zerial, M. Image-based analysis of lipid nanoparticle-mediated siRNA delivery, intracellular trafficking and endosomal escape. *Nat. Biotechnol.* **2013**, *31*, 638–46.

[6] Jeong, J. H., Mok, H., Oh, Y., and Park, T. G. (2009) siRNA Conjugate Delivery Systems. *Bioconjug. Chem.* **2009**, *20*, 5–14.

[7] Takemoto, H., Miyata, K., Hattori, S., Ishii, T., Suma, T., Uchida, S., Nishiyama, N., and Kataoka, K. Acidic pH-responsive siRNA conjugate for reversible carrier stability and accelerated endosomal escape with reduced IFNα-associated immune response. *Angew. Chemie - Int. Ed.* **2013**, *52*, 6218–6221.

[8] Lee, S. H., Mok, H., and Park, T. G. Di- and Triblock siRNA-PEG Copolymers: PEG Density Effect of Polyelectrolyte Complexes on Cellular Uptake and Gene Silencing Efficiency. *Macromol. Biosci.* **2011**, *11*, 410–418.

[9] Boutris, C., Chatzi, E. G., and Kiparissides, C. Characterization of the LCST behaviour of aqueous poly(N-isopropylacrylamide) solutions by thermal and cloud point techniques. *Polymer (Guildf).* **1997**, *38*, 2567–2570.

[10] Lv, W., Liu, S., Feng, W., Qi, J., Zhang, G., Zhang, F., and Fan, X. Temperature- and redox-directed multiple self assembly of poly(N-isopropylacrylamide) grafted dextran nanogels. *Macromol. Rapid Commun.* **2011**, *32*, 1101–1107.

[11] Gao, X., Cao, Y., Song, X., Zhang, Z., Xiao, C., He, C., and Chen, X. pH- and thermo-responsive poly(N-isopropylacrylamide-co-acrylic acid derivative) copolymers and hydrogels with LCST dependent on pH and alkyl side groups. *J. Mater. Chem. B* **2013**, *1*, 5578.

6. Appendix

Appendix 6.1. Cellular viability assay

Appendix 6.1.1. Cellular viability assay for HeLa-Luc cells using PLK1 expressing siRNA

In Chapter 4, I described that the coil-globule transition of the conjugated PNIPAAm segment plays a main role for an artificial control of luciferase expression for cultures HeLa-Luc cells. In brief, for the treatment of PNIPAAm-siLuc (10 nM siRNA) at 37 °C exhibited 80% of gene silencing after incubated for 48 h due to the globule form of the conjugated PNIPAAm exposed siLuc for a ready access to the gene silencing ability. On the other hand, for the treatment at 30 °C decreased to 20% of gene silencing due to the coil form of the conjugated PNIPAAm inhibited siLuc activity. According to the results, in this appendix, I investigated thermoresponsive behavior of the conjugated PNIPAAm to another siRNA sequence other than luciferase-targeting sequence; I utilized polo-like kinase 1 (PLK1) targeting siRNA (siPLK1) to the cell viability assay for cultured HeLa-Luc cells. PLK1 plays a main role in control of the cell cycle, and overexpression of PLK1 can cause for the canceration [1-3]. Knockdown of PLK1 caused the apoptosis in cancer cells, but not in normal cell lines [4].

In order to examine the viability of HeLa-Luc after the treatment with PNIPAAm-siPLK1, firstly, I prepared PNIPAAm-siPLK1 conjugation through freeze-thaw treatment using PNIPAAm-DBCO and azide-siPLK1. The synthetic manner, purification as well as characterization of PNIPAAm-siPLK1 are in a similar manner to that mentioned in Chapter 2. PEG-siPLK1 also was prepared as a control system. Then, I prepared lipoplexes of siPLK1 and its polymer conjugates (PNIPAAm-siPLK1 and PEG-siPLK1) with Lipofectamine RNAiMAX, and applied lipoplexes to cultured HeLa-Luc cells at final concentration of siRNA at 0.1 nM, 1 nM, 5 nM and 10 nM. Then, the cells were incubated at 37 °C and 30 °C.

To confirm the sequence-specific silencing capacity of siPLK1, I utilized siScramble (siScr) for the control experiment. After incubation of the cells for 72 h, CCK-8 solutions were applied into each treated well, and determined the absorbance at 450 nm using microplate reader. As the results, the viability of HeLa-Luc at 37 °C shows almost 40% after the treatment with PNIPAAm-siPLK1 at 10 nM siRNA, suggesting that globule form of the conjugated PNIPAAm exposes siPLK1 to inhibit the mPLK1, and leads to the cell death, which is close to the viability after the treatment with unconjugated siPLK1 (~40%). Meanwhile, for the treatment with PEG-siPLK1, cells showed high viability possibly the steric hindrance effect of the conjugated PEG segment inhibits the siPLK1 activity (Figure A-1a). On the contrary, at 30 °C, no cell death could be observed for the treatment from any samples (Figure 6-1b), probably because the PLK1 expression is weak at low temperature and thus, no apoptosis of treated cells could be observed. According to the results, it is would support the notion that the globule form of the conjugated PNIPAAm successfully offer for a

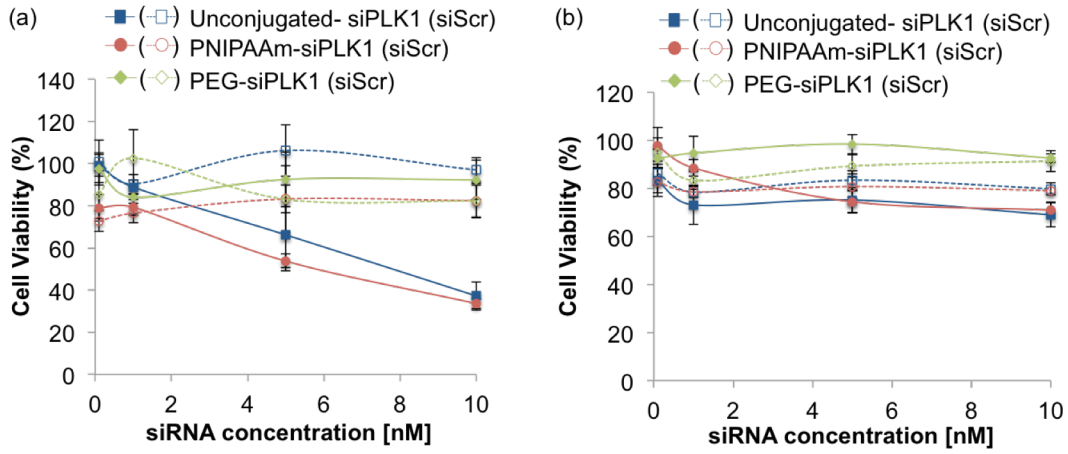

Figure 6-1. Cell viability assay for HeLa-Luc after the treatmenr with unconjugated siPLK1 and its polymer conjugates at 37 °C (a) and 30 °C (b) using Lipofectamine RNAiMAX. Results were shown as mean and standard error of mean obtained from six samples.

ready access of siRNA to initiate gene silencing pathway. In contrast, the steric hindrance effect of the conjugated PEG inhibits the activity of siRNA, and compromise gene silencing ability.

Appendix 6.1.2. References

[1] Benoit, D. S. W., Henry, S. M., Shubin, A. D., Hoffman, A. S., and Stayton, P. S. pH-Responsive Polymeric siRNA Carriers Sensitize Multidrug Resistant Ovarian Cancer Cells to Doxorubicin via Knockdown of Polo-like Kinase 1. *Mol. Pharm.* **2010**, *7*, 442–455.

[2] Ando, K., Ozaki, T., Yamamoto, H., Furuya, K., Hosoda, M., Hayashi, S., Fukuzawa, M., and Nakagawara, A. Polo-like kinase 1 (Plk1) inhibits p53 function by physical interaction and phosphorylation. *J. Biol. Chem.* **2004**, *279*, 25549–25561.

[3] Lee, S.-Y., Jang, C., and Lee, K.-A. Polo-like kinases (plks), a key regulator of cell cycle and new potential target for cancer therapy. *Dev. Reprod.* **2014**, *18*, 65.

[4] Spänkuch-Schmitt, B., Wolf, G., and Solbach, C. Downregulation of human polo-like kinase activity by antisense oligonucleotides induces growth inhibition in cancer cells. *Oncogene* **2002**, 3162–3171.

7. Achievements

Publication

[1] Noor Faizah Che Harun, Hiroyasu Takemoto, Takahiro Nomoto, Keishiro Tomoda, Makoto Matsui, Nobuhiro Nishiyama " Artificial Control of Gene Silencing Activity Based on siRNA Conjugation with Polymeric Molecule Having Coil-Globule Transition Behavior" *Bioconjugate Chemistry* **2016** *27*, 1961-1964.

Presentations

[1] Noor Faizah Che Harun, Hiroyasu Takemoto, Takahiro Nomoto, Keishiro Tomoda, Makoto Matsui and Nobuhiro Nishiyama " Development of Thermoresponsive Polymer-siRNA conjugates for controlled RNAi Activity" 65th SPSJ Annual Meeting, Kobe, Japan, May 2016 (Oral presentation)

[2] Noor Faizah Che Harun, Hiroyasu Takemoto, Takahiro Nomoto, Keishiro Tomoda, Makoto Matsui and Nobuhiro Nishiyama "Development of siRNA conjugated polymer with coil-globule transition behavior for an artificially controlled gene silencing activity" 65th Symposium on Macromolecules, Yokohama, Japan, September 2016 (Oral presentation)

[3] Noor Faizah Che Harun, Hiroyasu Takemoto, Takahiro Nomoto, Keishiro Tomoda, Makoto Matsui and Nobuhiro Nishiyama "Artificial control of siRNA bioactivity based on the phase transition behavior of the conjugated polymeric molecule" 11th SPSJ International Polymer Conference, December 2016 (Oral presentation).

8. Acknowledgements

For the first and foremost, I would like to convey my utmost sincere gratitude to my academic supervisor, Professor Nobuhiro Nishiyama for the continuous support of my Ph.D study and research, for his patience, motivation, enthusiasm, immense knowledge, and providing me with an excellent atmosphere for completing my research.

I appreciate all the members of staff at Nishiyama Laboratory who kindly helped me and provided insightful discussion about the research.

I have to express my gratitude to Dr. Takahiro Nomoto for his guidance, valuable comments for my research as well as to always positively motivate me during completing this research.

Particularly, I would like to express my utmost gratitude to Dr. Hiroyasu Takemoto, the direct my mentor, for assisting all of my research activity patiently not only for experimental planning but also for my future planning, which were necessary to proceed in a right way, helping me to develop my polymer synthesis as well as biological study skills and to understand my research area better. I also appreciate every single discussion time spent to me, especially for editing or reviewing any kind of manuscript I have to prepare. I have really enjoyed the experience working with you.

I am also very grateful to be surrounded by smart and friendly lab members who readily helped me anytime I have problem inside and outside laboratory. Thank you very much for any kind of times.

I also would like to express my sincere gratitude to the management team of Universiti Kuala Lumpur (UniKL) for accepting me as one of the academic staffs under Lectureship Scheme in UniKL and for helping me on every kind of management matters. Because of this, I am possible to pursue my dream to study for Ph.D. I deeply appreciate for all of the opportunities and co-operations that have been provided to me.

I have to also express my sincere gratitude to Majlis Amanah Rakyat (MARA), a Malaysia government agency for providing continuous financial support for my Ph.D study and daily life in Japan.

The most importantly, none of this would have been possible without love, courage and patient of my family members, especially my parents, my brothers and my sisters, for their unconditional love, warm support, and encourage, which allowed me to get this far in life.

"Alhamdulillah"

Noor Faizah binti Che Harun

Interdisciplinary Graduate School of Science and Engineering,

Tokyo Institute of Technology,

March 2017